

# GEOMETRICALLY HIGHER ORDER UNFITTED SPACE-TIME METHODS FOR PDES ON MOVING DOMAINS: GEOMETRY ERROR ANALYSIS\*

FABIAN HEIMANN AND CHRISTOPH LEHRENFELD<sup>†</sup>

**Abstract.** In [Heimann, Lehrenfeld, Preuß, SIAM J. Sci. Comp. 45(2), 2023, B139 - B165] new geometrically unfitted space-time Finite Element methods for partial differential equations posed on moving domains of higher-order accuracy in space and time have been introduced. For geometrically higher-order accuracy a parametric mapping on a background space-time tensor-product mesh has been used. In this paper, we concentrate on the geometrical accuracy of the approximation and derive rigorous bounds for the distance between the realized and an ideal mapping in different norms and derive results for the space-time regularity of the parametric mapping. These results are important and lay the ground for the error analysis of corresponding unfitted space-time finite element methods.

**Key words.** moving domains, unfitted FEM, level set method, isoparametric FEM, space-time FEM, higher-order FEM

**AMS subject classifications.** 65M60, 65M85, 65D30

**1. Introduction.** Finite element (FE) simulations play an important role in engineering and other computational sciences [6, 20]. In many of those applications, complex geometries are involved. The most straightforward strategy for taking these geometries into account is to generate a mesh following the geometry. For polytopal domains, for instance, a simplicial mesh can be generated in an exact fit with the physical domain. For other domains – imagine for instance a sphere – a polygonal approximation can be meshed and a mapping is applied to curve the boundary elements to arrive at a higher-order accurate domain approximation [10, 4]. In the last two decades, unfitted FEs have been proposed as an alternative approach to solving PDEs on complex domains [8]. The idea here is that the FE simulation is based on a background grid which does not take into account the geometry of the problem. Instead, the geometry is prescribed separately, e.g. implicitly by a level set function  $\phi$ . In that way, the computational task of mesh generation can be avoided, and new questions concerning e.g. numerical quadrature on the implicitly cut elements arise.

By design, the unfitted paradigm becomes particularly attractive for problems involving time-dependent domains, because in that case the mesh must otherwise be carefully transferred or regenerated. We focus on this setting in this article. Our main contribution is the development and mathematical validation of a strategy to provide a computationally feasible and higher-order accurate unfitted geometry description for time-dependent *smooth* domains. This provides a crucial component for unfitted FE simulations, in particular space-time discretisations for bulk- or surface problems. We presented such a bulk space-time FE method for the convection-diffusion problem in [19], whilst a similar method for surface problems have been considered in [35]. The rigorous mathematical error analysis of both methods, which will be the topic of forthcoming papers, heavily exploits the results from this paper. In that way, we split the mathematical analysis between mere geometry considerations, which are considered in this work, and the problem and method-specific analysis sections, which will be treated in separate works.

---

\*Submitted to the editors DATE.

<sup>†</sup>Institut für Numerische und Angewandte Mathematik, Universität Göttingen, (`{f.heimann, lehrenfeld}@math.uni-goettingen.de`).

A crucial distinction is that between second-order and higher-order accurate geometry representations in space on simplicial meshes: For a second-order accurate geometry description, for which the maximal distance between exact and discrete geometry should be of order  $h^2$ , where  $h$  denotes the mesh size, it suffices to generate an elementwise linear interpolant of the level set function and use the implied discrete geometry. This discrete geometry will be a simple polytope on each element, so that integration can be performed easily by tessellation<sup>1</sup> [22]. One option for obtaining a higher-order accurate geometry description suggests improving the quality of the second-order approximation using an isoparametric mapping [23, 29]. In this paper, we want to build on this idea, specifically, the numerical analysis in [29], and extend it to the space-time setting. We have seen numerically in [19] that the generalisation to tensor-product space-time level set representations is feasible. Compared to [19], where this statement is validated by numerical experiments, we provide a rigorous numerical analysis in this paper.

**1.1. Approaches in the literature.** We would like to relate our methods to the literature on *unfitted* discretisations.

First, the issue of numerical integration can be numerically solved with special integration techniques, cf. e.g. [36, 14]. To our best knowledge, whilst the methods make reasonable approximations of relevant quantities, their well-functioning has not yet been mathematically analysed rigorously. Some of these methods come with other restrictions such as quadrilateral (or hexahedral) elements or the necessity of local refinements within one element, which can potentially be computationally expensive for high-order accuracy demands. Similar integration strategies are also applied in other approaches in the literature. In particular, in [3], a variant space-time method exploiting cell agglomeration is presented and analysed. The cell-agglomeration technique is an alternative to the so-called Ghost-penalty stabilisation which is often used in methods such as [19]. Apart from these different strategies to ensure stability in the presence of small cuts, the method analysis in [3] does not take into account the inexactness of discrete geometries. We aim to follow the numerical implementation more closely in the sense of taking into account the discrete geometry in the detailed numerical analysis. We note that for the DG-in-time method of [19], an analysis assuming the exact handling of geometries has also been presented in [33], and an analysis involving a semi-discrete geometry in [17].

Further applications of the unfitted space-time methodology been investigated for an osmotic cell swelling problem in [38], the heat equation on two overlapping meshes in [21], Navier-Stokes equations in [1, 2], two-phase flow problems in [28, 22, 12, 13] and coupled surface-bulk problems in [39, 16].

Apart from the space-time discretisations on which we focus here, time-stepping methods provide an alternative approach to solving the same physical problems. In particular, those methods have been studied for a bulk convection-diffusion problem in low- [26] and high-order [30], the Stokes-like problems [37, 9, 31]. Moreover, Trace-FEM discretisations for surface problems have been studied [27, 5, 32].

**1.2. The spatial case of the unfitted isoparametric FEM.** In this section, we outline the main concepts in the construction and analysis of the isoparametric FEM for the *spatial* setting, as the construction and analysis of the *space-time* version share a similar structure. We refer to [23] and [29] for details on the *spatial* setting.

---

<sup>1</sup>Similar statements also hold for quadrilateral and hexahedral elements based on bi- and trilinear level set representations, see [18].

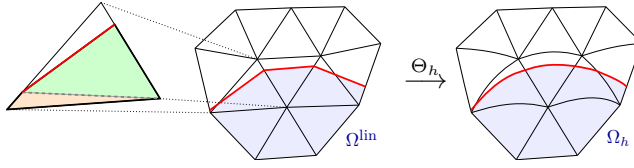


FIG. 1. Sketch of a simple subdivision for quadrature on  $T \cap \Omega^{\text{lin}}$ , the discrete geometry  $\Omega^{\text{lin}}$  and the mapped geometry  $\Omega_h$  obtained from the mapping  $\Theta_h$ . Reproduction from [19].

Assume we want to approximate the potentially complicated physical domain  $\Omega$ , which is embedded in some background domain  $\tilde{\Omega}$  equipped with a simplicial<sup>2</sup> mesh  $\mathcal{T}_h$ ,  $\bigcup_{T \in \mathcal{T}_h} \bar{T} = \tilde{\Omega}$ . Further, assume that a level set function  $\phi(x)$  encodes  $\Omega$  s.t.

$$(1.1) \quad \Omega = \{x \in \tilde{\Omega} \mid \phi(x) < 0\},$$

and that an  $\mathcal{T}_h$ -elementwise linear interpolation of  $\phi$ , denoted by  $\phi^{\text{lin}}$  is given. On

$$(1.2) \quad \Omega^{\text{lin}} := \{x \in \tilde{\Omega} \mid \phi^{\text{lin}}(x) < 0\}$$

the task of numerical integration is computationally feasible as the local polygonal part of  $\Omega^{\text{lin}}$  on each respective  $T \in \mathcal{T}_h$  can be subdivided in few simplices<sup>3</sup>, cf. l.h.s. of Figure 1 for an example. This allows for the construction of high-order accurate quadrature rules on  $\Omega^{\text{lin}}$  with *positive quadrature weights*. The isoparametric mapping now aims at providing a mesh deformation  $\Theta_h: \tilde{\Omega} \rightarrow \tilde{\Omega}$ , such that the image of  $\Omega^{\text{lin}}$  under this mapping is a computationally feasible and higher-order accurate approximation of  $\Omega$ , cf. r.h.s. of Figure 1 for an example.

The construction of this mapping starts with the construction of a theoretical and element-local counterpart of  $\Theta_h$ , i.e. a mapping  $\Psi^\Gamma: \bigcup\{T \in \mathcal{T}_h \mid T \cap \Omega^{\text{lin}} \neq \emptyset\} \rightarrow \tilde{\Omega}$  with the property  $\Psi^\Gamma(\partial\Omega^{\text{lin}}) = \partial\Omega$ . So, the criterion of computational feasibility is neglected for the moment to construct an “ideal” mapping. An appropriate search direction  $G$  is fixed and for all points within a cut element,  $x \in \{T \in \mathcal{T}_h \mid T \cap \Omega^{\text{lin}} \neq \emptyset\}$ ,  $\Psi^\Gamma(x)$  is defined to be the point which is the closest one along the search direction to reproduce the value of  $\phi^{\text{lin}}(x)$  now at  $\phi(\Psi^\Gamma(x))$ . For interpolation results within the isoparametric unfitted FEM exploiting this mapping, the boundedness in relevant norms of the extension of  $\Psi^\Gamma$  onto all of  $\tilde{\Omega}$ , which is called  $\Psi$  will be central. In [29], a FE blending procedure is suggested to arrive at  $\Psi = \mathcal{E}\Psi^\Gamma$ .

In the next step, a discrete FE approximation of the ideal mapping  $\Psi^\Gamma$ , which is called  $\Theta_h^\Gamma$ , is constructed. In practice, to reproduce the values of a higher-order discrete approximation of  $\phi$ , denoted by  $\phi_h$ , a discrete search direction  $G_h$  replaces the search direction  $G$  and a subsequent application of an Oswald-type interpolator is used to obtain inter-element continuity. Finally,  $\Theta_h^\Gamma$  is extended with the same blending procedure to yield  $\Theta_h := \mathcal{E}\Theta_h^\Gamma$ .

The desired result that the so-constructed discrete approximation is of higher-order is stated and proven in this framework as a small difference between  $\Psi$  and  $\Theta_h$ . In order to be able to include these results in a Strang-Lemma-type analysis of a particular discretisation of a PDE problem (in the case of [29] a two-domain Poisson problem is considered, in the case of [24] a fictitious domain problem and in

<sup>2</sup>We restrict to simplicial meshes for ease of presentation. Extensions to quadrilateral and hexahedral meshes, following [18], are however easily possible.

<sup>3</sup>The detailed distinction of cases for 2d and 3d is not complicated, but too long to be given in detail here. We refer the reader to [22].

[15] a surface Poisson problem), the mapping  $\Phi_h$  is defined as  $\Phi_h := \Psi \circ (\Theta_h)^{-1}$  and bounded close to the identity. Overall, the following three components are crucial for the success of the approach (in the spatial setting as well as in the *space-time* setting):

- *Robust quadrature rules* based on positive quadrature weights on  $\Omega^{\text{lin}}$ .
- *Geometrical accuracy*, i.e. higher-order bounds on  $\|\Phi_h - \text{id}\|$  in relevant norms.
- *Approximability of sufficiently smooth functions on deformed meshes*, which is transferred from standard interpolation results of the uncurved mesh  $\mathcal{T}_h$  if sufficiently high spatial derivatives of  $\Psi$  stay uniformly bounded.

**1.3. Structure of the paper.** For the *space-time* setting, the space-time mesh and the level set representation will be based on a tensor-product time-slab structure and numerical integration will be based on (carefully adjusted) iterated integrals over linear-in-space level set domains with an additional parametric space-time mesh deformation. In this setting, we want to essentially reproduce the aforementioned results for the spatial setting. Here, the interplay of temporal and spatial errors plays a crucial role and we aim for high-order error bounds under mild conditions on the anisotropy of space and time resolution. To this end, this paper is structured as follows<sup>4</sup>:

In [section 2](#), we introduce how the unfitted geometry in space-time is described by a level set function and the assumptions considered for the analysis. In [section 3](#), we introduce the ideal *space-time* mapping in the vicinity of the domain boundary, which means we construct the space-time mapping  $\Psi^\Gamma(x, t)$  and show relevant properties.

In [sections 4 to 6](#) we then construct mappings on the same part of the computational mesh that are discrete only in time, in space-time or only in space, respectively and show the proximity of these mappings to  $\Psi^\Gamma$  and one another in relevant norms. A discrete-in-time mapping is firstly introduced in [section 4](#) as a preparation for the definition of the fully discrete mapping on cut elements in [section 5](#). Another semi-discrete mapping, now discrete in space, is then introduced in [section 6](#). This mapping is needed in the analysis to preserve the usefulness of some error bounds on anisotropic space-time meshes with  $\Delta t \ll h$ .

In the subsequent [section 7](#), the extension of the ideal and the fully discrete mappings is discussed. Then, we elaborate on space-time interpolation based on the deformed meshes in [section 8](#). Finally, we end the paper with some numerical experiments in [section 9](#) and a conclusion in [section 10](#).

Several proofs that are tedious, but elementary or similar to other proofs presented in the main part or other literature are deferred to [Appendices A and B](#).

## 2. The space-time level set geometry description.

**2.1. The space-time geometry and some basic notation.** We assume that the space-time geometry  $Q$  of interest describes a time-dependent domain on a time interval  $[0, T]$ ,  $Q = \bigcup_{t \in [0, T]} \Omega(t) \times \{t\}$ . We assume that  $\Omega(t)$  is embedded into a sufficiently large spatial background domain  $\tilde{\Omega} \subseteq \mathbb{R}^d$ ,  $d = 1, 2, 3$ , for all  $t \in [0, T]$  so that  $Q \subset \tilde{\Omega} \times [0, T]$ . For the spatial boundary of the space-time domain, we introduce the symbol  $\partial^s$ , so that  $\partial^s Q := \bigcup_{t \in [0, T]} \partial\Omega(t) \times \{t\}$  is the spatial boundary of the space-time domain. We further assume that there is  $d_\Omega > 0$  so that  $\text{dist}(\partial\tilde{\Omega}, \partial\Omega(t)) > d_\Omega$  for all  $t \in [0, T]$ . On the space-time domains, we use differential operators,

<sup>4</sup>In this work a large number of symbols and definitions need to be handled by the reader. To facilitate backtracking, we have introduced hyperlinks to the respective definitions and symbols. These hyperlinks are marked in green and can be used to conveniently find the respective definitions.

e.g. the gradient operator  $\nabla$  or the general derivative operator  $D$ , for the *spatial* operations and use the notation  $\partial_t$  for the time derivative. On rare occasions we will also use the full space-time derivative which we denote by  $D_{\mathbf{x},t}$ . While gradients  $\nabla$  of scalars are understood as column vectors, for vector-valued functions, the gradient  $\nabla$  is understood as the row-wise gradient.

For the spatial identity operator we use the symbol  $\text{id}_x : \mathbb{R}^{d+1} \rightarrow \mathbb{R}^d$  and for the spatial identity matrix  $\text{Id}_x = \nabla \text{id}_x \in \mathbb{R}^{d \times d}$ . For the corresponding space-time versions we use  $\text{id}_{x,t} : \mathbb{R}^{d+1} \rightarrow \mathbb{R}^{d+1}$  and  $\text{Id}_{x,t} \in \mathbb{R}^{(d+1) \times (d+1)}$

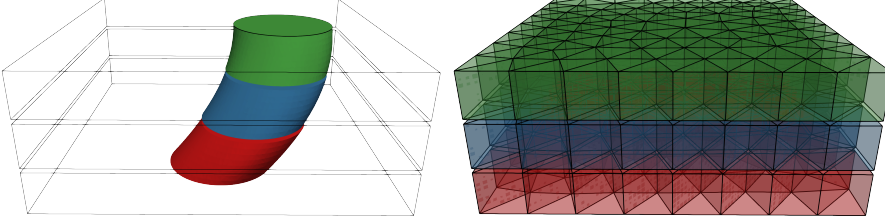


FIG. 2. Illustration of the space-time geometry obtained from a circle moving in a square background domain. The left figure shows the space-time domain  $Q$  embedded in a set of three time slabs, and the right figure shows the tensor-product background space-time mesh of three time slabs.

Let the time interval  $[0, T]$  be further subdivided into  $N$  (not necessarily equally spaced) time slices  $I_n := (t_{n-1}, t_n]$ ,  $n = 1, \dots, N$ ,  $t_0 = 0, t_N = T$  and let us assume a simplicial shape regular triangulation  $\mathcal{T}_h$  of  $\tilde{\Omega}$  to be given that is time-independent on each time interval  $I$ . Then, from  $\mathcal{T}_h$  and a time interval  $I_n$  we automatically obtain a tensor-product triangulation of the space-time domain, denoted by  $\mathcal{Q}_h^n$ , see Figure 2 for an illustration.

For geometry description and approximation, time intervals can be treated independently. Hence, we will fix one time interval  $I_n$  for our considerations in the following. However, to reflect the origin of the time interval as a time-stepping related object, we denote its length as  $\Delta t = t_n - t_{n-1} = |I_n|$ . We define the corresponding part of the space-time geometry as  $Q^n := Q \cap \tilde{Q}^n$  with the space-time background domain  $\tilde{Q}^n := \tilde{\Omega} \times I_n$ . For the spatial resolution, we define the mesh size  $h = \max_{T \in \mathcal{T}_h} h_T$  with the local mesh size  $h_T = \text{diam}(T)$ ,  $T \in \mathcal{T}_h$ .

On the tensor product background space-time mesh, we introduce the following FE space of continuous piecewise polynomials of order  $k_s$  in space and  $k_t$  in time:

$$(2.1) \quad V_h^{k_s, k_t} := W_h^{k_s} \otimes \mathcal{P}^{k_t}(I_n) \text{ with } W_h^{k_s} := \{v \in H^1(\tilde{\Omega}) \mid v|_T \in \mathcal{P}^{k_s}(T) \forall T \in \mathcal{T}_h\}.$$

where  $H^1$  denotes the usual (spatial) Sobolev space and  $\mathcal{P}^{k_t}(I_n) = \mathcal{P}^{k_t}(I_n; \mathbb{R})$  is the space of polynomials up to degree  $k_t$  on  $I_n$ . Analogously we define  $V_h^{k_s, k_t}(\mathcal{Q}_h^{\text{sub}})$  for a tensor-product sub-mesh  $\mathcal{Q}_h^{\text{sub}}$  built from the spatial sub-mesh  $\mathcal{T}_h^{\text{sub}}$  of  $\Omega^{\text{sub}}$  and  $I_n$  by replacing  $\tilde{\Omega}$  by the corresponding spatial domain  $\Omega^{\text{sub}}$ .

In the following we use  $\lesssim$  and  $\gtrsim$  to denote inequalities up to constants that are independent of the mesh size  $h$ , the time step size  $\Delta t$  and the cut configuration, i.e. the position of  $Q^n$  in the mesh. We use  $\simeq$  to imply  $\lesssim$  and  $\gtrsim$  simultaneously.

For the forthcoming analysis we are interested in the asymptotic behavior of the error in the space-time geometry approximation. We will therefore assume at several places that the mesh size  $h$  and the time step size  $\Delta t$  are *sufficiently small* without an explicit specification of the respective constants.

**2.2. The space-time level set description.** Crucial for the remainder of this work is the way that we assume the domain to be described by: Through a level

set function. The space-time levelset function  $\phi$  is defined on  $\tilde{Q}^n$  and its zero level set describes the space-time geometry. We will require some smoothness of  $\phi$  in the vicinity of its spatial boundary. For the neighborhood of the spatial boundary we first introduce a spatial neighborhood of size  $d_U > 0$  for a fixed time  $t \in I_n$  by  $U_s(t) := \{x \in \tilde{\Omega} \mid \text{dist}(x, \partial\Omega(t)) < d_U\}$ . A corresponding space-time neighborhood is obtained as  $U := \bigcup_{t \in I_n} U_s(t) \times \{t\}$ .

The upcoming discretisation will be controlled by two order parameters,  $q_s$  for the spatial and  $q_t$  for temporal order. We assume that  $\phi$  is sufficiently smooth in  $U$  and formulate the following assumption:

*Assumption 2.1.* There exists a function  $\phi \in C^0(\tilde{Q}^n; \mathbb{R})$  s.t.

$$(2.2) \quad \Omega(t) = \{x \in \tilde{\Omega} \mid \phi(x, t) < 0\}, \quad Q^n = \{(x, t) \in \tilde{Q}^n \mid \phi(x, t) < 0\},$$

which satisfies the following regularity assumptions on a neighbourhood  $U$  of  $\partial^s Q^n$  with a fixed  $d_U > 0$ :

$$(2.3\text{-}\phi\text{bnd}) \quad c_{\nabla\phi} \leq \|\nabla\phi\|_{\infty, U} \leq C_{\nabla\phi}, \quad \|\partial_t\phi\|_{\infty, U}, \|D^2\phi\|_{\infty, U}, \|\partial_t\nabla\phi\|_{\infty, U} \lesssim 1.$$

Moreover, the levelset function at each time  $t \in I_n$  fulfils a weak signed distance property:

$$(2.4\text{-}\phi\text{wsd}) \quad |\phi(x + \epsilon\nabla\phi(x), t) - \phi(x + \tilde{\epsilon}\nabla\phi(x), t)| \simeq |\epsilon - \tilde{\epsilon}| \quad \text{for } x \in U(t).$$

**DEFINITION 2.2.** We define the regularity index  $\ell_\phi$  of  $\phi$  as the largest integer value (or infinity) for which  $\phi \in C^0(\tilde{\Omega}) \cap C^2(U) \cap C^{\ell_\phi}(Q_h^U)$ .

We note that the simultaneous space-time regularity assumption could be weakened to a separate regularity assumption in space and time. However, this would complicate the analysis further and we therefore opt for the stronger variant here. We make the following assumption on the regularity index  $\ell_\phi$  of  $\phi$ :

*Assumption 2.3.*  $\ell_\phi \geq \max\{q_s, q_t\} + 2$ .

Note that the smoothness of  $\phi$  in  $U$  (together with (2.3- $\phi\text{bnd}$ )) implies a corresponding smoothness of  $\partial^s Q^n \in C^{\ell_\phi}$  and  $\partial\Omega(t)$ ,  $t \in I_n$ , respectively. Further, we note that with **Assumption 2.1** all (space-time) elements that are intersected by  $\partial^s Q^n$  and a finite number of neighbor elements can be guaranteed to lie within  $U$  for sufficiently small  $h$  and  $\Delta t$ . Let  $\mathcal{T}_h^U$  be the submesh of elements that are contained in  $U$  for all times  $t \in I_n$ , i.e.  $T \times I_n \subset U$  for all  $T \in \mathcal{T}_h^U$ . We denote the spatial domain corresponding to  $\mathcal{T}_h^U$  as  $\bar{U}$  and the set of space-time elements as  $\mathcal{Q}_h^U = \{T \times I_n \mid T \in \mathcal{T}_h^U\}$  with corresponding space-time domain  $Q_h^U$ .

**2.3. Discrete level set functions.** In practice, we will typically not have access to the exact level set function  $\phi$  but only to a discrete approximation. We assume that we are given a discrete level set approximation  $\phi_h \in V_h^{q_s, q_t}$  of  $\phi$  with  $q_s, q_t \in \mathbb{N}$  and that the following approximation assumption holds.

*Assumption 2.4.* For  $(m_s, m_t) \in \{0, \dots, q_s + 1\} \times \{0, 1\} \cup \{0\} \times \{0, \dots, q_t + 1\}$

$$(2.5\text{-}\phi_h\text{acc}) \quad \|\tilde{D}^{m_s} \partial_t^{m_t}(\phi - \phi_h)\|_{\infty, \mathcal{Q}_h^U} \lesssim h^{q_s+1-m_s} + \Delta t^{q_t+1-m_t}.$$

Note that with the regularity assumption in **Assumption 2.3**, we have  $m_s \leq q_s + 1 \leq \ell_\phi$  and  $m_t \leq q_t + 1 \leq \ell_\phi$  in **Assumption 2.4** so that it would hold for  $\phi_h$  being a suitable interpolation operator.



In the upcoming analysis we will make use of the tensor product structure of the FE space  $V_h^{q_s, q_t}$  and we assume a *nodal* basis  $\{\ell_i\}$  of  $\mathcal{P}^{q_t}(I_n)$  with nodes  $\{t_i\}$  so that  $\ell_j(t_i) = \delta_{ij}$ . We further define with  $I_{q_t}^t$  the temporal (nodal) interpolation operator applied in space-time, i.e.  $I_{q_t}^t : v(x, t) \mapsto \sum_{i=0}^{q_t} \ell_i(t)v(x, t_i)$ . We can hence develop  $\phi_h \in V_h^{q_s, q_t}$  in terms of spatial functions  $\phi_{h,i}(x, t) = \phi_h(x, t_i) \in W_h^{q_s}$  and have

$$(2.6) \quad \phi_h(x, t) = \sum_{i=0}^{q_t} \ell_i(t) \phi_{h,i}(x),$$

Note that we specifically opted for a nodal basis in time here. More general options would also be possible but would complicate the notation and analysis slightly. For notational consistency we also introduce  $\phi_i(x) = \phi(x, t_i)$ .

Next, we will assume the existence of two semi-discrete versions of  $\phi$  which have tensor product form and are only discrete in time and continuous in space or vice versa. These semi-discrete versions will be crucial for the construction of semi-discrete mappings in sections 4 and 6 that are needed to obtain robustness in the error bounds w.r.t. anisotropy in space and time.

*Assumption 2.5.* We assume that there is  $\phi_{\Delta t} \in \mathcal{P}^{q_t}(I_n; C^0(\tilde{\Omega}) \cap C^{q_s+1}(\mathcal{T}_h^U))$  with  $\phi_{\Delta t, i} := \phi_{\Delta t}(\cdot, t_i)$  s.t. for  $m_s = 0, \dots, q_s + 1$  there holds

$$(2.7a-\phi_{\Delta t|h, i}) \quad \|D^{m_s}(\phi_{\Delta t, i} - \phi_{h, i})\|_{\infty, \mathcal{T}_h^U} \lesssim h^{q_s+1-m_s}, \text{ which implies}$$

$$(2.7b-\phi_{\Delta t|h}) \quad \|D^{m_s}(\phi_{\Delta t} - \phi_h)\|_{\infty, \mathcal{Q}_h^U} \lesssim h^{q_s+1-m_s}, \text{ and}$$

$$(2.7c-\phi_{\Delta t \text{ acc}}) \quad \|D^{m_s}(\phi_{\Delta t} - \phi)\|_{\infty, \mathcal{Q}_h^U} \lesssim h^{q_s+1-m_s} + \Delta t^{q_t+1}.$$

*Assumption 2.6.* We assume that there is  $\phi_H \in C^{q_t+1}(I_n; W_h^{q_s})$  s.t. for  $m_t = 0, \dots, q_t + 1$  and  $m_s \in \{0, 1\}$  there holds

$$(2.8a-\phi_H|h) \quad \|\partial_t^{m_t}(\phi_H - \phi_h)\|_{\infty, \mathcal{Q}_h^U} \lesssim \Delta t^{q_t+1-m_t}, \text{ and}$$

$$(2.8b-\phi_H \text{ acc}) \quad \|D^{m_s} \partial_t^{m_t}(\phi_H - \phi)\|_{\infty, \mathcal{Q}_h^U} \lesssim h^{q_s+1-m_s} + \Delta t^{q_t+1-m_t}.$$

*Remark 2.7.* The previous assumptions are reasonable if  $\phi_h$  stems from a discretisation with separable temporal and spatial errors. Let us consider the simplest case where  $\phi_h$  is obtained from a tensor-product space-time interpolation,  $\phi_h = I^t I^s \phi$  with  $I^s$  a corresponding spatial interpolation operator. Then, we can set  $\phi_H = I^s \phi$  and  $\phi_{\Delta t} = I^t \phi$  and obtain the desired properties from continuity and the respective approximation properties of  $I^t$  and  $I^s$ , respectively. [Assumption 2.6](#) will explicitly be mentioned when used and corresponding weaker statements will be given in parallel for the case that the assumptions are not available.

We note that for sufficiently small  $h$  and  $\Delta t$  the weak signed distance property from [\(2.4- \$\phi\_{\text{wsd}}\$ \)](#) of  $\phi$  carries over to  $\bar{\phi} \in \{\phi_{\Delta t}, \phi_H, \phi_h\}$ :

$$(2.9-\phi_h \text{ wsd}) \quad |\bar{\phi}(x + \epsilon \nabla \bar{\phi}(x), t) - \bar{\phi}(x + \tilde{\epsilon} \nabla \bar{\phi}(x), t)| \simeq |\epsilon - \tilde{\epsilon}| \quad \text{for } x \in U(t).$$

**2.4. The reference geometry based on  $\phi^{\text{lin}}$ .** Dealing with piecewise higher-order polynomial level set functions is difficult in the context of robust numerical integration, cf. [subsection 1.1](#). This is why we introduce a reference geometry based on a linear approximation of  $\phi$  in space in the spirit of the spatial isoparametric FEM, cf. [subsection 1.2](#). For the function  $\phi_h \in V_h^{q_s, q_t}$ , we define the spatial piecewise linear

nodal interpolation:

$$(2.10) \quad \phi^{\text{lin}}(x, t) := (I_h^1 \phi_h(\cdot, t))(x) \stackrel{(2.6)}{=} \sum_{i=0}^{q_t} \ell_i(t) (I_h^1 \phi_{h,i}(x)) =: \sum_{i=0}^{q_t} \ell_i(t) \phi_i^{\text{lin}}(x),$$

where  $I_h^1 : C^0(\Omega) \rightarrow W_h^1$  denotes the spatial nodal interpolation operator. This implies

COROLLARY 2.8. *It holds for  $m = 0, 1$*

$$(2.11\text{-}\phi_{1\text{in}}|_h \text{acc}) \quad \|D^m(\phi_h - \phi^{\text{lin}})\|_{\infty, \mathcal{Q}_h^U} \lesssim h^{2-m}.$$

Also, the time derivative of  $\phi^{\text{lin}}$  is also (at each time) the spatial interpolation of  $\partial_t \phi_h$ :

$$(2.12) \quad (I_h^1 \partial_t \phi_h(\cdot, t))(x) = \sum_{i=0}^{q_t} (\partial_t \ell_i(t)) (I_h^1 \phi_{h,i}(x)) = \sum_{i=0}^{q_t} (\partial_t \ell_i(t)) \phi_i^{\text{lin}}(x) = \partial_t \phi^{\text{lin}}(x, t).$$

The same holds for the time derivatives of the gradients of  $\phi_h$  and  $\phi^{\text{lin}}$ . These results imply together with Assumption 2.4 the following result.

COROLLARY 2.9. *It holds for  $\bar{\phi} \in \{\phi_h, \phi_{\Delta t}\}$ ,  $m_s = 0, 1$  and  $m_t = 0, \dots, q_t + 1$ ,*

$$(2.13\text{a-}\phi^{\text{lin}} \text{acc}) \quad \|D^{m_s} \partial_t^{m_t} (\bar{\phi} - \phi^{\text{lin}})\|_{\infty, \mathcal{Q}_h^U} \lesssim h^{2-m_s},$$

$$(2.13\text{b-}\phi^{\text{lin}} \text{acc}) \quad \|D^{m_s} \partial_t^{m_t} (\phi - \phi^{\text{lin}})\|_{\infty, \mathcal{Q}_h^U} \lesssim h^{2-m_s} + \Delta t^{q_t+1-m_t}.$$

The function  $\phi^{\text{lin}}$  induces the linear (in space) domains

$$(2.14) \quad \Omega^{\text{lin}}(t) := \{x \in \tilde{\Omega} \mid \phi^{\text{lin}}(x, t) < 0\}, \text{ and } Q^{\text{lin}} := \bigcup_{t \in I_n} \Omega^{\text{lin}}(t) \times \{t\}.$$

We are now in a similar setting as for the merely spatial unfitted isoparametric FEM approach. We have a reference configuration with  $Q^{\text{lin}}$  of lower order accuracy (in space) described by  $\phi^{\text{lin}}$  and a higher-order accurate description with  $\phi_h$  which is however not directly suitable for numerical integration.

**2.5. A blending from cut to uncut elements.** For the construction of a mapping from  $Q^{\text{lin}}$  that approximates  $Q^n$  with higher-order accuracy we need to find a mapping  $\Theta_h^\Gamma$  that maps the spatial boundary  $\partial^s Q^{\text{lin}}$  close to  $\partial^s Q^n$ , and relatedly a mapping  $\Psi^\Gamma$ , mapping  $\partial^s Q^{\text{lin}}$  exactly onto  $\partial^s Q^n$ . Eventually, however, these mappings should be defined on the whole space-time slab  $\tilde{Q}^n$ . We will consider two different approaches for the construction and extension of the mapping for which we distinguish the choice of a triple  $(\mathcal{T}_h^\Gamma, \Omega^\Gamma, b)$ , where  $\mathcal{T}_h^\Gamma$  is a submesh of  $\mathcal{T}_h^U$  of *active elements*,  $\Omega^\Gamma$  is the corresponding domain and  $b : \tilde{Q}^n \rightarrow [0, 1]$  is a blending function. Corresponding to  $\mathcal{T}_h^\Gamma$  we further introduce the space-time submesh of active elements  $\mathcal{Q}_h^\Gamma := \bigcup_{T \in \mathcal{T}_h^\Gamma} T \times I_n$  and  $Q_h^\Gamma := \Omega^\Gamma \times I_n$  as the corresponding space-time domain. For notational convenience we define according to  $b(x, t)$  the time restrictions to  $t_i$  by  $b_i(x) := b(x, t_i)$  for  $i = 0, \dots, q_t$ .

1. In a first approach – the *FE blending* – we consider all space-time cut elements as  $\mathcal{T}_h^\Gamma$  and construct in a first step  $\Psi^\Gamma$  and  $\Theta_h^\Gamma$  within this cut region. Afterwards, in a second step, we will use a *FE blending* which is a continuous extension which vanishes within an  $\mathcal{O}(h)$  layer of one element from the cut elements in order to obtain  $\Psi = \mathcal{E}\Psi^\Gamma$ ,  $\Theta_h = \mathcal{E}\Theta_h^\Gamma$ .



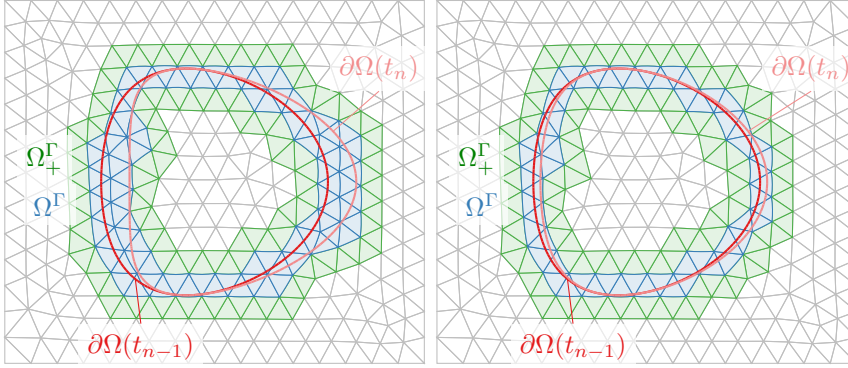


FIG. 3. Illustration of the discrete regions involved in the FE blending construction. We sketch the situation of a large (left) and small (right) time step. The solid and transparent red lines indicate the discrete interface at the beginning and end of the time step, respectively. The blue elements indicate the active mesh as it relates to the blending construction,  $\mathcal{T}_{b_1}^\Gamma$ . The green elements indicate the additional adjacent elements where the FE blending will operate.

2. In the second approach – the *smooth blending* – we use a smooth function in the construction of the mapping to transition between region where the mapping takes full effect to regions where the mapping is the identity. To accommodate for this, a wider stripe of elements than merely the cut elements is chosen for  $\mathcal{T}_h^\Gamma$  and the mappings  $\Psi^\Gamma$  and  $\Theta_h^\Gamma$  are constructed in the same way as in the first step of the FE blending. Then, the second step of extension becomes almost trivial as outside of  $\mathcal{T}_h^\Gamma$  the functions are set to identity.

We will unify the analysis of both cases by introducing two steps: The construction of a mapping on an *active set of elements* and a FE extension. In the case of the FE blending the active set of elements is merely the set of cut space-time elements while in the second case it is the set of space-time elements where the scalar blending function is smaller one. Note that in both cases for sufficiently small  $h$  the set of active elements lies within  $\mathcal{T}_h^U$  and hence within  $\bar{U}$ .

After defining a mapping on the active set of elements the FE extension is applied which however becomes trivial in the case of the smooth blending as the mapping will be the trivial mapping on the boundary of the *active* set of elements already.

*Remark 2.10* (Problems purely posed on space-time cut elements). If problems are to be solved only on the space-time cut elements as it is the case for surface PDEs when treated with TraceFEM approaches, problems with blendings vanish and the FE blending is a very natural (and simpler) choice. Furthermore, the additional more restrictive assumptions that we will introduce for the FE blending would not be needed for proper mappings only on the space-time cut elements.

**2.5.1. Finite element blending.** For the *FE blending* only cut space-time elements, respectively their spatial counterparts, become *active*. For the time slice under consideration,  $I_n$ , the set of *active* elements is

$$(2.15) \quad \mathcal{T}_{b_1}^\Gamma := \{T \in \mathcal{T}_h \mid \exists t \in I_n \partial\Omega^{\text{lin}}(t) \cap T \neq \emptyset\}, \quad \Omega_{b_1}^\Gamma = \bigcup \mathcal{T}_{b_1}^\Gamma.$$

We give an illustration for this active domain for two time step choices in Figure 3. We also show the domain of adjacent elements, which is the domain where the FE blending will decay. (More details about this will be given in section 7.)

For the blending function we set  $b_1(x, t) \equiv 0$  and obtain the triple  $(\mathcal{T}_h^\Gamma, \Omega^\Gamma, b) = (\mathcal{T}_{b_1}^\Gamma, \Omega_{b_1}^\Gamma, b_1)$ . This blending approach has also been discussed in [19]. It however

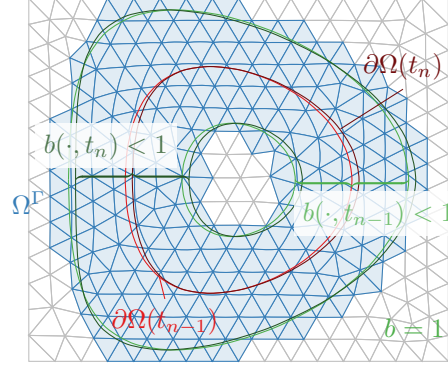


FIG. 4. Illustration of the discrete domain induced by a smooth blending function  $b$ . The surface is shown in red for the beginning and the end of a time step  $I_n$ . At the surface and the neighboring elements,  $b = 0$ . Away from the surface, the value of  $b$  increases until the green lines, where  $b = 1$  (dashed lines for  $b = 1$  at the end of the time step). The resulting region  $\Omega^\Gamma$ , constructed in line with [Assumption 2.13](#), is shown in blue. Compare with [Figure 7](#) for plots of example functions  $b$ .

comes at the price of additional assumptions on the regularity of the level set function and a CFL-type time step restriction which we formulate in the next two assumptions:

*Assumption 2.11.* We assume the additional regularity  $\ell_\phi \geq q_s + q_t + 2$ .

*Assumption 2.12.* We assume the time step restriction  $\Delta t \lesssim h$ .

In the case of the **FE** blending, we assume both assumptions to hold. An alternative that alleviates these restrictions is the *smooth blending* discussed next.

**2.5.2. Smooth blending.** For the second option of the blending, the *smooth blending*, we let the corresponding domains follow from a blending function  $b_2: \tilde{Q}^n \rightarrow [0, 1]$ , which has the properties summarised in the following assumption.

*Assumption 2.13.* In the case of the *smooth blending* we assume that there exists a blending function  $b_2 \in C^{\ell_\phi}(\tilde{Q}^n; [0, 1])$  with width  $w_b \in \mathbb{R}, 0 < w_b < \min\{d_\Omega, d_U\}$  such that

1. On all cut elements,  $b_2$  vanishes,  $b_2(x, t) = 0$  for all  $x \in \Omega_{b_1}^\Gamma, t \in I_n$ .
2. Sufficiently far away from the interface,  $b_2$  takes the value 1: For all  $t \in I_n$ , for all  $x \in \tilde{\Omega}$  such that  $\text{dist}(x, \partial\Omega^{\text{lim}}(t)) > w_b$ , there is  $b_2(x, t) = 1$ .
3.  $\|\partial_t^{m_t} D^{m_s} b_2\|_{\infty, \tilde{Q}^n} \leq C_b$  with  $C_b$  independent of  $h$  and  $\Delta t$ ,  $m_s + m_t \leq \ell_\phi$ .

This allows us to define the following counterparts of  $\mathcal{T}_{b_1}^\Gamma$  and  $\Omega_{b_1}^\Gamma$ :

$$(2.16) \quad \mathcal{T}_{b_2}^\Gamma := \{T \in \mathcal{T}_h \mid \exists t \in I_n \exists x \in T \ b_2(x, t) < 1\}, \quad \Omega_{b_2}^\Gamma := \bigcup \mathcal{T}_{b_2}^\Gamma.$$

For the *smooth blending* we obtain the triple  $(\mathcal{T}_h^\Gamma, \Omega^\Gamma, b) = (\mathcal{T}_{b_2}^\Gamma, \Omega_{b_2}^\Gamma, b_2)$ .

We illustrate the geometric domains for an example case in

Compared to [Assumption 2.12](#) we only require a much milder condition on the smallness of the time-step to ensure the well-posedness of the upcoming constructions:

*Assumption 2.14.* There exists  $\epsilon > 0$  such that

$$(2.17-\Delta t_{\text{bnd}}) \quad \Delta t^{q_t+1} \leq C_{\Delta t-h} h^{1+\epsilon}.$$

Note that this assumption allows for anisotropy in space and time resolution to a large extent. We refer to [Figure 5](#) for an illustration of the restrictions.

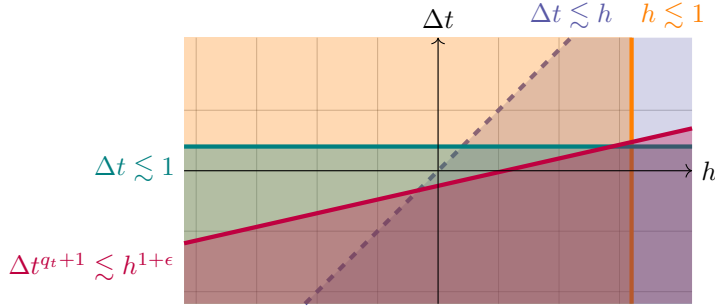


FIG. 5. Illustration of restrictions on time step and mesh size in a double logarithmic plot. The orange area corresponds to the restriction  $\Delta t$  sufficiently small, teal to  $h$  sufficiently small and purple to  $\Delta t^{q_t+1} \lesssim h^{1+\epsilon}$  in Assumption 2.14 and grey to  $\Delta t \lesssim h$  in Assumption 2.12.

*Remark 2.15* (Comparison of blending options). The FE blending causes the mesh deformation to decay within a layer of one element, i.e. width  $\mathcal{O}(h)$ , leading to  $\mathcal{O}(1/h)$  gradients. This restricts the boundedness proofs of the upcoming analysis to space-time refinement strategies with  $\Delta t \lesssim h$ . To allow for a wider range of combinations of space and time refinements, the smooth blending is well-suited as it implies a decay of the mesh deformation on a fixed width, i.e. of order  $\mathcal{O}(1)$ . Further, the FE blending leads to mesh deformations which are discontinuous along time slice boundaries, which necessitates a mesh transfer operation when the geometry is used in a FE simulation, cf. [19]. On the other hand, a continuous-in-time mesh deformation function can be obtained for the smooth blending variant. However, the major disadvantage of the smooth blending function is the larger bandwidth of active elements which scales like  $h^{-d}$  while it scales only with  $h^{1-d}$  for the FE blending.

**3. Construction of ideal mapping on cut elements.** As a first step, we introduce a mapping  $\Psi^\Gamma$  which maps  $Q^{\text{lin}}$  close to  $Q^n$ . Fix some space-time point  $(x, t) \in Q_h^\Gamma$ , we want to match the level set value of  $(1-b(x, t))\phi^{\text{lin}}(x, t) + b(x, t)\phi_h(x, t)$  with the level set value of  $\phi$  at a point  $y \in \tilde{\Omega}$ . For this, we define the (purely spatial) *search direction*  $G(x, t) := \nabla\phi(x, t)$ , and the *distance function*  $d(x, t): \Omega^\Gamma \rightarrow \mathbb{R}$  (this implies  $d: Q_h^\Gamma \rightarrow \mathbb{R}$ ) to be the (in absolute numbers) smallest value s.t.

$$(3.1\text{-ddef}) \quad \phi(x + d(x, t)G(x, t), t) = (1-b(x, t))\phi^{\text{lin}}(x, t) + b(x, t)\phi(x, t) \quad \forall (x, t) \in Q_h^\Gamma.$$

We correspondingly define  $d_i(x) := d(x, t_i)$  and  $G_i(x) := G(x, t_i)$ .

Note that for  $(x, t)$  such that  $b(x, t) = 1$ , the trivial solution is  $d(x, t) = 0$ . On the other side, for  $b(x, t) = 0$ , the condition reduces to

$$\phi(x + d(x, t)G(x, t), t) = \phi^{\text{lin}}(x, t) \quad \text{for all } (x, t) \in Q_h^\Gamma,$$

which is very similar to the construction in [29, Eq. (3.1)] for the merely spatial case. We illustrate this behaviour for a space-time point where  $\phi^{\text{lin}}(x, t) = 0$  and  $b(x, t) = 0$  (this case could be called “full blending”) in Figure 6: Starting from a point  $(x, t)$  with some value of  $\phi^{\text{lin}}(x, t)$ , in this case 0, we calculate the search direction  $G(x, t)$  and move so far along this direction until we obtain the same value in  $\phi(\dots, t)$ .

The function  $d$  has the following fundamental properties:

LEMMA 3.1. For  $h$  and  $\Delta t$  sufficiently small, the relation (3.1-ddef) defines a

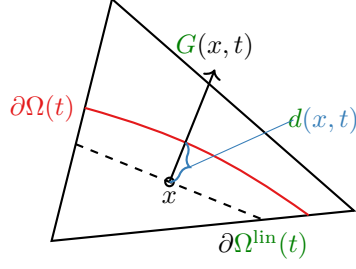


FIG. 6. Illustration of definition of the function  $d$  at a space-time point with  $\phi^{\text{lin}}(x, t) = 0$ .

unique  $d(x, t)$ , and  $d \in C^0(Q_h^\Gamma) \cap C^{\ell_\phi}(Q_h^\Gamma)$ . Furthermore, there holds

$$(3.2a\text{-dbnd}) \quad \|\partial_t^{m_t} D^{m_s} d\|_{\infty, Q_h^\Gamma} \lesssim h^{2-m_s} + \Delta t^{q_t+1-m_t} \text{ for } m_s, m_t \in \{0, 1\},$$

$$(3.2b\text{-dbnd}) \quad \|\partial_t^{m_t} d\|_{\infty, Q_h^\Gamma} \lesssim h^2 + \Delta t^{q_t+1-m_t} \text{ for } m_t \in \{0, \dots, q_t + 1\},$$

$$(3.2c\text{-dbnd}) \quad \|\partial_t^{m_t} D^{m_s} d\|_{\infty, Q_h^\Gamma} \lesssim 1 \text{ for } m_s = 0, \dots, q_s + 1, m_t = 0, \dots, q_t + 1, m_t + m_s \leq \ell_\phi,$$

*Proof.* The proof follows similar ideas as the proof of [29, Lemma 3.1]. Differences originate from the fact that  $\phi^{\text{lin}}$  deviates from  $\phi$  not only by spatial but also temporal errors and that we have to involve the blending function  $b(x, t)$  which was not considered in [29]. Furthermore, with the time-dependence more derivate terms become involved. We treat the proof of some basic properties in the main part and refer to appendices for the more technical proofs.

Well-posedness of  $d$ :

Define for fixed  $\alpha_0 > 0$  on  $\alpha \in [-\alpha_0 h, \alpha_0 h]$  at the point  $(x, t) \in Q_h^\Gamma$  the function

$$(3.3) \quad \begin{aligned} g(\alpha) &:= \phi(x + \alpha G(x, t), t) - (1 - b(x, t))\phi^{\text{lin}}(x, t) - b(x, t)\phi(x, t) \\ &= \phi(x + \alpha G(x, t), t) - \phi^{\text{lin}}(x, t) + b(x, t)(\phi^{\text{lin}}(x, t) - \phi(x, t)). \end{aligned}$$

As  $\phi \in C^{\ell_\phi}(Q_h^U)$ ,  $g \in C^{\ell_\phi}([-\alpha_0 h, \alpha_0 h])$  for  $h \leq h_0$  sufficiently small. This allows us to apply the Taylor series theorem, leading to

$$(3.4) \quad g(\alpha) = g(0) + g'(0)\alpha + 1/2 g''(\xi)\alpha^2 \quad \text{for some } \xi \in [\min\{0, \alpha\}, \max\{0, \alpha\}].$$

Combining (2.5- $\phi_h \text{acc}$ ) from Assumption 2.4 and (2.13b- $\phi^{\text{lin}} \text{acc}$ ) from Corollary 2.8, we obtain at point  $(x, t)$  that  $|g(0)| = |(1 - b)(\phi^{\text{lin}} - \phi)| \lesssim h^2 + \Delta t^{q_t+1} \lesssim h^{1+\epsilon}$  (with (2.17- $\Delta t \text{bnd}$ ) from Assumption 2.14). From the chain rule, we obtain furthermore  $g'(0) = \|\nabla \phi\|_2^2$ . We now claim that there is a unique  $\alpha \in [-\alpha_0 h, \alpha_0 h]$  such that  $g(\alpha) = 0$ . First assume that there are two such  $\alpha$  and denote them as  $\alpha_1$  and  $\alpha_2$ . Then they are equal by (3.3) and (2.4- $\phi \text{wsd}$ ) as at

$$0 = |g(\alpha_1) - g(\alpha_2)| \stackrel{(3.3)}{=} |\phi(x + \alpha_1 G(x, t), t) - \phi(x + \alpha_2 G(x, t), t)| \stackrel{(2.4-\phi \text{wsd})}{\simeq} |\alpha_1 - \alpha_2|.$$

For existence, we see that with (2.3- $\phi \text{bnd}$ ) and  $|g(0)| \leq (\alpha_0 h)^{1+\epsilon}$

$$g(\alpha_0 h) \stackrel{(3.4)}{=} g(0) + \|\nabla \phi\|_2^2 \alpha_0 h + 1/2 g''(\xi) \alpha_0^2 h^2 \geq c_{\nabla \phi}^2 (\alpha_0 h) - c(\alpha_0 h)^{1+\epsilon} - 1/2 (\alpha_0 h)^2$$

and hence  $g(\alpha_0 h) > 0$  for  $h \leq h_0$  sufficiently small and by the same argument,  $g(-\alpha_0 h) < 0$ . Then with the continuity of  $g$  and the intermediate value theorem, we obtain the existence of a root of  $g$ . Hence,  $d(x, t)$  is well defined as this root, has  $|d(x, t)| < \alpha_0 h$  and regularity  $d \in C^{\ell_\phi}(T)$ .

The proof of the estimates in (3.2a-d**bn**d) will be subdivided into the cases  $(m_t, m_s) \in \{\{0,0\}, (0,1), (1,1)\}$  while  $(m_t, m_s) = (1,0)$  will be treated within the proof of (3.2b-d**bn**d).

Proof of (3.2a-d**bn**d) for  $(m_t, m_s) = (0,0)$ :

Writing out the above Taylor expansion for  $g(d(x,t))$ , we obtain

$$(3.5) \quad \begin{aligned} g(d(x,t)) &= 0 = g(0) + \|\nabla\phi\|_2^2 d(x,t) + 1/2 g''(\xi) d^2(x,t) \\ &\Rightarrow d(x,t) \leq \|\nabla\phi\|_2^{-2} (-g(0) + 1/2 |g''(\xi)| (\alpha_0 h)^2) \stackrel{(2.3-\phi\text{bn}d)}{\lesssim} h^2 + \Delta t^{q_t+1}, \end{aligned}$$

With the above estimate on  $|g(0)|$  and the regularity  $\phi \in C^{q_s+q_t+2}(U)$ , the estimate is complete.

Proof of (3.2a-d**bn**d) for  $(m_t, m_s) = (0,1)$ :

Next, we apply the chain rule on (3.1-d**def**). We introduce  $\pi: \tilde{Q}^n \rightarrow \tilde{Q}^n, (x,t)^T \mapsto (x+d(x,t)G(x,t), t)^T$ , such that

$$(3.6-d|\pi) \quad \phi \circ \pi = (1-b)\phi^{\text{lin}} + b\phi = \phi^{\text{lin}} + b(\phi - \phi^{\text{lin}}).$$

For the spatial derivative, we obtain

$$(3.7) \quad \begin{aligned} \overbrace{\nabla\phi^{\text{lin}}(x,t) - \nabla\phi(\pi(x,t))}^{=:A} &= \nabla d \overbrace{G(x,t)^T \nabla\phi(\pi(x,t))}^{=:B} + \overbrace{d \nabla G(x,t)^T \nabla\phi(\pi(x,t))}^{=:C} \\ &+ \overbrace{\nabla b(\phi^{\text{lin}} - \phi)(x,t)}^{=:D} + \overbrace{b(\nabla\phi^{\text{lin}} - \nabla\phi)(x,t)}^{=:E} \end{aligned}$$

For the terms  $A, B, C, D, E$  we obtain the following estimates:

$$(3.8a) \quad A = \underbrace{\nabla\phi^{\text{lin}}(x,t) - \nabla\phi(x,t)}_{\lesssim h + \Delta t^{q_t+1}} + \underbrace{\nabla\phi(x,t) - \nabla\phi(\pi(x,t))}_{\lesssim |d|_{2,\infty,U} d \lesssim h^2 + \Delta t^{q_t+1}} \lesssim h + \Delta t^{q_t+1}.$$

$$(3.8b) \quad B = \|\nabla\phi(x,t)\|_2^2 + G(x,t)^T (\nabla\phi(\pi(x,t)) - \nabla\phi(x,t)) \gtrsim 1 - h^2 - \Delta t^{q_t+1},$$

$$(3.8c) \quad C \lesssim |d| |\phi|_{2,\infty} (1 + h^2 + \Delta t^{q_t+1}) \lesssim h^2 + \Delta t^{q_t+1},$$

$$(3.8d) \quad D \lesssim |b|_{H^1} (h^2 + \Delta t^{q_t+1}) \lesssim h^2 + \Delta t^{q_t+1}, \quad E \lesssim h + \Delta t^{q_t+1}.$$

Overall, this yields  $|\nabla d| \lesssim (h + \Delta t^{q_t+1}) / (1 - h^2 - \Delta t^{q_t+1})$ , which proves (3.2a-d**bn**d) for  $(m_t, m_s) = (0,1)$ .

Proofs of (3.2a-d**bn**d) for  $(m_t, m_s) = (1,1)$ , (3.2b-d**bn**d) and (3.2c-d**bn**d):

Similarly, the proofs of (3.2a-d**bn**d) for  $(m_t, m_s) = (1,1)$ , (3.2b-d**bn**d) for  $m_t \geq 1$  and (3.2c-d**bn**d) rely on (repeated) applications of the chain rule. We give the proofs in Appendices A.1 to A.3.  $\square$

Having introduced the function  $d(x,t)$ , we now define

$$(3.9-\Psi^\Gamma_{\text{def}}) \quad \Psi^\Gamma(x,t) := x + d(x,t)G(x,t) \text{ and } \Psi_i^\Gamma(x) := \Psi^\Gamma(x, t_i), \quad i = 0, \dots, q_t$$

Then, the previous lemma immediately implies with  $G(x,t) = \nabla\phi \in C^1(U) \cap C^{\ell_\phi}(Q_h^U)$  and  $\nabla\phi = \mathcal{O}(1)$  the following results for  $\Psi^\Gamma$ :

COROLLARY 3.2. *There holds*

$$(3.10a-\Psi^\Gamma_{\text{bn}d}) \quad \|\partial_t^{m_t} D^{m_s} (\Psi^\Gamma - \text{id}_x)\|_{\infty, Q_h^\Gamma} \lesssim h^{2-m_s} + \Delta t^{q_t+1-m_t}, \quad m_t, m_s \in \{0,1\},$$

$$(3.10b-\Psi^\Gamma_{\text{bn}d}) \quad \|\partial_t^{m_t} \Psi^\Gamma\|_{\infty, Q_h^\Gamma} \lesssim h^2 + \Delta t^{q_t+1-m_t}, \quad m_t \in \{0, \dots, q_t+1\}$$

$$(3.10c-\Psi^\Gamma_{\text{bn}d}) \quad \|D^{m_s} \partial_t^{m_t} \Psi^\Gamma\|_{\infty, Q_h^\Gamma} \lesssim 1, \quad m_s \leq q_s+1, m_t \leq q_t+1, m_t+m_s \leq \ell_\phi.$$

**4. Construction of discrete-in-time mapping on cut elements.** Before we turn to the realisable mapping in [section 5](#) we introduce a semi-discrete mapping  $\Psi_{\Delta t}^\Gamma$  on the active domain elements based on the semi-discrete level set approximations  $\phi_{\Delta t}$ .

We start with a mapping that is discrete in time based on the ansatz  $\Psi_{\Delta t}^\Gamma = \sum_{i=0}^{q_t} \ell_i(t) \Psi_{\Delta t,i}^\Gamma(x)$ . In analogy to [\(3.1-ddef\)](#), we use the *search direction*  $G_{\Delta t,i}(x) := \nabla \phi_{\Delta t}(x, t_i)$  and the *distance functions*  $d_{\Delta t,i}: \Omega^\Gamma \rightarrow \mathbb{R}$  which is defined to be the (in absolute numbers) smallest value s.t.

$$(4.1-d_{\Delta t,i} \text{def}) \quad \phi_{\Delta t,i}(x + d_{\Delta t,i} G_{\Delta t,i}) = (1 - b_i(x)) \phi_i^{\text{lin}}(x) + b_i(x) \phi_{\Delta t,i}(x) \quad \forall x \in \Omega^\Gamma.$$

We then define  $\Psi_{\Delta t,i}^\Gamma(x) := x + (d_{\Delta t,i} G_{\Delta t,i})(x)$  and thereby  $\Psi_{\Delta t}^\Gamma := \sum_{i=0}^{q_t} \ell_i(t) \Psi_{\Delta t,i}^\Gamma(x)$ . The following bounds on  $d_{\Delta t,i}$  and  $\Psi_{\Delta t,i}^\Gamma$ , for  $i = 0, \dots, q_t$  are the analogs of [Lemma 3.1](#) and [Corollary 3.2](#) restricted to  $t_i$  and right-hand side terms that are independent of  $\Delta t$ .

LEMMA 4.1. *For  $h$  sufficiently small, the relation [\(4.1-d\\_{\Delta t,i} def\)](#) defines unique functions  $d_{\Delta t,i}(x)$  and  $d_{\Delta t,i} \in C^0(\Omega^\Gamma) \cap C^{q_s+1}(\mathcal{T}_h^\Gamma)$ . Furthermore, there holds*

$$(4.2-d_{\Delta t} \text{bnd}) \quad \|D^{m_s} d_{\Delta t,i}\|_{\infty, \mathcal{T}_h^\Gamma} \lesssim \min\{1, h^{2-m_s}\} \quad \text{for } m_s \leq q_s + 1.$$

which implies  $\Psi_{\Delta t}^\Gamma \in C(Q_h^\Gamma)$  and

$$(4.3-\Psi_{\Delta t}^\Gamma \text{bnd}) \quad \|D^{m_s}(\Psi_{\Delta t}^\Gamma - \text{id}_x)\|_{\infty, \mathcal{Q}_h^\Gamma} \lesssim \min\{1, h^{2-m_s}\} \quad \text{for } m_s \leq q_s + 1.$$

*Proof.* The proof follows along the same lines as the proof of [Lemma 3.1](#). There, the r.h.s. bounds at the end are all reduced to the error terms  $\phi^{\text{lin}} - \phi$  and derivatives thereof. In the present case, we have to replace  $\phi^{\text{lin}} - \phi$  by  $\phi_i^{\text{lin}} - \phi_{\Delta t,i}$  (and derivatives thereof) so that with [\(2.13a-phi^{lin} acc\)](#) we can drop the dependency on the time step size and obtain the desired result.  $\square$

LEMMA 4.2. *There holds*

$$(4.4-\Psi_{\Delta t} \text{acc-a}) \quad \|\Psi_{\Delta t}^\Gamma - \Psi^\Gamma\|_{\infty, \mathcal{Q}_h^\Gamma} \lesssim h^{q_s+1} + \Delta t^{q_t+1}$$

$$(4.4-\Psi_{\Delta t}^\Gamma \text{acc-b}) \quad \|\nabla(\Psi_{\Delta t}^\Gamma - \Psi^\Gamma)\|_{\infty, \mathcal{Q}_h^\Gamma} \lesssim h^{q_s} + \Delta t^{q_t+1}$$

*Proof.* First, we note that with [\(3.10c-Psi^Gamma bnd\)](#) we have  $\|\Psi^\Gamma - I_{q_t}^t \Psi^\Gamma\|_{\infty, \mathcal{Q}_h^\Gamma} \lesssim \Delta t^{q_t+1}$ . Hence, it suffices to prove [\(4.4-Psi\\_{\Delta t} \text{acc-a}\)](#) and [\(4.4-Psi\\_{\Delta t}^\Gamma \text{acc-b}\)](#) at the nodes  $t_i$ .

Proof of [\(4.4-Psi\\_{\Delta t} \text{acc-a}\)](#) at  $t_i$ ,  $\|\Psi_{\Delta t,i}^\Gamma - \Psi_i^\Gamma\|_{\infty, \Omega^\Gamma} \lesssim h^{q_s+1} + \Delta t^{q_t+1}$  :

We have for  $x \in \Omega^\Gamma$  (we will drop the argument for  $d_i, d_{\Delta t,i}, G_i, G_{\Delta t,i}$  and  $b_i$  in the following chain of equations, so that e.g.  $G_i = G_i(x)$ )

$$(4.5) |d_i - d_{\Delta t,i}| \stackrel{(2.4-\phi \text{wsd})}{\simeq} |\phi_i(x + d_i G_i) - \phi_i(x + d_{\Delta t,i} G_i)| \\ \lesssim |\phi_i(x + d_i G_i) - \phi_i(x + d_{\Delta t,i} G_{\Delta t,i})| + |\phi_i(x + d_{\Delta t,i} G_{\Delta t,i}) - \phi_i(x + d_{\Delta t,i} G_i)| \\ \stackrel{(3.1-ddef) \& (4.1-d_{\Delta t,i} \text{def})}{\lesssim} |b_i(\phi_i(x) - \phi_{\Delta t,i}(x))| + |\nabla \phi_i|_\infty |d_{\Delta t,i}|_\infty |G_i - G_{\Delta t,i}|_\infty \lesssim h^{q_s+1} + \Delta t^{q_t+1}.$$

Hence  $|\Psi_{\Delta t,i}^\Gamma - \Psi_i^\Gamma| \lesssim |d_{\Delta t,i} - d_i| |G_i| + |d_i| |G_{\Delta t,i} - G_i|$  and the result follows with  $\|G\|_{\infty, \mathcal{Q}_h^\Gamma} \lesssim 1$ ,  $\|d\|_{\infty, \mathcal{Q}_h^\Gamma} \lesssim h^2 + \Delta t^{q_t+1}$  and  $\|\nabla \phi_{\Delta t} - G\|_{\infty, \mathcal{Q}_h^\Gamma} = \|\nabla(\phi_{\Delta t} - \phi)\|_{\infty, \mathcal{Q}_h^\Gamma} \lesssim h^{q_s} + \Delta t^{q_t+1}$ , cf. [\(2.7c-phi\\_{\Delta t} \text{acc}\)](#).

Proof of [\(4.4-Psi\\_{\Delta t}^\Gamma \text{acc-b}\)](#):

The proof follows similar strategies as the proof of [\(3.2a-dbnd\)](#) for  $(m_t, m_s) = (0, 1)$  and we give the details for the sake of completeness in [Appendix B.1](#).  $\square$



**5. Construction of fully discrete mapping on cut elements.** We now turn to the realisable discrete mapping  $P_h^\Gamma$  on the cut elements. Here, we try to mimic the construction of the continuous mapping  $\Psi^\Gamma$  in (3.9- $\Psi^\Gamma_{\text{def}}$ ) with adaptations due to the fact that  $\phi$  may not be available in general and  $\Psi^\Gamma$  is not a FE function.

**5.1. Discrete search directions.** To transfer the construction principle of the spatially continuous mappings in the previous sections to a computable setting, we need to first define a *discrete search direction*. We follow [29] in approximating  $G = \nabla\phi$  where two options are presented: Let  $x \in \Omega^\Gamma$ , then

$$(5.1) \quad G_{h,i}(x) := \nabla\phi_{h,i}(x) \quad \text{or} \quad G_{h,i}(x) := (P_h^\Gamma \nabla\phi_{h,i})(x), \quad i = 0, \dots, q_t.$$

and  $G_h(x, t) := \sum_{i=0}^{q_t} \ell_i(t) G_{h,i}(x)$ , s.t.  $G_h(x, t) = \nabla\phi_h(x, t)$  or  $G_h(x, t) = P_h^\Gamma \nabla\phi_h(x, t)$ , respectively, for  $(x, t) \in Q_h^\Gamma$ . Here,  $P_h^\Gamma : C(\mathcal{T}_h^\Gamma) \rightarrow W_h^k$  is an Oswald-type spatially averaged interpolation operator as in [29, Sect. 2.2]. It satisfies

$$(5.2) \quad P_h^\Gamma w = I_{q_s}^s w, \quad \|P_h^\Gamma w\|_{\infty, \Omega} \lesssim \|w\|_{\infty, \mathcal{T}_h} \quad \forall w \in C(\Omega^\Gamma)^d.$$

where  $I_{q_s}^s$  denotes a generic spatial interpolation operator. Then it holds

LEMMA 5.1. *For  $G_h = \nabla\phi_h$  or  $G_h = P_h^\Gamma \nabla\phi_h$  there holds for  $m = 0, 1$ :*

$$(5.3-G_h \text{acc}) \quad \|D^m(G_h - G)\|_{\infty, Q_h^\Gamma} \lesssim h^{q_s - m} + \Delta t^{q_t + 1}.$$

*Proof.* Let  $G_h = \nabla\phi_h$ . Then the result follows from (2.5- $\phi_h \text{acc}$ ). For  $G_h = P_h^\Gamma \nabla\phi_h$  a proof is given in Appendix B.2.  $\square$

**5.2. Construction of element-wise approximation of  $\Psi^\Gamma$  on active elements.** Next, our aim is to introduce a computable approximation of  $\Psi^\Gamma$ .

To this end, we recover that the higher-order approximation of  $\phi$  was given as  $\phi_h = \sum_{i=0}^{q_t} \ell_i(t) \phi_{h,i}(x)$ . Each of these  $\phi_{h,i}(x)$  can be used to construct a spatial approximation of  $\Psi_i^\Gamma$  as follows:

Let  $i = 0, \dots, q_t$  and  $\mathcal{E}_T \phi_{h,i}$  be the polynomial extension of  $\phi_{h,i}|_T$  for  $T \in \mathcal{T}_h^\Gamma$ . Then, we define the function  $d_{h,i} : \Omega^\Gamma \rightarrow [-\delta, \delta]$  for  $\delta > 0$  sufficiently small as follows: For  $x \in \Omega^\Gamma$ , let  $d_{h,i}(x)$  be the (in absolute value) smallest number such that

$$(5.4-d_{h,i} \text{def}) \quad \mathcal{E}_T \phi_{h,i}(x + (d_{h,i} G_{h,i})(x)) = (1 - b_i(x)) \phi_i^{\text{lin}}(x) + b_i(x) \phi_{h,i}(x).$$

We define the space-time function  $d_h : Q_h^\Gamma \rightarrow \mathbb{R}$  correspondingly.

**5.3. Accuracy of element-wise approximation of  $\Psi^\Gamma$  on active elements.** We aim to prove a variant of [29, Lemma 3.5]. To this end, we start by validating the proximity of  $\mathcal{E}_T \phi_{h,i}$  to  $\phi_{h,i}$  in a neighborhood of each element  $T \in \mathcal{T}_h^\Gamma$ .

LEMMA 5.2. *Fix  $T \in \mathcal{T}_h^\Gamma$  and  $i \in \{0, \dots, q_t\}$  and let  $y := x + \alpha G_{h,i}(x)$  be given such that  $|x - y| \lesssim h$  (which is the case if and only if  $|\alpha| \lesssim h$ ). Then, we have for  $m = 0, 1$*

$$(5.5a-\mathcal{E}_T \text{acc}) \quad |D^m(\mathcal{E}_T \phi_{h,i} - \phi_i)(y)| \lesssim h^{q_s + 1 - m} + \Delta t^{q_t + 1},$$

$$(5.5b-\mathcal{E}_T \text{acc}) \quad |D^m \partial_t(\mathcal{E}_T \phi_h - \phi)(y, t)| \lesssim h^{q_s + 1 - m} + \Delta t^{q_t}, \quad t \in I_n$$

$$(5.5c-\mathcal{E}_T \text{acc}) \quad |D^m(\mathcal{E}_T \phi_{h,i} - \phi_{\Delta t, i})(y)| \lesssim h^{q_s + 1 - m}.$$

*Proof.* The proof is similar to a result in [29, A. 1]. We provide it in Appendix B.3.  $\square$

Now, we come to the counterpart of [29, Lemma 3.5]:

LEMMA 5.3. *For all  $i = 0, \dots, q_t$ , and  $h$  sufficiently small, (5.4- $d_{h,i}$ def) defines a unique  $d_{h,i} : \Omega^\Gamma \rightarrow \mathbb{R}$  with  $d_{h,i} \in C(\Omega^\Gamma) \cap C^\infty(\mathcal{T}_h^\Gamma)$ . Furthermore:*

$$(5.6a-d_{h,vrt}) \quad d_{h,i}(x_V) = 0 \quad \text{for all vertices } x_V \text{ of } T \in \mathcal{T}_h^\Gamma,$$

$$(5.6b-d_{h,i}bnd) \quad \|d_{h,i}\|_{\infty, \Omega^\Gamma} \lesssim h^2 + \Delta t^{q_t+1}, \quad \|\nabla d_{h,i}\|_{\infty, \mathcal{T}_h^\Gamma} \lesssim h + \Delta t^{q_t+1}.$$

*Proof.* The first result of  $d_{h,i}$  vanishing on vertices follows from the construction of  $\phi_i^{\text{lin}}$  as the vertex interpolant of  $\phi_{h,i}$ . Next, we show the existence of a unique solution  $d_{h,i}$  of (5.4- $d_{h,i}$ def) for  $i \in \{0, \dots, q_t\}$ . We define, for a fixed  $\alpha_0 > 0$  at the point  $x \in \Omega^\Gamma$ , the function  $g : [-\alpha_0 h, \alpha_0 h] \rightarrow \mathbb{R}$  as follows:

$$(5.7) \quad g(\alpha) := \mathcal{E}_T \phi_{h,i}(x + \alpha G_{h,i}(x)) - (1 - b_i(x)) \phi_i^{\text{lin}}(x) - b_i(x) \phi_{h,i}(x)$$

We observe at  $x$  as argument for  $\phi_i$ ,  $b_i$ ,  $\phi_i^{\text{lin}}$  and  $\phi_{h,i}$ , respectively,

$$|\phi_i - (1 - b_i) \phi_i^{\text{lin}} - b_i \phi_{h,i}| = |(1 - b_i)(\phi_i - \phi_i^{\text{lin}}) - b_i(\phi_{h,i} - \phi_i)| \lesssim h^2 + \Delta t^{q_t+1},$$

due to (2.5- $\phi_h$ acc), (2.13b- $\phi^{\text{lin}}$ acc) and  $b_i \in [0, 1]$ . In combination with (5.5a- $\mathcal{E}_T$ acc), we obtain

$$g(\alpha) = \phi_i(x + \alpha G_{h,i}(x)) - \phi_i(x) + \mathcal{O}(h^2 + \Delta t^{q_t+1}).$$

Next, we exploit proximity of  $\phi_i$  and  $\phi_{h,i}$  w.r.t. both arguments,  $x$  and  $x + \alpha G_{h,i}(x)$  using (2.5- $\phi_h$ acc), so that

$$g(\alpha) = \phi_{h,i}(x + \alpha G_{h,i}(x)) - \phi_{h,i}(x) + \mathcal{O}(h^2 + \Delta t^{q_t+1}).$$

We can now apply a Taylor development as in (3.5) to obtain:

$$(5.8) \quad g(\alpha) = \alpha |\nabla \phi_{h,i}(x)|^2 + \mathcal{O}(h^2 + \Delta t^{q_t+1})$$

Note that  $d_{h,i}(x)$  is  $\alpha$  so that  $g(\alpha) = 0$ . We now apply a similar argument to the one in the proof of (3.5). Involving (2.17- $\Delta t$ bnd) to bound the remainder term by  $\mathcal{O}(h)$ , noting that  $|\nabla \phi_{h,i}(x)|$  is bounded from below and above for sufficiently small  $h$ , we can easily see that  $g(\pm \alpha_0 h) \leq 0$  for sufficiently small  $h$ . As  $g$  is continuous (more specifically a linear function with a higher-order perturbation), we can apply the intermediate value theorem to conclude that there exists a unique  $\alpha \in [-\alpha_0 h, \alpha_0 h]$  such that  $g(\alpha) = 0$ . Further, it satisfies the first estimate in (5.6b- $d_{h,i}$ bnd). The second estimate in (5.6b- $d_{h,i}$ bnd) is proven in Appendix B.4.  $\square$

In terms of  $d_{h,i}(x)$ , we then define

$$(5.9-\Psi_h^\Gamma \text{def}) \quad \Psi_{h,i}^\Gamma(x) := x + (d_{h,i} G_{h,i})(x), \quad \Psi_h^\Gamma(x, t) = \sum_{i=0}^{q_t} \ell_i(t) \Psi_{h,i}^\Gamma(x).$$

LEMMA 5.4. *There holds*

$$(5.10-\Psi_{\Delta t|_h}^\Gamma) \quad \|\Psi_{\Delta t}^\Gamma - \Psi_h^\Gamma\|_{\infty, Q_h^\Gamma} \lesssim h^{q_s+1}$$

*Proof.* We note that it suffices to prove  $\|\Psi_{\Delta t,i}^\Gamma - \Psi_{h,i}^\Gamma\|_{\infty, \Omega^\Gamma} \lesssim h^{q_s+1}$  for  $i = 0, \dots, q_t$ . Then the following is very similar to the proof of [29, Lemma 3.6] given in [29, A.2]. By the definitions of  $\Psi_{h,i}^\Gamma$  and  $\Psi_{\Delta t,i}^\Gamma$ , we have for  $x \in \Omega^\Gamma$

$$(5.11) \quad \begin{aligned} |(\Psi_{\Delta t,i}^\Gamma - \Psi_{h,i}^\Gamma)(x)| &= |(d_{\Delta t,i} G_{\Delta t,i} - d_{h,i} G_{h,i})(x)| \\ &\leq |(d_{\Delta t,i} - d_{h,i})(x)| |G_{\Delta t,i}(x)| + |d_{h,i}(x)| |(G_{\Delta t,i} - G_{h,i})(x)| \end{aligned}$$

Here, the second summand can be bounded by  $h^{q_s+1}$  with (2.7a- $\phi_{\Delta t|h,i}$ ) and  $m_s = 1$  from Assumption 2.5 and (5.6b- $d_{h,i}\text{bnd}$ ) from Lemma 5.3 together with (2.17- $\Delta t\text{bnd}$ ) so that  $|d_{h,i}(x)| \lesssim h$ . In the first summand,  $|G_{\Delta t,i}(x)|$  is bounded  $\lesssim 1$  due to (2.7c- $\phi_{\Delta t\text{acc}}$ ) and (2.3- $\phi\text{bnd}$ ), so that it remains to estimate  $|(d_{\Delta t,i} - d_{h,i})(x)|$ .

From the definitions of  $d_{\Delta t,i}$  and  $d_{h,i}$ , we obtain

$$\begin{aligned} \phi_{\Delta t,i}(x + (d_{\Delta t,i}G_{\Delta t,i})(x)) &= (1 - b_i(x))\phi_i^{\text{lin}}(x) + b_i(x)\phi_{\Delta t,i}(x) \\ \mathcal{E}_T\phi_{h,i}(x + (d_{h,i}G_{h,i})(x)) &= (1 - b_i(x))\phi_i^{\text{lin}}(x) + b_i(x)\phi_{h,i}(x), \\ (5.12) \quad \Rightarrow \phi_{\Delta t,i}(x + (d_{\Delta t,i}G_{\Delta t,i})(x)) &= \mathcal{E}_T\phi_{h,i}(x + (d_{h,i}G_{h,i})(x)) + \mathcal{O}(h^{q_s+1}) \end{aligned}$$

where we made use of  $m_s = 0$  in (2.7a- $\phi_{\Delta t|h,i}$ ) from Assumption 2.5. We set  $y_h := \Psi_{h,i}^\Gamma(x)$  and  $\tilde{y}_h := x + (d_{h,i}G_{\Delta t,i})(x)$ . Then, with (2.9- $\phi_h\text{wsd}$ ), it follows:

$$\begin{aligned} |d_{\Delta t,i}(x) - d_{h,i}(x)| &\simeq |\phi_{\Delta t,i}(x + (d_{\Delta t,i}G_{\Delta t,i})(x)) - \phi_{\Delta t,i}(x + (d_{h,i}G_{\Delta t,i})(x))| \\ (5.12) \quad &\stackrel{=}{=} |\mathcal{E}_T\phi_{h,i}(\overbrace{x + (d_{h,i}G_{h,i})(x)}^{=y_h}) - \phi_{\Delta t,i}(\overbrace{x + (d_{h,i}G_{\Delta t,i})(x)}^{=\tilde{y}_h})| + \mathcal{O}(h^{q_s+1}) \\ &\leq |(\mathcal{E}_T\phi_{h,i} - \phi_{\Delta t,i})(y_h)| + |\phi_{\Delta t,i}(y_h) - \phi_{\Delta t,i}(\tilde{y}_h)| + \mathcal{O}(h^{q_s+1}) \end{aligned}$$

Exploiting (5.5c- $\mathcal{E}_T\text{acc}$ ) in Lemma 5.2 the first summand in this expression can be bounded by  $\lesssim h^{q_s+1}$ . For the second summand, we have  $\|d_{h,i}\|_{\infty,\Omega^\Gamma} \lesssim h^2 + \Delta t^{q_t+1}$  with (5.6b- $d_{h,i}\text{bnd}$ ) from Lemma 5.3 and  $\|G_{h,i} - G_{\Delta t,i}\|_{\infty,\Omega^\Gamma} \lesssim h^{q_s}$  from  $m_s = 1$  in (2.7a- $\phi_{\Delta t|h,i}$ ) from Assumption 2.5 so that  $|y_h - \tilde{y}_h| \lesssim h^{q_s+2} + \Delta t^{q_t+1}h^{q_s} \lesssim h^{q_s+1}$  where we used (2.17- $\Delta t\text{bnd}$ ) in the last step. With the boundedness  $\|\nabla\phi_{\Delta t}\|_{\infty,U} \lesssim \|\nabla\phi\|_{\infty,U} \lesssim C_{\nabla\phi}$ , cf. (2.3- $\phi\text{bnd}$ ), we hence have

$$|\phi_{\Delta t,i}(y_h) - \phi_{\Delta t,i}(\tilde{y}_h)| \lesssim \|\nabla\phi_{\Delta t,i}\|_{\infty,\bar{U}}|y_h - \tilde{y}_h| \lesssim h^{q_s+1}.$$

Taking these results together, we have

$$(5.13) \quad \|d_{\Delta t,i} - d_{h,i}\|_{\infty,\Omega^\Gamma} \lesssim h^{q_s+1}.$$

With (5.11) and the previous considerations, this implies (5.10- $\Psi_{\Delta t|h}^\Gamma$ ).  $\square$

Each of these mappings  $\Psi_{h,i}^\Gamma$  ( $i = 0, \dots, q_t$ ) is close to the restriction of the mapping from the previous subsection,  $\Psi_i^\Gamma$ , as is stated in the following:

LEMMA 5.5. *For all  $i = 0, \dots, q_t$  and  $h$  sufficiently small,*

$$(5.14\text{-}\Psi_h^\Gamma\text{acc}) \quad \|\Psi_h^\Gamma - \Psi^\Gamma\|_{\infty,Q_h^\Gamma} \lesssim h^{q_s+1} + \Delta t^{q_t+1},$$

*Proof.* The statement follows from a triangle inequality  $\|\Psi_h^\Gamma - \Psi^\Gamma\|_{\infty,Q_h^\Gamma} \leq \|\Psi_h^\Gamma - \Psi_{\Delta t}^\Gamma\|_{\infty,Q_h^\Gamma} + \|\Psi_{\Delta t}^\Gamma - \Psi^\Gamma\|_{\infty,Q_h^\Gamma}$  and (5.10- $\Psi_{\Delta t|h}^\Gamma$ ) and (4.4- $\Psi_{\Delta t\text{acc-a}}$ ).  $\square$

**5.4. Continuous approximation of  $\Psi_h^\Gamma$  on active elements.** Note that  $\Psi^\Gamma$  is not necessarily continuous in space across element boundaries. Next, we define a spatially continuous version of  $\Psi_h^\Gamma$ ,  $\Theta_h^\Gamma$ , by applying the spatial interpolation operator  $P_h^\Gamma$  as before

$$(5.15) \quad \Theta_h^\Gamma(x, t) := P_h^\Gamma\Psi_h^\Gamma = \sum_{i=0}^{q_t} \ell_i(t)(P_h^\Gamma\Psi_{h,i}^\Gamma(x)).$$

We can now put the results for the time instances  $t_i$ ,  $i = 0, \dots, q_t$  together to obtain the following result in space-time:

LEMMA 5.6. For  $m_s = 0, \dots, q_s + 1$  and  $m_t = 0, \dots, q_t + 1$  the following holds:

$$(5.15a-\Theta_h^\Gamma \text{acc}) \quad \Delta t^{m_t} h^{m_s} \|D^{m_s} \partial_t^{m_t} (\Theta_h^\Gamma - \Psi^\Gamma)\|_{\infty, \mathcal{Q}_h^\Gamma} \lesssim h^{q_s+1} + \Delta t^{q_t+1},$$

$$(5.15b-\Theta_h^\Gamma \text{acc}) \quad \|\nabla(\Theta_h^\Gamma - \Psi^\Gamma)\|_{\infty, \mathcal{Q}_h^\Gamma} \lesssim h^{q_s} + \Delta t^{q_t+1}.$$

Let us stress that the second claim is stronger than the case  $m_s = 1$  and  $m_t = 0$  in the first estimate. Only restrictions as strong as  $\Delta t \lesssim h$  would let the first estimate imply the second. Below, in Lemma 6.4 – after having introduced another semi-discrete mapping – we will deduce an analog to (5.15b- $\Theta_h^\Gamma \text{acc}$ ) for the time derivative (using Assumption 2.6) which could only be implied from the first claim for  $h \lesssim \Delta t$ .

*Proof.* We prove both results one after another.

Proof of (5.15a- $\Theta_h^\Gamma \text{acc}$ ):

With  $P_h^\Gamma \Psi^\Gamma = I_{q_s}^\Gamma \Psi^\Gamma$  and hence  $I_{q_t}^t P_h^\Gamma \Psi^\Gamma = I_{q_t}^t I_{q_s}^s \Psi^\Gamma$  we can apply a triangle inequality to obtain one discrete (in time and space) difference  $P_h^\Gamma (\Psi_h^\Gamma - I_{q_t}^t \Psi^\Gamma)$  and an interpolation error (in time and space):

$$\begin{aligned} & \Delta t^{m_t} h^{m_s} \|\partial_t^{m_t} D^{m_s} (P_h^\Gamma \Psi_h^\Gamma - \Psi^\Gamma)\|_{\infty, \mathcal{Q}_h^\Gamma} \\ & \leq \Delta t^{m_t} h^{m_s} (\|\partial_t^{m_t} D^{m_s} P_h^\Gamma (\Psi_h^\Gamma - I_{q_t}^t \Psi^\Gamma)\|_{\infty, \mathcal{Q}_h^\Gamma} + \|\partial_t^{m_t} D^{m_s} (I_{q_t}^t I_{q_s}^s \Psi^\Gamma - \Psi^\Gamma)\|_{\infty, \mathcal{Q}_h^\Gamma}) \lesssim \dots \end{aligned}$$

Applying an inverse inequality on the discrete (in time and space) term, exploiting continuity of  $P_h^\Gamma$  and standard tensor product interpolation gives

$$\begin{aligned} \dots & \lesssim \|\Psi_h^\Gamma - I_{q_t}^t \Psi^\Gamma\|_{\infty, \mathcal{Q}_h^\Gamma} + (h^{q_s+1} + \Delta t^{q_t+1}) \|\Psi^\Gamma\|_{H^{q_s+1, q_t+1, \infty}(\mathcal{Q}_h^\Gamma)} \\ & \lesssim \|\Psi_h^\Gamma - \Psi^\Gamma\|_{\infty, \mathcal{Q}_h^\Gamma} + \|I_{q_t}^t \Psi^\Gamma - \Psi^\Gamma\|_{\infty, \mathcal{Q}_h^\Gamma} + (h^{q_s+1} + \Delta t^{q_t+1}) \|\Psi^\Gamma\|_{H^{q_s+1, q_t+1, \infty}(\mathcal{Q}_h^\Gamma)} \end{aligned}$$

Now, making use of (5.14- $\Psi_h^\Gamma \text{acc}$ ), standard temporal interpolation with the bounds from (3.10c- $\Psi^\Gamma \text{bnd}$ ) and (3.10c- $\Psi^\Gamma \text{bnd}$ ) for the last term we obtain the claim.

Proof of (5.15b- $\Theta_h^\Gamma \text{acc}$ ):

To circumvent using the inverse inequality on terms that involve temporal resolution quantities (and hence avoiding quotients of the form  $\Delta t^l/h$  for some  $l \in \mathbb{N}$ ) we start with a triangle inequality that involves  $P_h^\Gamma \Psi_{\Delta t}^\Gamma$  and  $\Psi_{\Delta t}^\Gamma$ :

$$\begin{aligned} \|\nabla(\Theta_h^\Gamma - \Psi^\Gamma)\|_{\infty, \mathcal{Q}_h^\Gamma} &= \|\nabla(P_h^\Gamma \Psi_h^\Gamma - \Psi^\Gamma)\|_{\infty, \mathcal{Q}_h^\Gamma} \\ &\leq \underbrace{\|\nabla P_h^\Gamma (\Psi_h^\Gamma - \Psi_{\Delta t}^\Gamma)\|_{\infty, \mathcal{Q}_h^\Gamma}}_A + \underbrace{\|\nabla(P_h^\Gamma \Psi_{\Delta t}^\Gamma - \Psi_{\Delta t}^\Gamma)\|_{\infty, \mathcal{Q}_h^\Gamma}}_B + \underbrace{\|\nabla(\Psi_{\Delta t}^\Gamma - \Psi^\Gamma)\|_{\infty, \mathcal{Q}_h^\Gamma}}_C \end{aligned}$$

We treat the three summands  $A$ ,  $B$  and  $C$  separately. In the first summand  $A$ , the gradient is applied to a spatially discrete function and we can apply an inverse inequality and continuity of the Oswald-interpolator to arrive at

$$A = \|\nabla P_h^\Gamma (\Psi_h^\Gamma - \Psi_{\Delta t}^\Gamma)\|_{\infty, \mathcal{Q}_h^\Gamma} \lesssim h^{-1} \|P_h^\Gamma (\Psi_h^\Gamma - \Psi_{\Delta t}^\Gamma)\|_{\infty, \mathcal{Q}_h^\Gamma} \lesssim h^{-1} \|\Psi_h^\Gamma - \Psi_{\Delta t}^\Gamma\|_{\infty, \mathcal{Q}_h^\Gamma}$$

Together with (5.10- $\Psi_{\Delta t}^\Gamma|_h$ ) in Lemma 5.4 we hence obtain the bound  $A \lesssim h^{q_s}$ .

For the second summand  $B$  we have that  $\Psi_{\Delta t}^\Gamma$  is continuous in space so that  $P_h^\Gamma$  becomes a classical interpolation operator  $P_h^\Gamma \Psi_{\Delta t}^\Gamma = I_{q_s}^s \Psi_{\Delta t}^\Gamma$  and we can apply standard interpolation results □

$$B = \|\nabla(I_{q_s}^s \Psi_{\Delta t}^\Gamma - \Psi_{\Delta t}^\Gamma)\|_{\infty, \mathcal{Q}_h^\Gamma} \lesssim h^{q_s} \|D^{q_s+1} \Psi_{\Delta t}^\Gamma\|_{\infty, \mathcal{Q}_h^\Gamma} \lesssim h^{q_s}$$

where we bounded the latter norm by 1 due to Lemma 4.1. Finally, we bound the last term by (4.4- $\Psi_{\Delta t}^\Gamma \text{acc-b}$ ),  $C = \|\nabla(\Psi_{\Delta t}^\Gamma - \Psi^\Gamma)\|_{\infty, \mathcal{Q}_h^\Gamma} \lesssim h^{q_s} + \Delta t^{q_t+1}$ . Putting the bounds for  $A$ ,  $B$  and  $C$  together yields the claim.

**6. Construction of discrete-in-space mapping on cut elements.** In this section, we define a semi-discrete mapping that is continuous in time and discrete in space. Throughout this section, we assume that [Assumption 2.6](#) is valid.

For the discrete search direction, we make the same choice as in the fully discrete setting, i.e. we define either  $G_H = \nabla \phi_H$  or  $G_H = (P_h^\Gamma \nabla \phi_H)$ .

We define the function  $d_H: Q_h^\Gamma \rightarrow [-\delta, \delta]$  for  $\delta > 0$  sufficiently small as follows: For  $x \in \Omega^\Gamma$ ,  $t \in I_n$ , let  $d_H(x, t)$  be the (in absolute value) smallest number such that

$$(6.1-d_H\text{def}) \quad \mathcal{E}_T \phi_H(x + (d_H G_H)(x, t), t) = (1 - b(x, t)) \phi^{\text{lin}}(x, t) + b(x, t) \phi_H(x, t).$$

In analogy to [\(5.5a- \$\mathcal{E}\_{T\text{acc}}\$ \)](#) in [Lemma 5.2](#) and [\(5.6b- \$d\_{h,i}\text{bnd}\$ \)](#) in [Lemma 5.3](#), we have the following result for  $d_H$ :

LEMMA 6.1. For  $T \in \mathcal{T}_h^\Gamma$ ,  $t \in I_n$  and  $y := x + \alpha(G_H)(x, t)$ ,  $|\alpha| \lesssim h$  there holds

$$(6.2a-\mathcal{E}_{T\text{acc}}) \quad |\partial_t^{m_t}(\mathcal{E}_T \phi_H - \phi)(y, t)| \lesssim h^{q_s+1} + \Delta t^{q_t+1-m_t}, \quad m_t = 0, 1.$$

For  $h$  sufficiently small, the relation [\(6.1- \$d\_H\text{def}\$ \)](#) defines a unique  $d_H \in C(Q_h^\Gamma)$  with

$$(6.2b-d_H\text{bnd}) \quad \|d_H\|_{\infty, Q_h^\Gamma} \lesssim h^2 + \Delta t^{q_t+1}.$$

$$(6.2c-d_H\text{bnd}) \quad \|\partial_t^{m_t} d_H\|_{\infty, Q_h^\Gamma} \lesssim 1, \quad m_t = 0, \dots, q_t + 1.$$

*Proof.* The proof of [\(6.2a- \$\mathcal{E}\_{T\text{acc}}\$ \)](#) follows the same lines of the proof of [\(5.5a- \$\mathcal{E}\_{T\text{acc}}\$ \)](#) and [\(5.5b- \$\mathcal{E}\_{T\text{acc}}\$ \)](#) with  $\phi_{h,i}(\cdot)$  replaced by  $\phi_H(\cdot, t)$  and exploiting [\(2.8b- \$\phi\_{H\text{acc}}\$ \)](#) instead of [\(2.5- \$\phi\_{h\text{acc}}\$ \)](#). The proof of [\(6.2b- \$d\_H\text{bnd}\$ \)](#) follows the same lines of the proof of [Lemma 5.3](#) when freezing  $t \in I_n$  and exchanging  $\phi_{h,i}(\cdot)$  with  $\phi_H(\cdot, t)$ ,  $G_{h,i}(\cdot)$  with  $G_H(\cdot, t)$  and  $\phi_i^{\text{lin}}(\cdot)$  with  $\phi^{\text{lin}}(\cdot, t)$ . These requirements [\(2.5- \$\phi\_{h\text{acc}}\$ \)](#) and [\(5.5a- \$\mathcal{E}\_{T\text{acc}}\$ \)](#) are replaced by [\(2.8b- \$\phi\_{H\text{acc}}\$ \)](#) and [\(6.2b- \$d\_H\text{bnd}\$ \)](#). Note that in contrast to [Lemma 5.3](#) and [Lemma 5.2](#) we do not consider spatial derivatives of  $d_H$  or  $\mathcal{E}_T \phi_H$ . [\(6.2c- \$d\_H\text{bnd}\$ \)](#) follows with similar arguments as in the proof of [\(3.2b- \$d\text{bnd}\$ \)](#) (for  $m_t > 1$ ) in [Appendix A.2](#). For completeness, we have included the proof in [Appendix B.5](#).  $\square$

In terms of  $d_H$ , we then define

$$(6.3-\Psi_H^\Gamma\text{def}) \quad \Psi_H^\Gamma(x, t) = x + (d_H G_h)(x, t).$$

LEMMA 6.2. There holds

$$(6.4-\Psi_H^\Gamma|_h) \quad \|\Psi_H^\Gamma - \Psi_h^\Gamma\|_{\infty, Q_h^\Gamma} \lesssim \Delta t^{q_t+1}.$$

*Proof.* By the definitions of  $\Psi_h^\Gamma$  and  $\Psi_H^\Gamma$ , we have for  $x \in \Omega^\Gamma$ ,  $t \in I_n$

$$(6.5) \quad \begin{aligned} |(\Psi_H^\Gamma - \Psi_h^\Gamma)(x, t)| &= |(d_H G_H - d_h G_h)(x, t)| \\ &\leq |(d_H - d_h)(x, t)| |G_h(x, t)| + |d_H(x, t)| |(G_H - G_h)(x, t)| \end{aligned}$$

The individual terms can now be bounded similarly to the procedure of the proof of [Lemma 5.4](#).  $|(d_H - d_h)(x, t)| \lesssim \Delta t^{q_t+1}$  follows effectively from [\(2.8a- \$\phi\_{H|h}\$ \)](#),  $|G_h| \lesssim 1$  follows from  $|G| \lesssim 1$  and proximity,  $|d_H| \lesssim h^2 + \Delta t^{q_t+1} \lesssim h$  follows from [\(6.2b- \$d\_H\text{bnd}\$ \)](#) and [\(2.17- \$\Delta t\text{bnd}\$ \)](#) and  $|(G_H - G_h)| \lesssim \frac{1}{h} \Delta t^{q_t+1}$  follows from [\(2.8a- \$\phi\_{H|h}\$ \)](#) and an inverse inequality. Inserting these bounds into [\(6.5\)](#) yields the claim.  $\square$

LEMMA 6.3. For all  $i = 0, \dots, q_t$  and  $h$  sufficiently small,

$$(6.6-\Psi_H^\Gamma\text{acc}) \quad \|\partial_t(\Psi_H^\Gamma - \Psi_h^\Gamma)\|_{\infty, Q_h^\Gamma} \lesssim h^{q_s+1} + \Delta t^{q_t},$$

*Proof.* The proof is given in [Appendix B.6](#).  $\square$

LEMMA 6.4. For  $m_s = 0, \dots, q_s + 1$  and  $m_t = 0, \dots, q_t + 1$  there holds:

$$(6.6\text{-}\Theta_h^\Gamma \text{acc}) \quad \|\partial_t(\Theta_h^\Gamma - \Psi^\Gamma)\|_{\infty, \mathcal{Q}_h^\Gamma} \lesssim h^{q_s+1} + \Delta t^{q_t}.$$

*Remark 6.5.* We note that this bound is an improved bound for [\(5.15a-}\Theta\\_h^\Gamma \text{acc\)}](#) with  $m_s = 0$  and  $m_t = 1$ . Only for  $h \lesssim \Delta t$  [\(6.6-}\Theta\\_h^\Gamma \text{acc\)}](#) follows from [\(5.15a-}\Theta\\_h^\Gamma \text{acc\)}](#) otherwise.

*Proof.* First, we want to work around the Oswald projection using a triangle inequality.

$$\begin{aligned} \|\partial_t(\Theta_h^\Gamma - \Psi^\Gamma)\|_{\infty, \mathcal{Q}_h^\Gamma} &= \|\partial_t(P_h^\Gamma \Psi_h^\Gamma - \Psi^\Gamma)\|_{\infty, \mathcal{Q}_h^\Gamma} \stackrel{=I_{q_s}^s \partial_t \Psi^\Gamma}{=} \\ &\leq \|\partial_t P_h^\Gamma(\Psi_h^\Gamma - \Psi^\Gamma)\|_{\infty, \mathcal{Q}_h^\Gamma} + \underbrace{\|P_h^\Gamma \partial_t \Psi^\Gamma - \partial_t \Psi^\Gamma\|_{\infty, \mathcal{Q}_h^\Gamma}}_{\lesssim h^{q_s+1} \|D^{q_s+1} \partial_t \Psi^\Gamma\|_{\infty, \mathcal{Q}_h^\Gamma}} \\ &\lesssim \|\partial_t(\Psi_h^\Gamma - \Psi^\Gamma)\|_{\infty, \mathcal{Q}_h^\Gamma} + h^{q_s+1} \quad (\text{with (5.2) and (3.10c-}\Psi_H^\Gamma \text{bnd)}) \end{aligned}$$

Hence, it only remains to bound  $\|\partial_t(\Psi_h^\Gamma - \Psi^\Gamma)\|_{\infty, \mathcal{Q}_h^\Gamma}$ . To circumvent using the inverse inequality on terms that involve spatial resolution quantities (and hence avoiding quotients of the form  $h^l/\Delta t$  for some  $l \in \mathbb{N}$ ) we apply another triangle inequality involving  $\Psi_H^\Gamma$ :

$$\|\partial_t(\Psi_h^\Gamma - \Psi^\Gamma)\|_{\infty, \mathcal{Q}_h^\Gamma} \leq \|\partial_t(\Psi_H^\Gamma - \Psi^\Gamma)\|_{\infty, \mathcal{Q}_h^\Gamma} + \|\partial_t(\Psi_h^\Gamma - \Psi_H^\Gamma)\|_{\infty, \mathcal{Q}_h^\Gamma} = I + II$$

The bound for  $I$  follows from [\(6.6-}\Psi\\_H^\Gamma \text{acc\)}](#). For  $II$  we shift in the time interpolant of  $\Psi_H^\Gamma$ ,  $I_{q_t}^t \Psi_H^\Gamma$ <sup>5</sup>, and apply a triangle inequality to obtain

$$\|\partial_t(\Psi_h^\Gamma - \Psi_H^\Gamma)\|_{\infty, \mathcal{Q}_h^\Gamma} \leq \|\partial_t(\Psi_h^\Gamma - I_{q_t}^t \Psi_H^\Gamma)\|_{\infty, \mathcal{Q}_h^\Gamma} + \|\partial_t(I_{q_t}^t \Psi_H^\Gamma - \Psi_H^\Gamma)\|_{\infty, \mathcal{Q}_h^\Gamma} = II_a + II_b \blacksquare$$

Next, for  $II_a$  we can apply an inverse inequality

$$\begin{aligned} II_a &= \|\partial_t(\Psi_h^\Gamma - I_{q_t}^t \Psi_H^\Gamma)\|_{\infty, \mathcal{Q}_h^\Gamma} \lesssim \Delta t^{-1} \|(\Psi_h^\Gamma - I_{q_t}^t \Psi_H^\Gamma)\|_{\infty, \mathcal{Q}_h^\Gamma} \\ &\lesssim \Delta t^{-1} \max_i \|\Psi_{h,i}^\Gamma - \Psi_H^\Gamma(\cdot, t_i)\|_{\infty, \Omega^\Gamma} \lesssim \Delta t^{-1} \|\Psi_h^\Gamma - \Psi_H^\Gamma\|_{\infty, \mathcal{Q}_h^\Gamma} \lesssim \Delta t^{q_t} \end{aligned}$$

where we exploited [\(6.4-}\Psi\\_H^\Gamma|\\_h\)](#). For  $II_b$  we have

$$\|\partial_t(I_{q_t}^t \Psi_H^\Gamma - \Psi_H^\Gamma)\|_{\infty, \mathcal{Q}_h^\Gamma} \lesssim \Delta t^{q_t} \|\partial_t^{q_t+1} \Psi_H^\Gamma\|_{\infty, \mathcal{Q}_h^\Gamma} \lesssim \Delta t^{q_t}$$

where the last inequality follows from the Leibniz rule

$$\|\partial_t^{q_t+1} \Psi_H^\Gamma\|_{\infty, \mathcal{Q}_h^\Gamma} \lesssim \sum_{k=0}^{q_t+1} \|\partial_t^{q_t+1-k} d_H\|_{\infty, \mathcal{Q}_h^\Gamma} \|\partial_t^k G_H\|_{\infty, \mathcal{Q}_h^\Gamma}$$

and the bounds [\(6.2c-d\\_H bnd\)](#) and [\(2.8b-}\phi\\_H \text{acc\)}](#).  $\square$

**7. Global space-time mappings.** In this section, we want to discuss the extension of the previously defined functions  $\Psi^\Gamma$  and  $\Theta_h^\Gamma$  onto the whole computational domain  $\tilde{\Omega} \times I_n$ . We recap that so far, both functions are defined on smaller sets  $\mathcal{Q}_h^\Gamma$ , whose specific structure depends on the choice of the [FE](#) or smooth blending.

<sup>5</sup>which is not necessarily the same as  $\Psi_h^\Gamma$



**7.1. Extension procedure for the smooth function blending.** The task of the extension is particularly straightforward for the smooth blending case because the blending function already ensures that the functions  $\Psi^\Gamma$  and  $\Theta_h^\Gamma$  smoothly transition towards identity on the (spatial) boundary of  $Q_h^\Gamma$ . Hence, we can give the following definition of the extension  $\mathcal{E} = \mathcal{E}_2$  for the smooth blending case for  $t \in I_n$ :

$$(7.1) \quad (\mathcal{E}_2 \Psi^\Gamma)(x, t) := \begin{cases} \Psi^\Gamma(x, t) & \text{if } x \in \Omega^\Gamma \\ \text{id}_x & \text{else.} \end{cases}, \quad \Psi := \mathcal{E} \Psi^\Gamma, \quad \Theta_h := \mathcal{E} \Theta_h^\Gamma.$$

We continue with the construction of the according  $\mathcal{E}_1$  for the FE blending.

**7.2. Extension procedure for FE blending.** We now introduce the extension procedure for the FE blending procedure. Hence, for the following assume that  $\Omega^\Gamma$  is the set of cut elements and the input functions  $\Psi^\Gamma$  and  $\Theta_h^\Gamma$  do not transition into identity at  $\partial Q_h^\Gamma$ .

As a first technical step, we introduce notation for all elements neighbouring  $\Omega^\Gamma$ :

$$(7.2a) \quad \mathcal{T}_{h,+}^\Gamma := \{T \in \mathcal{T}_h | \bar{T} \cap \overline{\Omega^\Gamma} \neq \emptyset\}, \quad \Omega_+^\Gamma := \bigcup \mathcal{T}_{h,+}^\Gamma,$$

$$(7.2b) \quad \mathcal{Q}_{h,+}^\Gamma := \{T \times I_n | T \in \mathcal{T}_{h,+}^\Gamma\}, \quad Q_{h,+}^\Gamma := \Omega_+^\Gamma \times I_n.$$

These are the elements that share at least one vertex with elements in the cut domain  $\mathcal{T}_h^\Gamma$ . On all the elements  $T \in \mathcal{T}_{h,+}^\Gamma \setminus \mathcal{T}_h^\Gamma$ , we will apply a blending step which realises a continuous transition from the given values on  $\partial\Omega^\Gamma$  to the identity on  $\partial\Omega_+^\Gamma$  by a construction involving barycentric coordinates on the reference element. It is described in detail in [29, Section 3.3] as  $\mathcal{E}^{\partial\Omega^\Gamma}$  and we assume from here on that this linear extension operation is given w.r.t. our set of relevant elements. Central for the applicability of this mapping is the following lemma, which gives bounds on  $\mathcal{E}^{\partial\Omega^\Gamma} w$  and spatial derivatives thereof in terms of higher derivatives of  $w$ : [29, Theorem 3.11]

**LEMMA 7.1.** *Let  $\mathcal{V}(\partial\Omega^\Gamma)$  denote the set of vertices in  $\partial\Omega^\Gamma$  and  $\mathcal{F}(\partial\Omega^\Gamma)$  the set of all edges ( $d = 2$ ) or faces ( $d = 3$ ) in  $\partial\Omega^\Gamma$ . The following estimate holds for  $m_s = 0, 1$  and sufficiently regular  $w$  s.t. the r.h.s. is well-defined and bounded:*

$$(7.3a\text{-}\mathcal{E}\text{bnd}) \quad \|D^{m_s} \mathcal{E}^{\partial\Omega^\Gamma} w\|_{\infty, \Omega_+^\Gamma \setminus \Omega^\Gamma} \lesssim \sum_{r=m_s}^{q_s+1} h^{r-m_s} \|D^r w\|_{\infty, \mathcal{F}(\partial\Omega^\Gamma)} + h^{-m_s} \|w\|_{\infty, \mathcal{V}(\partial\Omega^\Gamma)}.$$

Moreover, for  $m_s = 2, \dots, q_s + 1$ , for  $T \in \mathcal{T}_{h,+}^\Gamma \setminus \mathcal{T}_h^\Gamma$  and  $\mathcal{F}(T)$  the facets of  $T$  on  $\partial\Omega^\Gamma$

$$(7.3b\text{-}\mathcal{E}\text{bnd}) \quad \|D^{m_s} \mathcal{E}^{\partial\Omega^\Gamma} w\|_{\infty, T} \lesssim \sum_{r=m_s}^{q_s+1} h^{r-m_s} \|D^r w\|_{\infty, \mathcal{F}(T)}.$$

The extension can be applied to any continuous, piecewise (sufficiently) smooth function  $w$ . If the argument  $w$  is piecewise (spatial) polynomial,  $\mathcal{E}^{\partial\Omega^\Gamma} w$  will be as well, cf. [29, Lemma 3.9]. Applying the  $\mathcal{E}^{\partial\Omega^\Gamma}$  to the mapping  $\Psi^\Gamma$ , we define for  $t \in I_n$

$$(7.4) \quad (\mathcal{E}_1 \Psi^\Gamma)(x, t) = \begin{cases} \Psi^\Gamma(x, t) & \text{if } x \in \Omega^\Gamma \\ \text{id}_x + \mathcal{E}^{\partial\Omega^\Gamma}(\Psi^\Gamma(\cdot, t) - \text{id}_x) & \text{if } x \in \Omega_+^\Gamma \setminus \Omega^\Gamma \\ \text{id}_x & \text{else.} \end{cases}$$

As a first step in the proving of geometry approximation and interpolation results for  $\Psi, \Theta_h$ , we state a commutation property for the *spatial* extension  $\mathcal{E}^{\partial\Omega^\Gamma}$ .

LEMMA 7.2. For  $u \in C^{m_t}(I_n; C(\partial\Omega^\Gamma))$ ,  $m_t \in \mathbb{N}$  time derivatives and spatial extension commute, i.e.  $\partial_t^{m_t} \mathcal{E}^{\partial\Omega^\Gamma} u(\cdot, t) = \mathcal{E}^{\partial\Omega^\Gamma} \partial_t^{m_t} u(\cdot, t)$ .

*Proof.* For the proof of this lemma, we refer to the construction of  $\mathcal{E}^{\partial\Omega^\Gamma}$  in [29].  $\square$

**7.3. Interpolation results: Boundedness of  $\Psi$ .** We bound the difference between  $\Psi$  and  $\text{id}_x$  in different norms:

THEOREM 7.3. Let  $q_t^* = q_t + 1$  for the smooth blending and  $q_t^* = q_t$  for the FE blending. Then, it holds

$$(7.5a\text{-}\Psi\text{bnd}) \quad \|\Psi - \text{id}_x\|_{\infty, \tilde{\mathcal{Q}}^n} \lesssim h^2 + \Delta t^{q_t+1},$$

$$(7.5b\text{-}\Psi\text{bnd}) \quad \|\partial_t \Psi\|_{\infty, \tilde{\mathcal{Q}}^n} \lesssim h^2 + \Delta t^{q_t}.$$

$$(7.5c\text{-}\Psi\text{bnd}) \quad \|\nabla \Psi - \text{Id}_x\|_{\infty, \mathcal{Q}_h^n} \lesssim h + \Delta t^{q_t^*},$$

$$(7.5d\text{-}\Psi\text{bnd}) \quad \|D^{m_s} \partial_t^{m_t} \Psi\|_{\infty, \mathcal{Q}_h^n} \lesssim 1 \quad \text{for } m_s \leq q_s + 1, m_t \leq q_t^*, m_t + q_t \leq \ell_\phi.$$

*Remark 7.4.* (7.5a- $\Psi\text{bnd}$ )-(7.5c- $\Psi\text{bnd}$ ) can be summarized as in (3.10a- $\Psi^\Gamma\text{bnd}$ ) of Corollary 3.2 only for the smooth blending case. For the FE blending case, the bound for the first spatial derivative is weaker by one order in  $\Delta t$ . Furthermore, the bound (7.5d- $\Psi\text{bnd}$ ) requires a stronger limitation on the order of the time derivative for the FE blending than for the smooth blending.

*Proof.* We start with the smooth function blending. By construction of the extension operator, only the space-time mesh  $\mathcal{Q}_h^\Gamma$  needs to be discussed, where  $\Psi = \Psi^\Gamma$ . Hence, all results follow from Corollary 3.2. Next, we note that the same argument applies to  $\mathcal{Q}_h^\Gamma$  for the FE blending. For  $\mathcal{Q}_{h,+}^\Gamma \setminus \mathcal{Q}_h^\Gamma$  with the FE blending, we apply Lemma 7.2 and Lemma 7.1 (at every  $t \in I_n$ ) to gain control over  $\|\partial_t^{m_t} D^{m_s} (\Psi - \text{id}_x)\|_{\infty, \mathcal{Q}_{h,+}^\Gamma \setminus \mathcal{Q}_h^\Gamma} = \|D^{m_s} \mathcal{E}^{\partial\Omega^\Gamma} \partial_t^{m_t} (\Psi^\Gamma - \text{id}_x)\|_{\infty, \mathcal{Q}_{h,+}^\Gamma \setminus \mathcal{Q}_h^\Gamma}$ . The structure of Lemma 7.1 suggests a distinction of cases  $m_s = 2, \dots, q_s + 1$  (case 1),  $m_s = 0$  (case 2) and  $m_s = 1$  (case 3).

Case 1, proof of (7.5d- $\Psi\text{bnd}$ ) for  $m_s = 2, \dots, q_s + 1$ :

We start with applying (7.3b- $\mathcal{E}\text{bnd}$ ) in order to yield for  $m_s = 2, \dots, q_s + 1$

$$(7.6) \quad \begin{aligned} & \|D^{m_s} \partial_t^{m_t} \Psi\|_{\infty, \mathcal{Q}_{h,+}^\Gamma \setminus \mathcal{Q}_h^\Gamma} = \|D^{m_s} \mathcal{E}^{\partial\Omega^\Gamma} \partial_t^{m_t} \Psi^\Gamma\|_{\infty, \mathcal{Q}_{h,+}^\Gamma \setminus \mathcal{Q}_h^\Gamma} \\ & \stackrel{(7.3b\text{-}\mathcal{E}\text{bnd})}{\lesssim} \max_{F \in \mathcal{F}(T)} \sum_{r=m_s}^{q_s+1} \underbrace{h^{r-m_s}}_{\lesssim 1} \|D^r \partial_t^{m_t} \Psi^\Gamma\|_{\infty, F \times I_n} \lesssim 1 \quad \text{by } (3.10c\text{-}\Psi^\Gamma\text{bnd}). \end{aligned}$$

In the last step we exploited Assumption 2.11 so that to bound  $\|D^r \partial_t^{m_t} \Psi^\Gamma\|_{\infty, F \times I_n}$  with (3.10c- $\Psi^\Gamma\text{bnd}$ ) we have for the indices  $r$  and  $m_t$  the bounds  $r \leq q_s + 1$ ,  $m_t \leq q_t + 1$  and  $r + m_t \leq q_s + q_t + 2 \leq \ell_\phi$ .

Case 2, proof of (7.5a- $\Psi\text{bnd}$ ), (7.5b- $\Psi\text{bnd}$ ) and (7.5d- $\Psi\text{bnd}$ ) for  $m_s = 0$ :

$$(7.3a\text{-}\mathcal{E}\text{bnd}) \quad \begin{aligned} & \|\partial_t^{m_t} (\Psi - \text{id}_x)\|_{\infty, \mathcal{Q}_{h,+}^\Gamma \setminus \mathcal{Q}_h^\Gamma} = \|D^0 \mathcal{E}^{\partial\Omega^\Gamma} \partial_t^{m_t} (\Psi^\Gamma - \text{id}_x)\|_{\infty, \mathcal{Q}_{h,+}^\Gamma \setminus \mathcal{Q}_h^\Gamma} \\ & \lesssim \max_{F \in \mathcal{F}(\partial\Omega^\Gamma)} \sum_{r=0}^{q_s+1} h^r \|D^r \partial_t^{m_t} (\Psi^\Gamma - \text{id}_x)\|_{\infty, F \times I_n} + \underbrace{\|\partial_t^{m_t} (\Psi^\Gamma - \text{id}_x)\|_{\infty, \mathcal{V}(\partial\Omega^\Gamma) \times I_n}}_{\lesssim h^2 + \Delta t^{q_t+1-m_t} \text{ by } (3.10b\text{-}\Psi^\Gamma\text{bnd})} \end{aligned}$$

Different values of  $m_t$ , yield the different results: For  $m_t = 0, 1$ , we bound all the summands  $r = 2, \dots, q_s + 1$  by  $h^2$ , again by (3.10c- $\Psi^\Gamma\text{bnd}$ ). The summand for  $r = 0$  can be bounded with  $\lesssim h^2 + \Delta t^{q_t+1-m_t}$  by (3.10a- $\Psi^\Gamma\text{bnd}$ ). The summand  $r = 1$

similarly with  $h(h + \Delta t^{q_t+1-m_t}) \lesssim h^2 + \Delta t^{q_t+1-m_t}$ . This concludes the proofs of (7.5a- $\Psi_{\text{bnd}}$ ) and (7.5b- $\Psi_{\text{bnd}}$ ). For  $m_t = 2, \dots, q_t + 1$ , we combine  $h^r \lesssim 1$  with (3.10c- $\Psi_{\text{bnd}}^\Gamma$ ) (using Assumption 2.11) to yield (7.5d- $\Psi_{\text{bnd}}$ ).

Case 3, proof of (7.5c- $\Psi_{\text{bnd}}$ ) and (7.5d- $\Psi_{\text{bnd}}$ ) for  $m_s = 1$ :

We start by observing

$$(7.7) \quad \begin{aligned} & \|D^1 \mathcal{E}^{\partial\Omega^\Gamma} \partial_t^{m_t} (\Psi^\Gamma - \text{id}_x)\|_{\infty, \mathcal{Q}_{h,\lambda}^\Gamma \setminus \mathcal{Q}_h^\Gamma} \\ & \stackrel{(7.3a-\mathcal{E}_{\text{bnd}})}{\lesssim} \max_{F \in \mathcal{F}(\partial\Omega^\Gamma)} \sum_{r=1}^{q_s+1} h^{r-1} \|D^r \partial_t^{m_t} (\Psi^\Gamma - \text{id}_x)\|_{\infty, F \times I_n} + \frac{1}{h} \overbrace{\|\partial_t^{m_t} (\Psi^\Gamma - \text{id}_x)\|_{\infty, \mathcal{V}(\partial\Omega^\Gamma) \times I_n}}^{\lesssim h^2 + \Delta t^{q_t+1-m_t} \text{ by (3.10b-}\Psi_{\text{bnd}}^\Gamma)} \end{aligned}$$

We first note that – for the purposes of proving (7.5d- $\Psi_{\text{bnd}}$ ) – by Assumption 2.12, we obtain in regards to the last summand  $\frac{1}{h}(h^2 + \Delta t^{q_t+1-m_t}) \lesssim h + \Delta t^{q_t-m_t}$ . Together with  $m_t \leq q_t$  required for the FE blending, the boundedness of this summand follows. In relation to the other summands, we confirm boundedness as before from (3.10c- $\Psi_{\text{bnd}}^\Gamma$ ).  $\square$

We introduce the following Sobolev spaces of space-time functions with weak derivatives of possibly non-uniform degree in space and time: Let  $Q$  be a space-time domain, then we define for  $r, s \in \mathbb{N}$

$$(7.8) \quad H_{\square}^{r,s}(Q) := \{u \mid \partial_t^q D^\alpha u \in L^2(Q), p, q \in \mathbb{N}, p = |\alpha| \leq r, p \leq s\}.$$

We will only need the spaces or corresponding norms for the cases  $(r, s) \in \mathbb{N} \times \{0, 1\} \cup \{0, 1\} \times \mathbb{N}$  in the following.

*Remark 7.5.* The concept of mixed regularities in space and time can further be generalized and refined within the concept of  $t$ -anisotropic Sobolev spaces. In that context, Sobolev spaces  $H^{r,s}$  are typically defined through interpolation between spaces with bounded derivatives for  $(r, 0)$ , i.e. only higher-order spatial derivatives and  $(0, s)$ , i.e. only higher-order temporal derivatives. In our simpler definition (7.8)  $(r, s)$ -regularity implies that also the weak  $(r, s)$ -derivative, i.e. the combined  $r$ -th order spatial and  $s$ -th order temporal derivative, exists. We indicate this stronger notion by the rectangle in the index<sup>6</sup> and note that w.r.t. the standard (isotropic) Sobolev space  $H^m(Q)$  there holds  $H^{r+s}(Q) \subseteq H_{\square}^{r,s}(Q) \subseteq H^{\min(r,s)}(Q)$ .

**COROLLARY 7.6.** *Let  $q_t^* = q_t + 1$  for the smooth and  $q_t^* = q_t$  for the FE blending. There holds*

$$(7.9) \quad \|\Psi\|_{H_{\square}^{q_s+1,1}(\mathcal{Q}_h^n)} + \|\Psi\|_{H_{\square}^{1,q_t^*}(\mathcal{Q}_h^n)} \lesssim 1.$$

**7.4. Space-Time mapping functions.** In the following, we introduce canonical variants of the mappings with a space-time range,  $\Psi^{\text{st}}: \tilde{Q}^n \rightarrow \tilde{Q}^n$  and  $\Theta_h^{\text{st}}: \tilde{Q}^n \rightarrow \tilde{Q}^n$  are the space-time variants of  $\Psi$  and  $\Theta_h$  with

$$(7.10) \quad \Psi^{\text{st}}(x, t) := (\Psi(x, t), t), \quad \Theta_h^{\text{st}}(x, t) := (\Theta_h(x, t), t).$$

In these terms, we also define the discrete space-time domain of integration:

$$(7.11) \quad \mathcal{Q}_h^n := \Theta_h^{\text{st}}(Q^{\text{lin}}), \quad \Omega_h(t) := \Theta_h(\Omega^{\text{lin}}(t), t).$$

<sup>6</sup>as opposed to a triangle that would correspond to the usual  $t$ -anisotropic Sobolev spaces  $H^{r,s}(Q) = H_{\triangle}^{r,s}(Q) := \{u \mid \partial_t^p D^\alpha u \in L^2(Q), p, q \in \mathbb{N}, q = |\alpha|, \frac{q}{r} + \frac{p}{s} \leq 1\}$ .

**7.5. Geometry approximation results.** Taking together results from the previous parts, we obtain a higher-order bound on the difference between  $\Psi$  and  $\Theta_h$ :

**THEOREM 7.7.** *Let  $q_t^* = q_t + 1$  for the smooth and  $q_t^* = q_t$  for the FE blending. Then, for  $(m_s, m_t) \in \{(0, 0), (0, 1), (1, 0)\}$  it holds*

$$(7.12a-\Theta_{h\text{acc}}) \quad \Delta t^{m_t} h^{m_s} \|D^{m_s} \partial_t^{m_t} (\Theta_h - \Psi)\|_{\infty, \mathcal{Q}_h^n} \lesssim h^{q_s+1} + \Delta t^{q_t+1},$$

$$(7.12b-\Theta_{h\text{acc}}) \quad \|\nabla(\Theta_h - \Psi)\|_{\infty, \mathcal{Q}_h^n} \lesssim h^{q_s} + \Delta t^{q_t^*}.$$

Under assumption [Assumption 2.6](#) there further holds

$$(7.12c-\Theta_{h\text{acc}}) \quad \|\partial_t(\Theta_h - \Psi)\|_{\infty, \mathcal{Q}_h^n} \lesssim h^{q_s+1} + \Delta t^{q_t}.$$

*Proof.* First, we observe that for the smooth blending the claims (7.12a- $\Theta_{h\text{acc}}$ ) and (7.12b- $\Theta_{h\text{acc}}$ ) follow directly from (5.15a- $\Theta_h^{\Gamma\text{acc}}$ ) and (5.15b- $\Theta_h^{\Gamma\text{acc}}$ ). In the case of the FE blending the same results are obtained by making use of [Lemma 7.1](#) and [Assumption 2.12](#). For completeness, we give the proof in [Appendix B.7](#). (7.12c- $\Theta_{h\text{acc}}$ ) follows directly from [Lemma 6.4](#) and – in the case of the FE blending – the commuting property of the spatial extension  $\mathcal{E}^{\partial\Omega^\Gamma}$ , cf. [Lemma 7.2](#).  $\square$

Taking the results of this lemma together with [Theorem 7.3](#), we conclude that for  $h$  and  $\Delta t$  sufficiently small, the mapping  $\Phi_h$  introduced as follows is a bijection:

$$(7.13) \quad \Phi_h^{\text{st}} := \Psi^{\text{st}} \circ (\Theta_h^{\text{st}})^{-1}$$

By this definition,  $\Phi_h^{\text{st}}$  translates between the higher-order geometry approximation and the exact domain,  $\Phi_h^{\text{st}}(Q_h^n) = Q^n$ . The previous results imply bounds on  $\Phi_h^{\text{st}}$ :

**COROLLARY 7.8.** *Let  $q_t^* = q_t + 1$  for the smooth and  $q_t^* = q_t$  for the FE blending. Then, it holds for  $(m_s, m_t) \in \{(0, 0), (0, 1), (1, 0)\}$*

$$(7.14a-\Phi_h^{\text{st}\text{bnd}}) \quad \Delta t^{m_t} h^{m_s} \|D^{m_s} \partial_t^{m_t} (\Phi_h^{\text{st}} - \text{id}_x)\|_{\infty, \mathcal{Q}_h^n} \lesssim h^{q_s+1} + \Delta t^{q_t+1}.$$

$$(7.14b-\Phi_h^{\text{st}\text{bnd}}) \quad \|\nabla \Phi_h^{\text{st}} - \text{Id}_x\|_{\infty, \bar{Q}^n} \lesssim h^{q_s} + \Delta t^{q_t^*},$$

If further [Assumption 2.6](#) holds, there is

$$(7.14c-\Phi_h^{\text{st}\text{bnd}}) \quad \|\partial_t \Phi_h^{\text{st}}\|_{\infty, \bar{Q}^n} \lesssim h^{q_s+1} + \Delta t^{q_t}.$$

*Proof.* We observe that  $\Phi_h^{\text{st}} - \text{id}_x = (\Psi^{\text{st}} - \Theta_h^{\text{st}}) \circ (\Theta_h^{\text{st}})^{-1}$ . Then, with [Theorem 7.3](#) and [Theorem 7.7](#), we obtain boundedness of  $\Theta_h^{\text{st}}$  as well as of  $(\Theta_h^{\text{st}})^{-1}$ , and the result follows from (7.12a- $\Theta_{h\text{acc}}$ )-(7.12c- $\Theta_{h\text{acc}}$ ).  $\square$

**7.6. Properties of  $\Theta_h$ .** Note that due to a triangle inequality, taking into account (7.12a- $\Theta_{h\text{acc}}$ )-(7.12c- $\Theta_{h\text{acc}}$ ) and (7.5c- $\Psi_{\text{bnd}}$ ) we can conclude the following bound on the difference between  $\Theta_h$  and  $\text{id}_x$ :

**COROLLARY 7.9.** *Let  $q_t^* = q_t + 1$  for the smooth and  $q_t^* = q_t$  for the FE blending. Then, there holds*

$$(7.15) \quad \|\Theta_h^{\text{st}} - \text{id}_x\|_{\infty, \bar{Q}^n} \lesssim h^2 + \Delta t^{q_t+1}, \quad \|\nabla \Theta_h^{\text{st}} - \text{Id}_x\|_{\infty, \bar{Q}^n} \lesssim h + \Delta t^{q_t^*}.$$

This implies that the norm of a function defined on  $\Omega^{\text{lin}}(t)$  or  $Q^{\text{lin}}$  is equivalent to the function lifted to  $\Omega_h(t)$  or  $Q_h^n$ , respectively, in accordance with  $\Theta_h$ :

**LEMMA 7.10.** *Let  $w \in L^2(Q^{\text{lin}})$  and  $v_t \in L^2(\Omega^{\text{lin}}(t))$  for  $t \in I_n$ . Then it holds*

$$(7.16) \quad \|w\|_{Q^{\text{lin}}} \simeq \|w \circ (\Theta_h^{\text{st}})^{-1}\|_{Q_h^n}, \quad \|v_t\|_{\Omega^{\text{lin}}(t)} \simeq \|v_t \circ \Theta_h(\cdot, t)^{-1}\|_{\Omega_h(t)}$$

*Proof.* From [Corollary 7.9](#), we have  $\det(\nabla \Theta_h^{\text{st}}) = 1 + \mathcal{O}(h + \Delta t^{q_t})$ .  $\square$

**7.7. An identity about the discrete space-time normal.** We define the outward pointing *space-time normals* to the space-time domains  $Q^n$  and  $Q_h^n$  on the *spatial* boundary as  $n$  and  $n_h$  respectively. We can give bounds between the difference of these two normals (after lifting them on the same domain):

LEMMA 7.11. *With Assumption 2.6 there holds*

$$(7.17) \quad \|n \circ \Phi_h^{\text{st}} - n_h\|_{\infty, \partial^s Q_h^n} \lesssim h^{q_s} + \Delta t^{q_t}.$$

*Proof.* We start with the same argument as given above of [29, Eq. (A.20)], which builds on the observation that the tangent space is transported by the mapping  $\Phi_h^{\text{st}}$ : Fix a point  $(x, t) \in \partial^s Q^h$  and let  $t_1, \dots, t_d$  be an orthonormal basis of  $n_h^\perp$ . The tangent space to  $\partial^s Q = \Phi_h^{\text{st}}(\partial^s Q^h)$  is given by  $\text{span}\{D_{\mathbf{x},t}\Phi_h^{\text{st}}(x, t)t_j \mid 1 \leq j \leq d\} = n^\perp$ . Hence, we have  $n(\Phi_h^{\text{st}}(x, t)) \in \text{span}\{(D_{\mathbf{x},t}\Phi_h^{\text{st}}(x, t))^{-T}n_h\}$ , so that we can write  $n \circ \Phi_h^{\text{st}} = (D_{\mathbf{x},t}\Phi_h^{\text{st}})^{-T}n_h / \|(D_{\mathbf{x},t}\Phi_h^{\text{st}})^{-T}n_h\|$ . With the help of Corollary 7.8, we have  $(D_{\mathbf{x},t}\Phi_h^{\text{st}})^{-T} = \text{Id}_{x,t} + \mathcal{O}(h^{q_s} + \Delta t^{q_t})$  from which we obtain the claim after a triangle inequality.

*Remark 7.12.* Without Assumption 2.6 an additional term  $h^{q_s+1}/\Delta t$  would enter from the estimates in Corollary 7.8 yielding a worse estimate of the form  $\|n \circ \Phi_h^{\text{st}} - n_h\|_{\infty, \partial^s Q_h^n} \lesssim h^{q_s} + \Delta t^{q_t} + h^{q_s+1}/\Delta t$ .

**8. Interpolation on  $\Psi$ -deformed space-time meshes.** In the analysis of numerical discretizations in the isoparametric setting, we have a mismatch in the domains of definition, as the solution  $u$  is defined on the physical domain, whereas discrete functions are fundamentally defined on  $Q^{\text{lin}} / Q_h^n$ . As the function  $\Psi$  maps from the piecewise linear reference geometry to the exact geometry, it is instructive to search for a discrete variant of the function  $\hat{u} = u^e \circ \Psi^{\text{st}}$ , for an extension  $u^e$  of  $u$ . To obtain this approximation, we will apply a result from [33] and discuss the relevant implications in relation to the geometry approximation.

Note that the domain of definition of  $\hat{u}$  depends on the physical problem of interest. In a surface problem, it would be reasonable to use the set  $Q_{h1}^\Gamma := \bigcup_{T \in \mathcal{T}_{b1}^\Gamma} T \times I_n$  as the smallest set of complete elements containing all relevant information. For a bulk problem, the following sets serve the purpose of the domain of definition

$$(8.1) \quad Q_\mathcal{E}^{\text{lin}} := \bigcup \{T \times I_n \mid (T \times I_n) \cap Q^{\text{lin}} \neq \emptyset\}, \quad \Omega_\mathcal{E}^{\text{lin}} := \bigcup \{T \mid (T \times I_n) \cap Q^{\text{lin}} \neq \emptyset\}.$$

From now on, we adopt the point of view of the bulk problem and interpolate on  $Q_\mathcal{E}^{\text{lin}}$ , but the respective results on the smaller set  $Q_{h1}^\Gamma$  follow.

We now show interpolation results on the space-time domain  $Q_\mathcal{E}^{\text{lin}}$ .

LEMMA 8.1. *There exists an interpolation operator  $\Pi_W^n : L^2(Q_\mathcal{E}^{\text{lin}}) \rightarrow V_h^{k_s, k_t}(Q_\mathcal{E}^{\text{lin}})$ , s.t. for all functions  $\hat{u} \in L^2(Q_\mathcal{E}^{\text{lin}})$  with sufficient regularity, s.t. the r.h.s. expressions in the following estimates are well-defined and bounded, there holds for the interpolation error  $\hat{e}_u = \hat{u} - \Pi_W^n \hat{u}$  and  $\ell_s \in \{1, \dots, k_s + 1\}$ ,  $\ell_t \in \{1, \dots, k_t + 1\}$ :*

$$(8.2a) \quad \|\hat{e}_u\|_{Q_\mathcal{E}^{\text{lin}}} \lesssim \Delta t^{\ell_t} \|\hat{u}\|_{H_{\square}^{0, \ell_t}(Q_\mathcal{E}^{\text{lin}})} + h^{\ell_s} \|\hat{u}\|_{H_{\square}^{\ell_s, 0}(Q_\mathcal{E}^{\text{lin}})},$$

$$(8.2b) \quad \|\partial_t \hat{e}_u\|_{Q_\mathcal{E}^{\text{lin}}} \lesssim \Delta t^{\ell_t-1} \|\hat{u}\|_{H_{\square}^{0, \ell_t}(Q_\mathcal{E}^{\text{lin}})} + h^{\ell_s} \|\hat{u}\|_{H_{\square}^{\ell_s, 1}(Q_\mathcal{E}^{\text{lin}})} \quad \text{if } \ell_t \geq 2,$$

$$(8.2c) \quad \|\nabla \hat{e}_u\|_{Q_\mathcal{E}^{\text{lin}}} \lesssim \Delta t^{\ell_t} \|\hat{u}\|_{H_{\square}^{1, \ell_t}(Q_\mathcal{E}^{\text{lin}})} + h^{\ell_s-1} \|\hat{u}\|_{H_{\square}^{\ell_s, 0}(Q_\mathcal{E}^{\text{lin}})} \quad \text{if } \ell_s > 2,$$

$$(8.2d) \quad \|\hat{e}_u(\cdot, t_n)\|_{\Omega_\mathcal{E}^{\text{lin}}} \lesssim \Delta t^{\ell_t-\frac{1}{2}} \|\hat{u}\|_{H_{\square}^{0, \ell_t}(Q_\mathcal{E}^{\text{lin}})} + \Delta t^{-\frac{1}{2}} h^{\ell_s} \|\hat{u}\|_{H_{\square}^{\ell_s, 0}(Q_\mathcal{E}^{\text{lin}})} \quad \text{if } \ell_t \geq 2.$$

*Proof.* We apply [33, Theorem 3.18 and Lemma 3.21]. Note that we choose the polygonal spatial domain  $\Omega_{\mathcal{E}}^{\text{lin}}$ , which corresponds to  $\Omega$  internally in [33, Sec. 3.3].  $\square$

This result asks for upper bounds for  $\|\hat{u}\|_{H_{\square}^{0,\ell_t}(Q_{\mathcal{E}}^{\text{lin}})}$ ,  $\|\hat{u}\|_{H_{\square}^{\ell_s,0}(Q_{\mathcal{E}}^{\text{lin}})}$ , as well as for  $\|\nabla\hat{u}\|_{H_{\square}^{0,\ell_t}(Q_{\mathcal{E}}^{\text{lin}})}$  and  $\|\partial_t\hat{u}\|_{H_{\square}^{\ell_s,0}(Q_{\mathcal{E}}^{\text{lin}})}$ . Those will be influenced both by the regularity of  $\hat{u}$ . For  $\hat{u} = u^e \circ \Psi^{\text{st}}$  this regularity crucially also depends on  $\Psi^{\text{st}}$  where we need the bounds derived before.

LEMMA 8.2. *Bounds on higher-order spatial or temporal derivatives of  $\Psi^{\text{st}}$  imply bounds on higher-order derivatives of  $u^e \circ \Psi^{\text{st}}$  by norms of  $u^e$  as follows for  $\ell_t, \ell_s \in \mathbb{N}$ :*

$$(8.3a) \quad \|\Psi^{\text{st}}\|_{H_{\square}^{0,\ell_t}(Q_{\mathcal{E}}^{\text{lin}})} \lesssim 1 \quad \implies \quad \|u^e \circ \Psi^{\text{st}}\|_{H_{\square}^{0,\ell_t}(Q_{\mathcal{E}}^{\text{lin}})} \lesssim \|u^e\|_{H^{\ell_t}(\Psi^{\text{st}}(Q_{\mathcal{E}}^{\text{lin}}))},$$

$$(8.3b) \quad \|\Psi^{\text{st}}\|_{H_{\square}^{\ell_s,0}(Q_{\mathcal{E}}^{\text{lin}})} \lesssim 1 \quad \implies \quad \|u^e \circ \Psi^{\text{st}}\|_{H_{\square}^{\ell_s,0}(Q_{\mathcal{E}}^{\text{lin}})} \lesssim \|u^e\|_{H^{\ell_s}(\Psi^{\text{st}}(Q_{\mathcal{E}}^{\text{lin}}))},$$

$$(8.3c) \quad \|\Psi^{\text{st}}\|_{H_{\square}^{\ell_s,1}(Q_{\mathcal{E}}^{\text{lin}})} \lesssim 1 \quad \implies \quad \|\partial_t(u^e \circ \Psi^{\text{st}})\|_{H_{\square}^{\ell_s,0}(Q_{\mathcal{E}}^{\text{lin}})} \lesssim \|u^e\|_{H^{\ell_s+1}(\Psi^{\text{st}}(Q_{\mathcal{E}}^{\text{lin}}))},$$

$$(8.3d) \quad \|\Psi^{\text{st}}\|_{H_{\square}^{1,\ell_t}(Q_{\mathcal{E}}^{\text{lin}})} \lesssim 1 \quad \implies \quad \|\nabla(u^e \circ \Psi^{\text{st}})\|_{H_{\square}^{0,\ell_t}(Q_{\mathcal{E}}^{\text{lin}})} \lesssim \|u^e\|_{H^{\ell_t+1}(\Psi^{\text{st}}(Q_{\mathcal{E}}^{\text{lin}}))}.$$

*Proof.* The proof relies on a Faa di Bruno formula in combination with the l.h.s. bounds. The proof is given in Appendix B.8 for completeness.  $\square$

The previous two results do not depend on the results of the previous sections but display the need and purpose of the higher-order bounds on  $\Psi^{\text{st}}$ . Combining the bounds for  $\Psi^{\text{st}}$  with the interpolation results, allows to derive interpolation results for isoparametrically mapped space-time FE spaces for space-time discretizations.

**9. Numerical examples.** We conclude the paper with a section on numerical experiments. Note that in [19], we already studied numerically convection-diffusion discretisations involving our geometry approximation with FE blending. Hence, we complement these results with some further numerical investigations.

All experiments are performed with `ngsxfem` [25], an unfitted FE extension of `ngsolve`. Reproduction data are available at <https://gitlab.gwdg.de/fabian.heimann/repro-ho-unf-space-time-fem-geom>. The linear systems are solved with the direct solvers `umfpack` and `pardiso` of IntelMKL.

To fix a specific setting, we choose a polynomial order parameter  $k = 1, \dots, 6$  and set all geometry approximation and discrete FE space orders to this,  $k = k_s = k_t = q_s = q_t$ . Similarly, we focus in the first subsections on simultaneous space-time refinements, i.e. we introduce parameters  $i = i_s = i_t$ , where the time step  $\Delta t$  and the mesh size  $h$  satisfy  $\Delta t = T \cdot 2^{-i_t-2}$ ,  $h = 0.9 \cdot 2^{-i_s}$ . For the evolving geometry, we use the first example of [19], where a circular geometry in 2D deforms into a kite. It is described in terms of the following level set function  $\phi$

$$\rho(t, y) = (1 - y^2) \cdot t, \quad r = \sqrt{(x - \rho)^2 + y^2}, \quad \phi = r - r_0, \quad r_0 = 1,$$

where  $\tilde{\Omega} = [-1.6, 2.1] \times [-1.6, 1.6]$ ,  $T = 0.5$ . We use unstructured simplicial meshes of the maximal mesh size  $h$  given above.

For the smooth blending function, we use the following construction: Fixing a smoothness order parameter  $s \in \mathbb{N}$  we define  $b$  for a blending width parameter  $w_b$ :

$$(9.1) \quad b = \begin{cases} 0 & \text{if } |\phi| \leq w_b, \\ 1 & \text{if } 2w_b < |\phi|, \text{ with } \pi_s(x) = \begin{cases} 2^{s-1}x^s & \text{if } x \leq \frac{1}{2} \\ 1 - 2^{s-1}(1-x)^s & \text{else.} \end{cases} \\ \pi_s\left(\frac{|\phi| - w_b}{w_b}\right) & \text{else,} \end{cases}$$



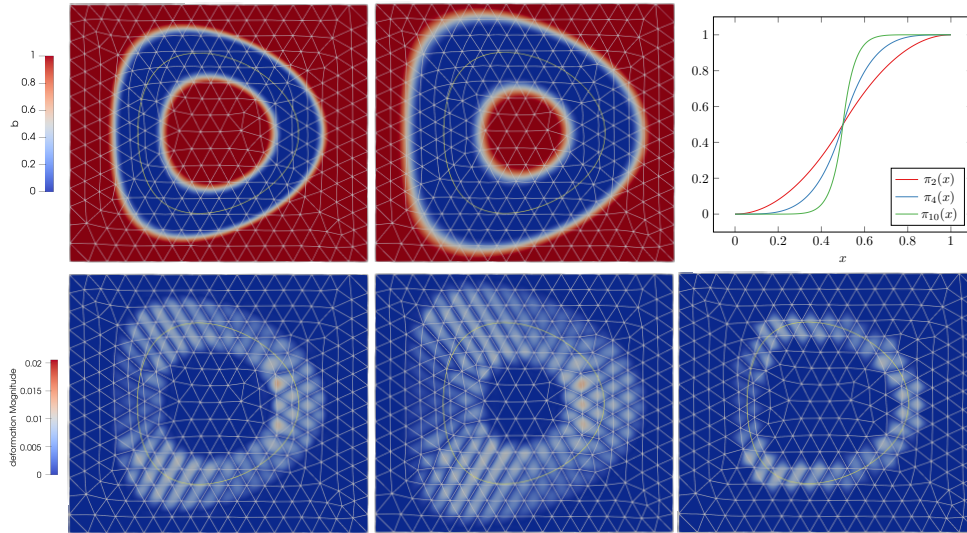


FIG. 7. Upper row left and middle: Two examples of blending functions  $b$  at a fixed time for increasing values of  $w_b$ . Upper row right: Examples of the function  $\pi_s$  involved in the definition of  $b$  in terms of  $\phi$ , (9.1). Bottom row left and middle: Absolute value of the deformation stemming from the smooth blending functions respectively above. Bottom row right: Absolute value of the deformation from the FE blending for the same discretisation parameters and a small time step.

We show examples of this blending function with the resulting deformation magnitudes in Figure 7, as well as a plot of  $\pi_s$ .

We note that in view of the analysis, the blending width needs to be chosen sufficiently large ( $w_b \gtrsim h$ ) so that all cut elements of a time slice have vanishing  $b$ , cf. first point of Assumption 2.13. Numerically, we also include studies where cut elements are only partially contained in the region with vanishing  $b$ .

**9.1. Geometrical Accuracy.** In the first numerical experiment, we want to study the geometrical accuracy of the suggested method. We measure numerically the distance between the numerical domain and the exact geometry on  $\partial\Omega_h(t)$ . To this end, we take the maximal value of the exact level-set function on the discrete higher-order geometry  $\partial\Omega_h(t)$ . As the chosen level-set function is a signed distance function up to a constant this yields a proper distance measure that we denote by  $\text{dist}^*$  which is equivalent to the Euclidean distance. In Figure 8 we observe for the chosen (equal) orders and refinements in space and time and with the smooth blending that  $\max_{t \in I_n} \text{dist}^*(\partial\Omega_h(t), \partial\Omega(t)) \lesssim h^{k+1} \simeq \Delta t^{k+1}$  which is in agreement with the theoretical predictions from Corollary 7.8. We note that this study for the FE blending was already included in [19] with similar results. We conclude that for the geometry approximation at the interface, both blending options work properly.

**9.2. Interpolation Quality.** As the next step, we solve a Ghost-penalty ([7, 8, 33, 17]) stabilized  $L^2$  projection problem for a function  $u = \cos(\pi \frac{t}{\tau_0}) \cdot \sin(\pi t)$ . The discrete approximation  $u_h \in V_h^{k_s, k_t}(Q_{\mathcal{E}}^{\text{lin}}) \circ \Theta_h^{\text{st}-1}$  solves  $a(u_h, v_h) = (u_h, v_h)_{Q_h^n} + J(u_h, v_h) = (u, v_h)_{Q_h^n}$  for all  $v_h \in V_h^{k_s, k_t}(Q_{\mathcal{E}}^{\text{lin}}) \circ \Theta_h^{\text{st}-1}$ . where  $J(\cdot, \cdot)$  is defined as in [19] but without the  $\frac{1}{h^2}$  scaling. We measure the numerical error in this refinement process in terms of the norms:  $\|\cdot\|_{L^2(\Omega_h(T))}$ , and  $\|\cdot\|_{L^2(\mathcal{Q}_h)}$  with  $\mathcal{Q}_h = \bigcup_n Q_h^n$ . With these two  $L^2$  norms, we choose two reasonable candidate norms for a first investigation, but of course also gradients in space or time derivatives could be included. (See

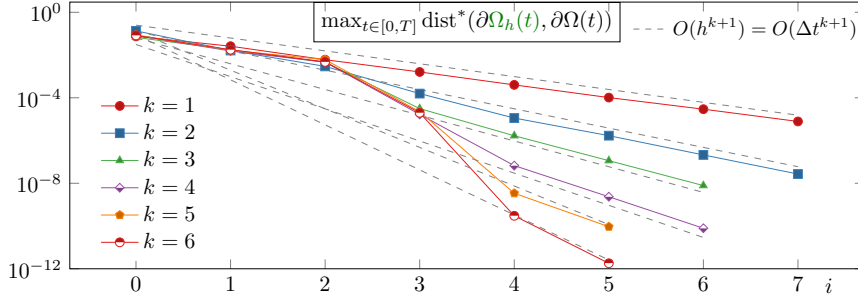


FIG. 8. Convergence of geometrical accuracy in terms of  $\text{dist}^*$  for simultaneous space and time refinements for the smooth blending on the kite geometry,  $s = 4$ ,  $w_b = 0.1$ .

e.g. [33]) We observe the results shown in Table 1. As the function  $u$  is smooth,

$k$	$i$	FE blending		smooth blend., $w_b = 0.1$		smooth blend., $w_b = 0.2$	
		err: $L^2(T), L^2(Q_h)$	(eoc)	err: $L^2(T), L^2(Q_h)$	(eoc)	err: $L^2(T), L^2(Q_h)$	(eoc)
2	0	$1.24 \cdot 10^{-1}$	$6.22 \cdot 10^{-2}$	$1.41 \cdot 10^{-1}$	$6.59 \cdot 10^{-2}$	$1.51 \cdot 10^{-1}$	$6.75 \cdot 10^{-2}$
	1	$3.13 \cdot 10^{-2}$	$1.42 \cdot 10^{-2}$	$3.56 \cdot 10^{-2}$	$1.61 \cdot 10^{-2}$	$3.30 \cdot 10^{-2}$	$1.57 \cdot 10^{-2}$
	2	$3.85 \cdot 10^{-3}$	$1.65 \cdot 10^{-3}$	$4.41 \cdot 10^{-3}$	$1.73 \cdot 10^{-3}$	$3.09 \cdot 10^{-3}$	$1.32 \cdot 10^{-3}$
	3	$4.01 \cdot 10^{-4}$	$1.67 \cdot 10^{-4}$	$3.39 \cdot 10^{-4}$	$1.36 \cdot 10^{-4}$	$2.72 \cdot 10^{-4}$	$1.21 \cdot 10^{-4}$
	4	$4.25 \cdot 10^{-5}$	$1.83 \cdot 10^{-5}$	$3.46 \cdot 10^{-5}$	$1.55 \cdot 10^{-5}$	$3.11 \cdot 10^{-5}$	$1.41 \cdot 10^{-5}$
	5	$4.99 \cdot 10^{-6}$	$2.17 \cdot 10^{-6}$	$4.25 \cdot 10^{-6}$	$1.91 \cdot 10^{-6}$	$3.79 \cdot 10^{-6}$	$1.74 \cdot 10^{-6}$
4	0	$3.66 \cdot 10^{-2}$	$2.16 \cdot 10^{-2}$	$1.03 \cdot 10^{-1}$	$3.78 \cdot 10^{-2}$	$1.07 \cdot 10^{-1}$	$4.34 \cdot 10^{-2}$
	1	$1.96 \cdot 10^{-3}$	$9.39 \cdot 10^{-4}$	$1.18 \cdot 10^{-2}$	$5.88 \cdot 10^{-3}$	$2.15 \cdot 10^{-2}$	$8.60 \cdot 10^{-3}$
	2	$5.91 \cdot 10^{-5}$	$2.61 \cdot 10^{-5}$	$3.78 \cdot 10^{-3}$	$1.38 \cdot 10^{-3}$	$8.18 \cdot 10^{-4}$	$4.62 \cdot 10^{-4}$
	3	$7.13 \cdot 10^{-7}$	$2.33 \cdot 10^{-7}$	$1.24 \cdot 10^{-4}$	$3.52 \cdot 10^{-5}$	$3.48 \cdot 10^{-6}$	$1.45 \cdot 10^{-6}$
	4	$1.41 \cdot 10^{-8}$	$4.90 \cdot 10^{-9}$	$4.82 \cdot 10^{-7}$	$1.84 \cdot 10^{-7}$	$9.91 \cdot 10^{-8}$	$4.14 \cdot 10^{-8}$
	5	$3.38 \cdot 10^{-10}$	$1.17 \cdot 10^{-10}$	$1.52 \cdot 10^{-8}$	$5.61 \cdot 10^{-9}$	$2.90 \cdot 10^{-9}$	$1.15 \cdot 10^{-9}$
6	0	$2.04 \cdot 10^{-2}$	$8.75 \cdot 10^{-3}$	$5.84 \cdot 10^{-2}$	$2.27 \cdot 10^{-2}$	$1.30 \cdot 10^{-1}$	$4.23 \cdot 10^{-2}$
	1	$7.71 \cdot 10^{-4}$	$3.64 \cdot 10^{-4}$	$1.89 \cdot 10^{-2}$	$7.86 \cdot 10^{-3}$	$8.72 \cdot 10^{-3}$	$5.16 \cdot 10^{-3}$
	2	$4.09 \cdot 10^{-5}$	$8.95 \cdot 10^{-6}$	$2.22 \cdot 10^{-3}$	$1.06 \cdot 10^{-3}$	$9.44 \cdot 10^{-4}$	$2.48 \cdot 10^{-4}$
	3	$1.21 \cdot 10^{-8}$	$2.62 \cdot 10^{-9}$	$7.49 \cdot 10^{-5}$	$2.49 \cdot 10^{-5}$	$9.27 \cdot 10^{-7}$	$3.32 \cdot 10^{-7}$
	4	$2.30 \cdot 10^{-11}$	$4.94 \cdot 10^{-12}$	$1.22 \cdot 10^{-7}$	$4.53 \cdot 10^{-8}$	$2.05 \cdot 10^{-8}$	$7.48 \cdot 10^{-9}$

TABLE 1

Numerical results for stabilized  $L^2$  projection problem on unfitted domain approximated isoparametrically. The function  $u$  is smooth and the discretisation orders in space and time, and the respective geometry approximation orders are chosen to be  $k$ , and  $i$  denotes simultaneous refinements in space and time. In the columns, different blending options are used: The FE blending, and two variants of the smooth blending with  $w_b \in \{0.1, 0.2\}$  and  $s = 4$ . Estimated orders of convergence are calculated based on the  $L^2(Q_h)$ -norm. See Table 2 for  $k \in \{1, 3, 5\}$ , and Table 3 for  $k = 4, s = 10$ .

and we chose the geometry approximation and discrete function space orders to be  $k = k_s = k_t = q_s = q_t$ , we expect e.g. for the  $L^2(Q_h)$ -norm from Lemma 8.1 in combination of the boundedness of the according norms of  $\hat{u}$  by means of Lemma 8.2 and Corollary 7.6 that for the smooth blending

$$\|u^e - u_h\|_{Q_h} \lesssim h^{\max(q_s, k_s)+1} + \Delta t^{\max(q_t, k_t)+1} \simeq h^{k+1} \simeq \Delta t^{k+1},$$

and for the FE blending

$$\|u^e - u_h\|_{Q_h} \lesssim h^{\max(q_s, k_s)+1} + \Delta t^{\max(q_t, k_t)+1} \simeq h^{k+1} + \Delta t^k.$$

Numerically, after a slightly different behavior in the pre-asymptotic regime, we observe that in all cases

$$\|u^\varepsilon - u_h\|_{\mathcal{Q}_h} \lesssim h^{k+1} \simeq \Delta t^{k+1}.$$

This confirms the mathematical analysis for the smooth blending. For the **FE** blending, we obtain similar results, so that the theoretical loss of one order in time is not showing in the particular example.

*Remark 9.1* (Approximation in the  $L^2(T)$  norm). In [Table 1](#), we have also included results for the respective numerical interpolation errors in the  $L^2(T)$  norm. Numerically, we observe the same convergence orders in this norms as with the  $L^2(\mathcal{Q}_h)$  space-time norm, i.e. errors of order  $\mathcal{O}(h^{k+1}) \simeq \mathcal{O}(\Delta t^{k+1})$ . Our theoretical results would guarantee only  $\mathcal{O}(h^{k+\frac{1}{2}}) \simeq \mathcal{O}(\Delta t^{k+\frac{1}{2}})$ , cf. [Lemma 8.1](#).

**9.3. Boundedness of  $\nabla\Psi$  under general space-time refinements for the **FE** blending.** In this section, we want to investigate numerically if specifically the refinement restriction of [Assumption 2.12](#) is necessary in the case of the **FE** blending. To this end, we fix a large time step,  $\Delta t = T$  (one time step) or  $\Delta t = T/2$  (two time steps), for the kite geometry and refine the mesh with  $h = 0.9 \cdot 0.5^{i_s}$  for  $i = i_s = 1, 2, \dots$ . Considering the proof of [Theorem 7.3](#), one would expect that potentially for fine meshes, a temporal error scaled by  $\frac{1}{h}$  might result in an unbounded summand for e.g. the upper bound on  $\|\nabla\Psi\|_\infty$ . This, in turn, could become problematic for the interpolation procedure. To investigate whether we can observe this behavior in practice, we calculate a numerical approximation of  $\Psi$  as follows: First, we use integration points of a third-order numerical integration on the cut elements  $\mathcal{T}_{b_1}^\Gamma \times I_n$  as sample points to calculate  $d$  explicitly from its definition by a Newton search (based on the given level set  $\phi$ ). Next, we use these sampled points to derive an approximate discrete function  $\tilde{d}$  by solving a **FE** interpolation problem. Finally, we combine this function with the exact  $G$ , and apply the blending procedure (which implicitly follows from setting a discrete function on  $\mathcal{T}_{b_1}^\Gamma$ ) and calculate  $\|\nabla\tilde{\Psi}\|_\infty$  of this function. As a numerical compromise, we focus on one intermediate time level for each  $I_n$  to construct  $\tilde{\Psi}$  and calculate  $\|\nabla\tilde{\Psi}\|_\infty$ . Two results are shown in [Figure 9](#). We observe that asymptotically,  $\|\nabla\tilde{\Psi}\|_\infty$  scales as  $\frac{1}{h}$ , whereas the error of the  $L^2$  interpolation problem remains constant. We conclude that the assumption [Assumption 2.12](#) seems necessary to avoid unbounded spatial gradients of  $\tilde{\Psi}$  (and hence  $\Psi$ ), although the interpolation error might not deteriorate immediately. Let us stress that very fine spatial meshes were necessary to trigger the problem. We note in passing that the behavior of  $\|\nabla\Theta_h\|_\infty$  is different from  $\Psi$ , we observe a norm decay with  $\mathcal{O}(h)$ .

**10. Conclusion and Outlook.** We have presented a strategy to solve the problem of higher-order numerical integration on implicitly defined (smooth) space-time domains, arising within the context of unfitted space-time discretisations on moving domains. Crucial for the strategy are two space-time mesh deformations, a computable mesh deformation  $\Theta_h^{\text{st}}$  and an ideal mesh deformation  $\Psi^{\text{st}}$ , which is not computationally feasible. The focus of this work is the detailed and rigorous analysis of the geometry approximation approach which revealed important properties such as proximity and boundedness which are important to understand the geometrical approximation and interpolation properties of **FE** methods on the deformed meshes.

A major output of this study is collected in [Theorem 7.7](#) which gives bounds on the proximity of  $\Psi^{\text{st}}$  and  $\Theta_h^{\text{st}}$  (in different norms). Notable is the dependence of these results – especially for the anisotropic cases where  $\Delta t \not\propto h$  – on the chosen

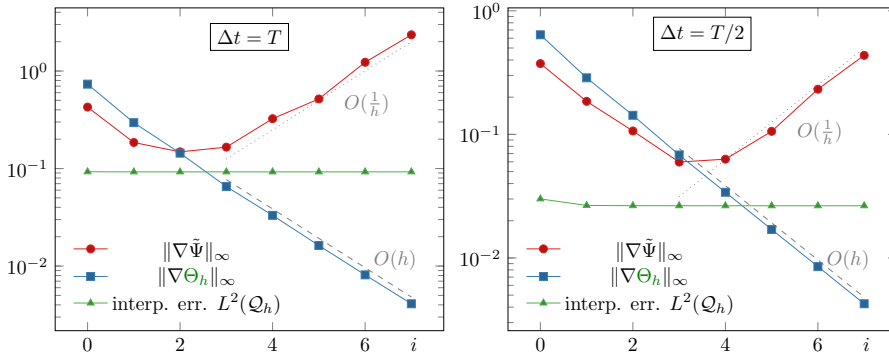


FIG. 9. Numerical studies about  $\|\nabla\tilde{\Psi}\|_\infty$  and  $\|\nabla\Theta_h\|_\infty$  for the FE blending in the limit  $h \rightarrow 0$  and  $\Delta t$  large and fixed. In both cases,  $\|\nabla\Theta_h\|_\infty$  scales with  $O(h)$ , and  $\|\nabla\tilde{\Psi}\|_\infty$  with  $O(\frac{1}{h})$ . The corresponding interpolation error remains constant.

blending from deformations on cut elements to the exterior. Only the *smooth* blending yields optimal results here, whereas the FE blending can slightly suffer from a mesh-dependent decay of the mesh deformation. Proximity and the effect of the different blendings are also studied and validated numerically.

A second output of major importance in this study is the boundedness of  $\Psi^{\text{st}}$  in higher-order derivatives which directly relates to the application of (optimal) space-time interpolation estimates. The corresponding results are collected in Corollary 7.6. Also here, we observe a dependence on the chosen blending.

Both the geometry approximation and interpolation results can now be taken into account in the rigorous mathematical analysis of unfitted space-time discretisations for different problems. In particular, we will apply the techniques to the DG discretisation in [19] in upcoming work. Apart from this method for a bulk convection-diffusion problem, the structures proven in this paper can be applied similarly to other problems, such as surface problems (see e.g. [35, 34]) or multi-domain problems (see e.g. [33]).<sup>7</sup>

#### REFERENCES

- [1] M. ANSELMANN AND M. BAUSE, *CutFEM and ghost stabilization techniques for higher order space-time discretizations of the Navier-Stokes equations*, (2021), <https://arxiv.org/abs/2103.16249>.
- [2] M. ANSELMANN AND M. BAUSE, *Higher order Galerkin-collocation time discretization with Nitsche's method for the Navier-Stokes equations*, Math. Comput. Simul., 189 (2021), pp. 141–162, <https://doi.org/10.1016/j.matcom.2020.10.027>.
- [3] S. BADIA, H. DILIP, AND F. VERDUGO, *Space-time unfitted finite element methods for time-dependent problems on moving domains*, Computers & Mathematics with Applications, 135 (2023), pp. 60–76, <https://doi.org/https://doi.org/10.1016/j.camwa.2023.01.032>, <https://www.sciencedirect.com/science/article/pii/S089812212300038X>.
- [4] C. BERNARDI, *Optimal finite-element interpolation on curved domains*, SIAM Journal on Numerical Analysis, 26 (1989), pp. 1212–1240, <https://doi.org/10.1137/0726068>, <https://doi.org/10.1137/0726068>.
- [5] P. BRANDNER, T. JANKUHN, S. PRAETORIUS, A. REUSKEN, AND A. VOIGT, *Finite element discretization methods for velocity-pressure and stream function formulations of surface stokes equations*, SIAM Journal on Scientific Computing, 44 (2022), pp. A1807–A1832, <https://doi.org/10.1137/21M1403126>, <https://doi.org/10.1137/21M1403126>, <https://arxiv.org/abs/https://doi.org/10.1137/21M1403126>.

<sup>7</sup>To see how the corresponding geometry analysis for the merely spatial problem, [29], finds application to a range of different problems, we refer the reader to [24], [15], and [26].

- [6] S. C. BRENNER AND L. R. SCOTT, *The mathematical theory of finite element methods*, Springer, 2008.
- [7] E. BURMAN, *Ghost penalty*, C.R. Math. Acad. Sci. Paris, 348 (2010), pp. 1217–1220, <https://doi.org/10.1016/j.crma.2010.10.006>.
- [8] E. BURMAN, S. CLAUS, P. HANSBO, M. G. LARSON, AND A. MASSING, *Cutfem: discretizing geometry and partial differential equations*, Int. J. Numer. Methods Eng., 104 (2015), pp. 472–501, <https://doi.org/10.1002/nme.4823>.
- [9] E. BURMAN, S. FREI, AND A. MASSING, *Eulerian time-stepping schemes for the non-stationary Stokes equations on time-dependent domains*, Numer. Math., (2022), <https://doi.org/10.1007/s00211-021-01264-x>.
- [10] P. CIARLET AND P.-A. RAVIART, *Interpolation theory over curved elements, with applications to finite element methods*, Computer Methods in Applied Mechanics and Engineering, 1 (1972), pp. 217–249, [https://doi.org/10.1016/0045-7825\(72\)90006-0](https://doi.org/10.1016/0045-7825(72)90006-0), <https://www.sciencedirect.com/science/article/pii/0045782572900060>.
- [11] G. M. CONSTANTINE AND T. H. SAVITS, *A multivariate faa di bruno formula with applications*, Transactions of the American Mathematical Society, 348 (1996), pp. 503–520, <http://www.jstor.org/stable/2155187> (accessed 2023-02-06).
- [12] T. FRACHON AND S. ZAHEDI, *A cut finite element method for incompressible two-phase navier–stokes flows*, Journal of Computational Physics, 384 (2019), pp. 77–98, <https://doi.org/https://doi.org/10.1016/j.jcp.2019.01.028>, <https://www.sciencedirect.com/science/article/pii/S0021999119300798>.
- [13] T. FRACHON AND S. ZAHEDI, *A cut finite element method for two-phase flows with insoluble surfactants*, Journal of Computational Physics, 473 (2023), p. 111734, <https://doi.org/https://doi.org/10.1016/j.jcp.2022.111734>, <https://www.sciencedirect.com/science/article/pii/S0021999122007975>.
- [14] T.-P. FRIES AND S. OMERović, *Higher-order accurate integration of implicit geometries*, International Journal for Numerical Methods in Engineering, 106 (2016), pp. 323–371, <https://doi.org/https://doi.org/10.1002/nme.5121>, <https://onlinelibrary.wiley.com/doi/abs/10.1002/nme.5121>, <https://arxiv.org/abs/https://onlinelibrary.wiley.com/doi/pdf/10.1002/nme.5121>.
- [15] J. GRANDE, C. LEHRENFELD, AND A. REUSKEN, *Analysis of a high-order trace finite element method for PDEs on level set surfaces*, SIAM Journal on Numerical Analysis, 56 (2018), pp. 228–255, <http://epubs.siam.org/doi/abs/10.1137/16M1102203>.
- [16] P. HANSBO, M. G. LARSON, AND S. ZAHEDI, *A cut finite element method for coupled bulk-surface problems on time-dependent domains*, Comput. Methods Appl. Mech. Engrg., 307 (2016), pp. 96–116, <https://doi.org/10.1016/j.cma.2016.04.012>.
- [17] F. HEIMANN, *On Discontinuous- and Continuous-In-Time Unfitted Space-Time Methods for PDEs on Moving Domains*, Master’s thesis, University of Göttingen, (2020), <https://doi.org/10.25625/CDCMYT>.
- [18] F. HEIMANN AND C. LEHRENFELD, *Numerical Integration on Hyperrectangles in Isoparametric Unfitted Finite Elements*, in European Conference on Numerical Mathematics and Advanced Applications, Springer, 2019, pp. 193–202, [https://doi.org/10.1007/978-3-319-96415-7\\_16](https://doi.org/10.1007/978-3-319-96415-7_16).
- [19] F. HEIMANN, C. LEHRENFELD, AND J. PREUSS, *Geometrically Higher Order Unfitted Space-Time Methods for PDEs on Moving Domains*, SIAM Journal on Scientific Computing, 45 (2023), pp. B139–B165, <https://doi.org/10.1137/22M1476034>, <https://doi.org/10.1137/22M1476034>.
- [20] T. J. HUGHES, *The finite element method: linear static and dynamic finite element analysis*, Courier Corporation, 2012.
- [21] M. G. LARSON AND C. LUNDHOLM, *Space-time cutfem on overlapping meshes: Simple discontinuous mesh evolution*, (2023), <https://arxiv.org/abs/2301.13517>.
- [22] C. LEHRENFELD, *On a Space-Time Extended Finite Element Method for the Solution of a Class of Two-Phase Mass Transport Problems*, PhD thesis, RWTH Aachen, February 2015, <http://publications.rwth-aachen.de/record/462743>.
- [23] C. LEHRENFELD, *High order unfitted finite element methods on level set domains using isoparametric mappings*, Comput. Methods Appl. Mech. Eng., 300 (2016), pp. 716 – 733, <https://doi.org/10.1016/j.cma.2015.12.005>.
- [24] C. LEHRENFELD, *A higher order isoparametric fictitious domain method for level set domains*, in Geometrically Unfitted Finite Element Methods and Applications, S. P. A. Bordas, E. Burman, M. G. Larson, and M. A. Olshanskii, eds., Springer International Publishing, 2017, pp. 65–92, <https://doi.org/10.1007/978-3-319-71431-8>.
- [25] C. LEHRENFELD, F. HEIMANN, J. PREUSS, AND H. VON WAHL, *‘ngsxfem’: Add-on to NGSolve*



- for geometrically unfitted finite element discretizations, *J. Open Source Softw.*, 6 (2021), p. 3237, <https://doi.org/10.21105/joss.03237>.
- [26] C. LEHRENFELD AND M. A. OLSHANSKII, *An Eulerian finite element method for PDEs in time-dependent domains*, *ESAIM: M2AN*, 53 (2019), pp. 585–614, <https://doi.org/10.1051/m2an/2018068>.
- [27] C. LEHRENFELD, M. A. OLSHANSKII, AND X. XU, *A stabilized trace finite element method for partial differential equations on evolving surfaces*, *SIAM Journal on Numerical Analysis*, 56 (2018), pp. 1643–1672, <https://doi.org/10.1137/17M1148633>, <https://doi.org/10.1137/17M1148633>, <https://arxiv.org/abs/https://doi.org/10.1137/17M1148633>.
- [28] C. LEHRENFELD AND A. REUSKEN, *Analysis of a Nitsche XFEM-DG discretization for a class of Two-Phase Mass Transport Problems*, *SIAM J. Numer. Anal.*, 51 (2013), pp. 958–983, <https://doi.org/10.1137/120875260>.
- [29] C. LEHRENFELD AND A. REUSKEN, *Analysis of a high order unfitted finite element method for an elliptic interface problem*, *IMA J. Numer. Anal.*, 38 (2018), pp. 1351–1387, <https://doi.org/10.1093/imanum/drx041>.
- [30] Y. LOU AND C. LEHRENFELD, *Isoparametric unfitted bdf-finite element method for pdes on evolving domains*, *SIAM Journal on Numerical Analysis*, 60 (2022), pp. 2069–2098, <https://doi.org/10.1137/21M142126X>, <https://doi.org/10.1137/21M142126X>, <https://arxiv.org/abs/https://doi.org/10.1137/21M142126X>.
- [31] M. NEILAN AND M. OLSHANSKII, *An eulerian finite element method for the linearized navier-stokes problem in an evolving domain*, arXiv preprint arXiv:2308.01444, (2023).
- [32] M. A. OLSHANSKII, A. REUSKEN, AND P. SCHWERING, *An eulerian finite element method for tangential navier-stokes equations on evolving surfaces*, (2023), <https://arxiv.org/abs/2302.00779>.
- [33] J. PREUSS, *Higher order unfitted isoparametric space-time FEM on moving domains*, Master’s thesis, University of Göttingen, (2018), <https://doi.org/10.25625/UACWXS>.
- [34] A. REUSKEN AND H. SASS, *Analysis of a space-time unfitted finite element method for PDEs on evolving surfaces*, (2024), <https://arxiv.org/abs/2401.01215>.
- [35] H. SASS AND A. REUSKEN, *An accurate and robust Eulerian finite element method for partial differential equations on evolving surfaces*, *Computers & Mathematics with Applications*, 146 (2023), pp. 253–270, <https://doi.org/https://doi.org/10.1016/j.camwa.2023.06.040>, <https://www.sciencedirect.com/science/article/pii/S0898122123002924>.
- [36] R. I. SAYE, *High-order quadrature methods for implicitly defined surfaces and volumes in hyperrectangles*, *SIAM Journal on Scientific Computing*, 37 (2015), pp. A993–A1019, <https://doi.org/10.1137/140966290>, <https://doi.org/10.1137/140966290>, <https://arxiv.org/abs/https://doi.org/10.1137/140966290>.
- [37] H. VON WAHL, T. RICHTER, AND C. LEHRENFELD, *An unfitted Eulerian finite element method for the time-dependent Stokes problem on moving domains*, *IMA J. Numer. Anal.*, (2021), <https://doi.org/10.1093/imanum/drab044>.
- [38] A. C. WENDLER, *Monolithic Unfitted Space-Time FEM for an Osmotic Cell Swelling Problem*, Master’s thesis, University of Göttingen, (2022), <https://doi.org/10.25625/0KPEON>.
- [39] S. ZAHEDI, *A space-time cut finite element method with quadrature in time*, in *Geometrically Unfitted Finite Element Methods and Applications - Proceedings of the UCL Workshop 2016*, *Lecture Notes in Computational Science and Engineering*, Springer, 2018, [https://doi.org/10.1007/978-3-319-71431-8\\_9](https://doi.org/10.1007/978-3-319-71431-8_9).

**Selected proofs.** In this section, we collect some proofs that are either tedious, but elementary or similar to other proofs presented in the main part or other literature.

## Appendix A. Selected proofs for Lemma 3.1.

### A.1. Proof of (3.2a-dbnad) for $(m_t, m_s) = (1, 1)$ .

*Proof.* We start to consider the first time derivative of (3.7) and bounding the left-hand side (term A) by  $\mathcal{O}(h + \Delta t^{q_t})$ :

$$\begin{aligned} \partial_t(\nabla\phi^{\text{lin}}(x, t) - \nabla\phi(\pi(x, t))) &= \underbrace{\partial_t\nabla\phi^{\text{lin}}(x, t) - \partial_t\nabla\phi(x, t)}_{\lesssim h + \Delta t^{q_t} \text{ by (2.13b-}\phi^{\text{lin}}\text{acc)}} + \underbrace{\partial_t\nabla\phi(x, t) - \partial_t\nabla\phi(\pi(x, t))}_{\lesssim |\phi|_{3, \infty, U} d \lesssim h^2 + \Delta t^{q_t + 1}} \end{aligned}$$

Now, we have to apply the product rule on all the right-hand-side terms. We start

with the first two summands (related to terms  $B$  and  $C$ ):

$$\begin{aligned}
& \partial_t(\nabla dG(x, t)^T \nabla \phi(\pi(x, t)) + d \nabla G^T \nabla \phi(\pi(x, t))) \\
&= (\partial_t \nabla d)G(x, t)^T \nabla \phi(\pi(x, t)) + \nabla d(\partial_t G(x, t)^T) \nabla \phi(\pi(x, t)) \quad (\text{I}) + (\text{II}) \\
& \quad + \nabla dG(x, t)^T \partial_t \nabla \phi(\pi(x, t)) + (\partial_t d) \nabla G^T \nabla \phi(\pi(x, t)) \quad (\text{III}) + (\text{IV}) \\
& \quad + d(\partial_t \nabla G^T) \nabla \phi(\pi(x, t)) + d \nabla G^T (\partial_t \nabla \phi(\pi(x, t))). \quad (\text{V}) + (\text{VI})
\end{aligned}$$

For I, we observe that the argument in (3.8b) can be applied here as well to yield

$$\text{I} \simeq (\partial_t \nabla d)(1 + h^2 + \Delta t^{q_t+1})$$

For II, we observe that the argument of (A.5) can be transferred here, where just the bound on  $\nabla d$  from (3.2a-dbnd) is applied to yield

$$\text{II} \lesssim h + \Delta t^{q_t+1}$$

Regarding the third term, we argue as follows:

$$\begin{aligned}
\text{III} &= \nabla dG(x, t)^T \partial_t \nabla \phi(\pi(x, t)) \lesssim \nabla d|\phi|_{1, \infty, U} (\partial_t \nabla \phi(x, t) + \mathcal{O}(h^2 + \Delta t^{q_t+1})) \\
&\lesssim \nabla d|\phi|_{1, \infty, U} |\phi|_{2, \infty, U} \lesssim h + \Delta t^{q_t+1} \text{ by (3.2a-dbnd)}.
\end{aligned}$$

For the fourth term, we combine the argument of (3.8c) with (A.6) to obtain

$$\text{IV} \lesssim (\partial_t d)|\phi|_{2, \infty} (1 + h^2 + \Delta t^{q_t+1}) \lesssim h^2 + \Delta t^{q_t}$$

For V, we give the following adaptation of the argument in (3.8c):

$$\text{V} = d(\partial_t \nabla G^T) \nabla \phi(\pi(x, t)) \lesssim d|\phi|_{3, \infty, U} (1 + \mathcal{O}(h^2 + \Delta t^{q_t+1})) \lesssim h^2 + \Delta t^{q_t+1}$$

by (3.2a-dbnd). Lastly, for VI, we have

$$(A.1) \quad \text{VI} = d \nabla G^T (\partial_t \nabla \phi(\pi(x, t))) \lesssim d|\phi|_{2, \infty, U} (\partial_t \nabla \phi(x, t) + h^2 + \Delta t^{q_t+1})$$

$$(A.2) \quad \lesssim d|\phi|_{2, \infty, U}^2 \lesssim h^2 + \Delta t^{q_t+1} \text{ by (3.2a-dbnd)}.$$

Next, we investigate the time derivatives from the two remaining summand on the right-hand side of (3.7):

$$\begin{aligned}
& \partial_t(\nabla b(\phi^{\text{lin}} - \phi)(x, t) + b(\nabla \phi^{\text{lin}} - \nabla \phi)(x, t)) \\
&= (\partial_t \nabla b)(\phi^{\text{lin}} - \phi) + \nabla b(\partial_t \phi^{\text{lin}} - \partial_t \phi) + \partial_t b(\nabla \phi^{\text{lin}} - \nabla \phi) + b(\partial_t \nabla \phi^{\text{lin}} - \partial_t \nabla \phi) \\
&\lesssim h + \Delta t^{q_t},
\end{aligned}$$

by the known techniques/ previous results.

Taking all these results together, we obtain

$$(A.3) \quad (\partial_t \nabla d)(1 + h^2 + \Delta t^{q_t+1}) \lesssim h + \Delta t^{q_t},$$

which finishes the proof of (3.2a-dbnd) for  $(m_t, m_s) = (1, 1)$ .  $\square$



**A.2. Proof of (3.2b-dbnd) for  $m_t \geq 1$ .**

*Proof.* We split the cases  $m_t = 1$  and  $m_t > 1$ .

Proof of (3.2b-dbnd) for  $m_t = 1$ :

We exploit the chain rule on (3.6-d $\pi$ ) similarly as in the proof of (3.2a-dbnd):

$$(A.4) \quad \begin{aligned} & (\partial_t \phi^{\text{lin}} - (\partial_t \phi) \circ \pi) \\ &= (\partial_t d) \underbrace{G^T(\nabla \phi) \circ \pi + d(\partial_t G)^T(\nabla \phi) \circ \pi}_{\stackrel{(3.8b)}{\simeq} 1+h^2+\Delta t^{q_t+1}} + \partial_t b \underbrace{(\phi^{\text{lin}} - \phi)}_{\lesssim h^2+\Delta t^{q_t+1}} + b \underbrace{(\partial_t \phi^{\text{lin}} - \partial_t \phi)}_{\lesssim h^2+\Delta t^{q_t}} \end{aligned}$$

For the l.h.s. there obviously holds

$$\begin{aligned} (\partial_t \phi^{\text{lin}} - (\partial_t \phi) \circ \pi) &= \underbrace{(\partial_t \phi^{\text{lin}} - \partial_t \phi)}_{\lesssim h^2+\Delta t^{q_t} \text{ by (2.13b-}\phi^{\text{lin}}\text{acc)}} + \underbrace{((\partial_t \phi) - (\partial_t \phi) \circ \pi)}_{\lesssim \|\partial_t \nabla \phi\|_\infty d \lesssim h^2+\Delta t^{q_t+1}} \lesssim h^2 + \Delta t^{q_t}. \end{aligned}$$

For the remaining summand, we argue with (3.2a-dbnd) to see

$$(A.5) \quad d(\partial_t G)^T(\nabla \phi) \circ \pi \lesssim d \|\partial_t \nabla \phi\|_\infty (\|\nabla \phi\|_\infty + h^2 + \Delta t^{q_t+1}) \lesssim h^2 + \Delta t^{q_t+1}$$

Taking these results together, we obtain

$$(A.6) \quad \partial_t d(1 + h^2 + \Delta t^{q_t+1}) \lesssim h^2 + \Delta t^{q_t},$$

which implies the claim in (3.2b-dbnd) for  $m_t = 1$ .

Proof of (3.2b-dbnd) for  $m_t > 1$ :

In regards to  $2 \leq m_t \leq q_t + 1$ , we proceed similarly as in the proof of (3.2b-dbnd) for  $m_t = 1$ . First, we note that for the time derivatives of  $b(\phi - \phi^{\text{lin}})$ , it holds with (2.13b- $\phi^{\text{lin}}\text{acc}$ ) and Assumption 2.13

$$\partial_t^{m_t} (b(\phi - \phi^{\text{lin}})) = \sum_{j=0}^{m_t} \binom{m_t}{j} (\partial_t^j b) (\partial_t^{m_t-j} (\phi - \phi^{\text{lin}})) \lesssim h^2 + \Delta t^{q_t+1-m_t}$$

With  $\phi \circ \pi = \phi^{\text{lin}} + b(\phi - \phi^{\text{lin}})$  and hence  $\partial_t^{m_t} (\phi \circ \pi) = \partial_t^{m_t} \phi^{\text{lin}} + \partial_t^{m_t} (b(\phi - \phi^{\text{lin}}))$  this implies together with another application of (2.13b- $\phi^{\text{lin}}\text{acc}$ )

$$\partial_t^{m_t} (\phi \circ \pi - \phi) \lesssim \partial_t^{m_t} (\phi^{\text{lin}} - \phi) + h^2 + \Delta t^{q_t+1-m_t} \lesssim h^2 + \Delta t^{q_t+1-m_t}.$$

Now we want to exchange  $(\partial_t^{m_t} \phi)$  with  $(\partial_t^{m_t} \phi) \circ \pi$  and note that  $\|\nabla \partial_t^{m_t} \phi\|_\infty \lesssim 1$ , so that with (3.2a-dbnd) for  $m_t = m_s = 0$  we obtain

$$(A.7) \quad \partial_t^{m_t} (\phi \circ \pi) - (\partial_t^{m_t} \phi) \circ \pi \lesssim h^2 + \Delta t^{q_t+1-m_t}.$$

We exploit this in now showing the result (3.2b-dbnd) for  $2 \leq m_t \leq q_t + 1$  by induction. So assume that (3.2b-dbnd) holds for  $0, \dots, m_t - 1$ . By induction (over  $m_t$ ) we can easily calculate the following equation

$$\partial_t^{m_t} (\phi \circ \pi) - (\partial_t^{m_t} \phi) \circ \pi = \sum_{j=0}^{m_t-1} \partial_t^j \left[ (\nabla \partial_t^{m_t-1-j} \phi) \circ \pi \cdot (\partial_t(dG)) \right].$$

Next, we want to separate the summand for  $j = m_t - 1$  and the remaining terms where we note that with (A.7) we already have a proper bound for the l.h.s. of the equation.

So, let's consider the summands for  $j < m_t - 1$ :  $\partial_t^j \left[ (\nabla \partial_t^{m_t-1-j} \phi) \circ \pi \cdot (\partial_t(dG)) \right]$ . According to the Leibniz rule, we will consider the products of terms for  $j_1 + j_2 = j$  where the  $j_1$ -th time derivative acts on  $(\nabla \partial_t^{m_t-1-j} \phi) \circ \pi$  and the ones where the  $j_2$ -th time derivative acts on  $\partial_t(dG)$ . For the former ones, we note that repeated application of the chain rule yields

$$\begin{aligned} \partial_t^{j_1} ((\nabla \partial_t^{m_t-1-j_1} \phi) \circ \pi) &\lesssim (\nabla \partial_t^{m_t-1} \phi) \circ \pi + \sum_{k=1}^{j_1} (\partial_t^{m_t-1-k} D^{k+1} \phi) \circ \pi \sum_{k=1}^{j_1} \partial_t^k(dG) \\ &\lesssim 1 + \sum_{k=1}^{j_1} \partial_t^k(dG) \end{aligned}$$

For the latter ones we have  $\partial_t^{j_2} \partial_t(dG) = \partial_t^{j_2+1}(dG)$  so that the products of the two terms are bounded by  $\partial_t^{j_2+1}(dG) + \sum_{k=1}^{j_1} \partial_t^k(dG) \partial_t^{j_2+1}(dG) \lesssim \partial_t^{m_t-1}(dG)$ . With the regularity of  $G$  the crucial remaining terms are the derivatives on  $d$  for which we can apply the induction hypothesis so that the summands for  $j < m_t - 1$  are bounded by  $h^2 + \Delta t^{q_t+2-m_t}$ . We hence find

$$(A.8) \quad \partial_t^{m_t-1} [(\nabla \phi) \circ \pi \cdot (\partial_t(dG))] \lesssim h^2 + \Delta t^{q_t+1-m_t}.$$

Now, applying the Leibniz rule again we obtain the summand  $(\nabla \phi) \circ \pi \cdot \partial_t^{m_t-1}(dG)$  and the remaining summands have the same bounds as the previously treated terms. Splitting the remaining term further as  $(\nabla \phi) \circ \pi \cdot \partial_t^{m_t-1}(dG) = (\nabla \phi) \circ \pi \cdot G \cdot \partial_t^{m_t-1}d + R$  with the remainder term  $R$ , we notice that  $R$  is again bounded as before. With  $(\nabla \phi) \circ \pi \cdot G \simeq 1$  we hence finally have

$$\partial_t^{m_t} d \lesssim h^2 + \Delta t^{q_t+1-m_t}.$$

which implies the claim (by induction).  $\square$

### A.3. Proof of (3.2c-dbnad).

*Proof.* Fix  $T \in \mathcal{T}_h^\Gamma$ ,  $\alpha_s \in \mathbb{N}_0^d$  and  $\alpha_t \in \mathbb{N}_0$  such that  $|\alpha_s| \leq q_s + 1$ ,  $\alpha_t \leq q_t + 1$ . Then, we aim to show

$$(A.9) \quad \|D^{(\alpha_s, \alpha_t)} d\|_{\infty, T \times I_n} \lesssim 1.$$

To this end, we introduce the function  $F(x, t, y) = \phi(x + yG(x, t), t) - \phi^{\text{lin}}(x, t) + b(x, t)(\phi^{\text{lin}}(x, t) - \phi(x, t))$ . Then the function  $d(x, t) = y(x, t)$  solves the implicit equation  $F(x, t, y(x, t)) = 0$ .

By the implicit function theorem, then we obtain for all  $\alpha \in \mathbb{N}_0^{d+1}$  with  $|\alpha| = 1$

$$(A.10) \quad D^\alpha d = - \underbrace{\left( \frac{\partial F}{\partial y}(x, t, d(x, t)) \right)^{-1}}_{:=A(x, t)} \cdot D_{(x, t)}^\alpha F(x, t, d(x, t)) = -A \cdot D_{(x, t)}^\alpha F(x, t, d(x, t)).$$

Hence, for all  $\alpha \in \mathbb{N}_0^{d+1}$  with  $0 < |\alpha| \leq q_s + q_t + 2$  (the boundedness of the zeroth and even first derivatives of  $d$  follow from the even stronger bounds in the previous equations), we find  $\alpha_1, \alpha_r \in \mathbb{N}_0^{d+1}$  s.t.  $|\alpha_1| = 1$  and  $\alpha = \alpha_1 + \alpha_r$ , so that we can conclude,

$$(A.11) \quad D^\alpha d = D^{\alpha_r} D^{\alpha_1} d = -D^{\alpha_r} A \cdot D_{(x, t)}^{\alpha_1} F(x, t, d(x, t))$$

$$(A.12) \quad = - \sum_{\nu \leq \alpha_r} \binom{\alpha}{\nu} (D^\nu A) \cdot D^{\alpha-\nu} D_{(x, t)}^{\alpha_1} F(x, t, d(x, t))$$

by the application of a Leibniz formula for multi-index derivatives. We are left with the task of showing boundedness of  $D^\alpha A$  for all  $\alpha \in \mathbb{N}_0^{d+1}$  s.t.  $|\alpha| \leq q_s + q_t + 1$  and of  $D^\alpha F$  for  $\alpha \in \mathbb{N}_0^{d+1}$  with  $|\alpha| \leq q_s + q_t + 2$ .

Concerning the boundedness of  $A$  itself, we start with the following observation in regard to its denominator:

$$\frac{\partial F}{\partial y}(x, t, d(x, t)) = \nabla \phi(x + d(x, t)G(x, t), t) \nabla \phi(x, t) = \|\nabla \phi(x, t)\|_2^2 + \mathcal{O}(h^2 + \Delta t^{q_t+1})$$

Hence, for sufficiently small meshes and time-steps, this expression is not only  $\leq 1$  (as would be also implied by the boundedness of the derivatives of  $F$  shown below) but even  $\simeq 1$ . We can conclude that  $A \lesssim 1$  and even higher negative powers,  $(\frac{\partial F}{\partial y}(x, t, d(x, t)))^{-k} \lesssim 1$  for  $k \in \mathbb{N}$ . This is helpful to show the general boundedness of  $D^\alpha A$ , as we can write  $A = i \circ \frac{\partial F}{\partial y}(x, t, d(x, t))$ , where  $i: x \mapsto 1/x$ . Then  $D^\alpha A$  can be calculated by a higher-dimensional Faa di Bruno formula such as [10, Lemma 3], leaving us with a sum of combinatorial factors and (higher) derivatives of  $i$  and  $\frac{\partial F}{\partial y}(x, t, d(x, t))$ . Then the boundedness follows from the previous observations with the bounds on (derivatives of)  $F$ .

Now in regards to  $D^\alpha F$ , we discuss the summands individually in the order: 1)  $\phi^{\text{lin}}(x, t)$ , 2)  $b(x, t)(\phi^{\text{lin}}(x, t) - \phi(x, t))$ , 3)  $\phi(x + yG(x, t), t)$ .

Regarding 1): We note that  $D^\alpha \phi^{\text{lin}}(x, t) = 0$  if a higher spatial derivative than the first is considered. Else,  $\|D^\alpha \phi^{\text{lin}}(x, t)\| \leq \|D^\alpha \phi(x, t)\| - \|D^\alpha \phi^{\text{lin}}(x, t) - D^\alpha \phi(x, t)\|$ , where the first summand is bounded by  $\phi \in C^{q_s+q_t+2}(U)$  and the second can be bounded by (2.13b- $\phi^{\text{lin}}\text{acc}$ ).

Regarding 2): From the previous point, we take the result  $\|D^\alpha \phi^{\text{lin}}\|_\infty \lesssim 1$  for all  $\alpha$  with  $|\alpha| < q_s + q_t + 2$ . Moreover,  $D^\alpha b$  and  $D^\alpha \phi$  are bounded similarly by the assumptions  $b, \phi \in C^{k_s+k_t+2}$ . This suffices to show

$$(A.13) \quad \|D^\alpha (b(x, t)(\phi^{\text{lin}}(x, t) - \phi(x, t)))\|_\infty \lesssim 1,$$

as all terms that appear in a Leibniz formula for multi-index derivatives as given above are bounded.

Regarding 3): So it remains to consider the summand  $(x, t, y) \mapsto \phi(x + yG(x, t), t)$ , which means  $D_{(x,t)}^\alpha \phi(x + yG(x, t), t)$ , where the evaluation point  $y = d(x, t)$  will be chosen. We define the helper function  $\pi: (x, t) \mapsto (x + yG(x, t), t)$ , so that we have to bound  $D_{(x,t)}^\alpha \phi \circ \pi$ . To this end, we again apply [10, Lemma 3], so that bounds on the corresponding functions  $\phi$  and  $\pi$  are sufficient. In regards to  $\phi$ , the assumption  $\phi \in C^{q_t+q_s+2}(U)$  suffices. For  $\pi$  we note that as  $G(x, t) = \nabla \phi(x, t)$ , the previously mentioned assumption implies that  $G(x, t) \in C^{q_t+q_s+1}$ , so that the result follows.  $\square$

## Appendix B. Further selected proofs.

### B.1. Proof of (4.4- $\Psi_{\Delta t}^\Gamma \text{acc-b}$ ).

*Proof.* We prove the bound at  $t_i$ ,  $\|\nabla(\Psi_{\Delta t, i}^\Gamma - \Psi_i^\Gamma)\|_{\infty, \Omega^\Gamma} \lesssim h^{q_s} + \Delta t^{q_t+1}$ . There holds

$$\begin{aligned} |\nabla(\Psi_{\Delta t, i}^\Gamma - \Psi_i^\Gamma)| &= |\nabla(d_{\Delta t, i} G_{\Delta t, i} - d_i G_i)| \\ &= |G_{\Delta t, i} - G_i| |d_{\Delta t, i}| + |G_i| |\nabla(d_{\Delta t, i} - d_i)| + |d_{\Delta t, i} - d_i| |\nabla G_i| + |d_i| |\nabla(G_{\Delta t, i} - G_i)| \end{aligned}$$

From (2.7c- $\phi_{\Delta t} \text{acc}$ ) (with  $m_s = 1$  and  $m_s = 2$ ), (4.2- $d_{\Delta t} \text{bnd}$ ), (4.4- $\Psi_{\Delta t} \text{acc-a}$ ), (2.3- $\phi \text{bnd}$ ) and (3.2) we can bound the first, third and fourth summand by the desired bound.

Further we have  $|G_i| \lesssim 1$  due to (2.3- $\phi_{\text{bnd}}$ ) so that it only remains to bound  $|\nabla(d_{\Delta t,i} - d_i)|$ .

Again, we start with (3.1- $d_{\text{def}}$ ) and (4.1- $d_{\Delta t,i}$ - $\text{def}$ ) and fix a time  $t_i$ ,  $i = 0, \dots, q_t$  and  $x \in \Omega^\Gamma$ .

$$\begin{aligned} (\phi_i \circ \Psi_i^\Gamma)(x) &= R(x) := (1 - b_i(x))\phi_i^{\text{lin}}(x) + b_i(x)\phi_i(x) \text{ and} \\ (\phi_{\Delta t,i} \circ \Psi_{\Delta t,i}^\Gamma)(x) &= R_{\Delta t}(x) := (1 - b_i(x))\phi_i^{\text{lin}}(x) + b_i(x)\phi_{\Delta t,i}(x). \end{aligned}$$

where we defined  $R$  and  $R_{\Delta t}$  for later use. For  $x \in \Omega^\Gamma$  we set  $y = \Psi_i^\Gamma(x)$  and  $y_{\Delta t} = \Psi_{\Delta t,i}^\Gamma(x)$  and obtain from the chain rule, recalling  $G_i = \nabla\phi_i$  and some elementary calculus

$$\begin{aligned} \nabla R(x) &= \nabla(\phi_i \circ \Psi_i^\Gamma)(x) \\ &= \nabla\phi_i(y) + (G_i(x) \cdot G_i(y))\nabla d_i(x) + d_i(x)\nabla G_i(x)\nabla\phi_i(y) \\ \nabla R_{\Delta t}(x) &= \nabla(\phi_{\Delta t,i} \circ \Psi_{\Delta t,i}^\Gamma)(x) \\ &= \nabla\phi_{\Delta t,i}(y_{\Delta t}) + (G_{\Delta t,i}(x) \cdot G_{\Delta t,i}(y_{\Delta t}))\nabla d_{\Delta t,i}(x) + d_{\Delta t,i}(x)\nabla G_{\Delta t,i}(x)\nabla\phi_{\Delta t,i}(y_{\Delta t}) \end{aligned}$$

Subtracting both equations and moving the terms involving  $\nabla d_i(x)$  and  $\nabla d_{\Delta t,i}(x)$  to one side we obtain the equation  $A = B - C - D$  with the expressions

$$\begin{aligned} A &:= (G_i(x) \cdot G_i(y))\nabla d_i(x) - (G_{\Delta t,i}(x) \cdot G_{\Delta t,i}(y_{\Delta t}))\nabla d_{\Delta t,i}(x), \\ B &:= \nabla(R - R_{\Delta t})(x), \quad C := \nabla\phi_i(y) - \nabla\phi_{\Delta t,i}(y_{\Delta t}), \\ D &:= (d_i(x)\nabla G_i(x)\nabla\phi_i(y) - d_{\Delta t,i}(x)\nabla G_{\Delta t,i}(x)\nabla\phi_{\Delta t,i}(y_{\Delta t})) \end{aligned}$$

We will start splitting the term  $A$  further with

$$\begin{aligned} A &= (G_i(x) \cdot G_i(y))\nabla d_i(x) - (G_{\Delta t,i}(x) \cdot G_{\Delta t,i}(y_{\Delta t}))\nabla d_{\Delta t,i}(x) \\ &= \underbrace{(G_i(x) \cdot G_i(y))\nabla(d_i - d_{\Delta t,i})(x)}_{=: A_1} - \underbrace{(G_i(x) \cdot G_i(y) - G_{\Delta t,i}(x) \cdot G_{\Delta t,i}(y_{\Delta t}))\nabla d_{\Delta t,i}(x)}_{=: A_2} \end{aligned}$$

For  $A_1$  we note that  $|y - x| = |\Psi_i^\Gamma(x) - x| = |(d_i G_i)(x)|$  and hence with (3.2a- $d_{\text{bnd}}$ )  $|y - x| \lesssim h^2 + \Delta t^{q_t+1}$ . Further we have  $|\nabla G_i| = |D^2\phi_i| \lesssim 1$  from (2.3- $\phi_{\text{bnd}}$ ) so that  $G_i(y) = G_i(x) + \mathcal{O}(h^2 + \Delta t^{q_t+1})$ . This yields

$$G_i(x) \cdot G_i(y) = \|\nabla\phi_i(x)\|^2(1 + \mathcal{O}(h^2 + \Delta t^{q_t+1})) \stackrel{(2.3-\phi_{\text{bnd}})}{\simeq} 1,$$

so that we can rearrange the balance  $A = B - C - D$  to

$$|\nabla(d_i - d_{\Delta t,i})(x)| \lesssim |A_2| + |B| + |C| + |D|$$

We will now bound each of these terms separately with  $\lesssim h^{q_s} + \Delta t^{q_t+1}$  which will yield the desired result.

$A_2$ : With  $|y - y_{\Delta t}| = |(\Psi_i^\Gamma - \Psi_{\Delta t,i}^\Gamma)(x)|$  and the bound from (4.4- $\Psi_{\Delta t}$ - $\text{acc-a}$ ) we have

$$G_{\Delta t,i}(y_{\Delta t}) = G_{\Delta t,i}(y) + \mathcal{O}(h^{q_s+1} + \Delta t^{q_t+1}) \cdot \|DG_{\Delta t,i}\|_{\infty, \Omega^\Gamma}$$

where  $\|DG_{\Delta t,i}\|_{\infty, \Omega^\Gamma} \lesssim 1$  with (2.7c- $\phi_{\Delta t}$ - $\text{acc}$ ) and  $m_s = 1$  and (2.3- $\phi_{\text{bnd}}$ ). From (2.7c- $\phi_{\Delta t}$ - $\text{acc}$ ) we also obtain  $G_{\Delta t,i}(y) = G_i(y) + \mathcal{O}(h^{q_s} + \Delta t^{q_t+1})$  so that together with (2.3- $\phi_{\text{bnd}}$ ) we have

$$G_{\Delta t,i}(x) \cdot G_{\Delta t,i}(y_{\Delta t}) = G_i(x) \cdot G_i(y) + \mathcal{O}(h^{q_s} + \Delta t^{q_t+1})$$

With (4.2- $d_{\Delta t}$ bnd) (for the derivative) we then make the rough estimate  $A_2 \lesssim h^{q_s} + \Delta t^{q_t+1}$ .

B: A bound for  $B$  follows easily with Assumption 2.13 and (2.7c- $\phi_{\Delta t}$ acc):

$$|\nabla(R - R_{\Delta t})(x)| \lesssim \underbrace{|\nabla b_i(x)|}_{\lesssim 1} \underbrace{|\phi_i - \phi_{\Delta t,i}(x)|}_{\lesssim h^{q_s+1} + \Delta t^{q_t+1}} + \underbrace{|b_i(x)|}_{\lesssim 1} \underbrace{|\nabla(\phi_i - \phi_{\Delta t,i})(x)|}_{\lesssim h^{q_s} + \Delta t^{q_t+1}} \lesssim h^{q_s} + \Delta t^{q_t+1}$$

C: For  $C$  we again apply (2.7c- $\phi_{\Delta t}$ acc) with  $m_s = 1$  to obtain

$$|\nabla \phi_i(y) - \nabla \phi_{\Delta t,i}(y_{\Delta t})| \lesssim \underbrace{|\nabla(\phi_i - \phi_{\Delta t,i})(y)|}_{\lesssim h^{q_s} + \Delta t^{q_t+1}} + \underbrace{|\nabla \phi_{\Delta t,i}(y) - \nabla \phi_{\Delta t,i}(y_{\Delta t})|}_{\lesssim \|D^2 \phi_{\Delta t,i}\|_{\infty, \bar{U}} |y - y_{\Delta t}|}$$

Now, we have  $\|D^2 \phi_{\Delta t,i}\|_{\infty, \bar{U}} \lesssim \|D^2 \phi_i\|_{\infty, \bar{U}} \lesssim 1$  due to (2.7c- $\phi_{\Delta t}$ acc) with  $m_s = 2$  and (2.3- $\phi$ bnd) and  $|y - y_{\Delta t}| \lesssim h^{q_s+1} + \Delta t^{q_s+1}$  with (4.4- $\Psi_{\Delta t}$ acc-a), so that also  $|C|$  has the desired upper bound.

D: Telescoping  $a_1 b_1 c_{1,1} - a_2 b_2 c_{2,2} = (a_1 - a_2) b_1 c_{1,1} + a_2 (b_1 - b_2) c_{1,1} + a_2 b_2 (c_{1,1} - c_{1,2}) + a_2 b_2 (c_{1,2} - c_{2,2})$  we obtain

$$\begin{aligned} (d_i(x) \nabla G_i(x) \nabla \phi_i(y) - d_{\Delta t,i}(x) \nabla G_{\Delta t,i}(x) \nabla \phi_{\Delta t,i}(y_{\Delta t})) &= D_1 + D_2 + D_3 + D_4 \text{ with} \\ D_1 &= (d_i - d_{\Delta t,i})(x) \nabla G_i(x) \nabla \phi_i(y) \\ D_2 &= d_{\Delta t,i}(x) \nabla (G_i - G_{\Delta t,i})(x) \nabla \phi_i(y) \\ D_3 &= d_{\Delta t,i}(x) \nabla G_{\Delta t,i}(x) (\nabla \phi_i(y) - \nabla \phi_{\Delta t,i}(y)) \\ D_4 &= d_{\Delta t,i}(x) \nabla G_{\Delta t,i}(x) (\nabla \phi_{\Delta t,i}(y) - \nabla \phi_{\Delta t,i}(y_{\Delta t})) \end{aligned}$$

With (4.5) and (2.3- $\phi$ bnd) we find  $|D_1| \lesssim h^{q_s+1} + \Delta t^{q_t+1}$ . Next, with (4.2- $d_{\Delta t}$ bnd) and (2.7c- $\phi_{\Delta t}$ acc) (with  $m_s = 2$ ) and (2.3- $\phi$ bnd) we get  $|D_2| \lesssim h^2 \cdot (h^{q_s-1} + \Delta t^{q_t+1}) \cdot 1$  which suffices for the desired bound. Next, with (4.2- $d_{\Delta t}$ bnd), (2.3- $\phi$ bnd) and (2.7c- $\phi_{\Delta t}$ acc) (with  $m_s = 1$ ) we also have  $|D_3| \lesssim h^2 \cdot 1 \cdot (h^{q_s} + \Delta t^{q_t+1})$  which again suffices. Finally, with (4.2- $d_{\Delta t}$ bnd), (2.3- $\phi$ bnd),  $\|D^2 \phi_{\Delta t,i}\|_{\infty, \bar{U}} \lesssim \|D^2 \phi_i\|_{\infty, \bar{U}} \lesssim 1$  due to (2.7c- $\phi_{\Delta t}$ acc) with  $m_s = 2$  and (2.3- $\phi$ bnd) and  $|y - y_{\Delta t}| \lesssim h^{q_s+1} + \Delta t^{q_s+1}$  with (4.4- $\Psi_{\Delta t}$ acc-a), we have  $|D_4| \lesssim h^2 \cdot 1 \cdot (h^{q_s+1} + \Delta t^{q_t+1})$  which concludes the proof.  $\square$

## B.2. Proof of Lemma 5.1 for $G_h = P_h^\Gamma \nabla \phi_h$ .

*Proof.* Let  $G_h = P_h^\Gamma \nabla \phi_h$ . We will make use of an inverse inequality to deal with the spatial derivative of  $P_h^\Gamma \nabla \phi_h$ . To circumvent using the inverse inequality on terms that involve temporal resolution quantities we apply a triangle inequality introducing  $P_h^\Gamma \nabla \phi_{\Delta t}$  and  $\nabla \phi_{\Delta t}$ . Exploit smoothness of  $\phi_{\Delta t}$  so that  $P_h^\Gamma \nabla \phi_{\Delta t} = I_{q_s}^s \nabla \phi_{\Delta t}$  we obtain

$$\begin{aligned} &\|D^m (P_h^\Gamma \nabla \phi_h - \nabla \phi)\|_{\infty, \mathcal{Q}_h^\Gamma} \\ &\leq \underbrace{\|D^m P_h^\Gamma \nabla (\phi_h - \phi_{\Delta t})\|_{\infty, \mathcal{Q}_h^\Gamma}}_{=:A} + \underbrace{\|D^m (I_{q_s}^s \nabla \phi_{\Delta t} - \nabla \phi_{\Delta t})\|_{\infty, \mathcal{Q}_h^\Gamma}}_{=:B} + \underbrace{\|D^m \nabla (\phi_{\Delta t} - \phi)\|_{\infty, \mathcal{Q}_h^\Gamma}}_{=:C} \end{aligned}$$

For  $A$  we apply an inverse inequality, exploit continuity of  $P_h^\Gamma$  and (2.7c- $\phi_{\Delta t}$ acc):

$$A \lesssim h^{-m} \|P_h^\Gamma \nabla (\phi_h - \phi_{\Delta t})\|_{\infty, \mathcal{Q}_h^\Gamma} \lesssim h^{-m} \|\nabla (\phi_h - \phi_{\Delta t})\|_{\infty, \mathcal{Q}_h^\Gamma} \lesssim h^{q_s-m}$$

For  $B$  we apply standard interpolation estimates

$$B \lesssim h^{q_s-m} \|D^{q_s+1} \phi_{\Delta t}\|_{\infty, \mathcal{Q}_h^\Gamma} \lesssim h^{q_s-m}$$

where the boundedness (by a constant) of  $D^{q_s+1}\phi_{\Delta t}$  follows from (2.7c- $\phi_{\Delta t}$ acc) with  $m_s = q_s + 1$  and the regularity of  $\phi$ . Finally, for  $C$  we can directly apply (2.7c- $\phi_{\Delta t}$ acc) with  $m_s = m + 1$  to get  $C \lesssim h^{q_s-m}$ . This concludes the proof.  $\square$

### B.3. Proof of Lemma 5.2.

*Proof.* We apply a several-variable version of Taylor's theorem with Lagrange remainder on  $\mathcal{E}_T\phi_{h,i} - \phi_i$  where we recall that  $\mathcal{E}_T\phi_{h,i} \in \mathcal{P}^{q_s}$ : We obtain the existence of  $\xi \in (0, 1)$  s.t.

$$\begin{aligned} |D^m(\mathcal{E}_T\phi_{h,i} - \phi_i)(y)| &= \left| \sum_{r=0}^{q_s-m} (r!)^{-1} D^{r+m}(\mathcal{E}_T\phi_{h,i} - \phi_i)(x) \overbrace{(y-x, \dots, y-x)}^{r \text{ times}} \right. \\ &\quad \left. - (q_s+1-m)!^{-1} D^{q_s+1}\phi_i(x + \xi(y-x)) \underbrace{(y-x, \dots, y-x)}_{(q_s+1-m) \text{ times}} \right| \\ &\lesssim \sum_{r=0}^{q_s} |D^r(\phi_{h,i} - \phi_i)|_{\infty, T} |y-x|^r + |y-x|^{q_s+1-m}. \end{aligned}$$

We have  $|D^r(\phi_{h,i} - \phi_i)|_{\infty, T} \lesssim h^{q_s+1-r} + \Delta t^{q_t+1}$  by (2.5- $\phi_h$ acc) and  $|y-x| \lesssim h$  so that (5.5a- $\mathcal{E}_T$ acc) follows. The second equation follows along the same lines noting that  $\mathcal{E}_T$  only acts on the spatial variable and that (2.5- $\phi_h$ acc) also provides the corresponding bounds for the temporal derivatives for any  $t \in I_n$ . Finally, for the third equation, we can apply the same approach to get

$$|D^m(\mathcal{E}_T\phi_{h,i} - \phi_{\Delta t,i})(y)| \lesssim \sum_{r=0}^{q_s} |D^r(\phi_{h,i} - \phi_{\Delta t,i})|_{\infty, T} h^r + h^{q_s+1-m} \lesssim h^{q_s+1-m}$$

with (2.7b- $\phi_{\Delta t|h}$ ).  $\square$

### B.4. Proof of the second estimate in (5.6b- $d_{h,i}$ bnd).

*Proof.* We treat the second estimate in (5.6b- $d_{h,i}$ bnd). For this, we take the gradient of both sides of (5.4- $d_{h,i}$ def). We start with the r.h.s. term and take  $x$  as argument for  $\phi_i^{\text{lin}}$ ,  $b_i$  and  $\phi_{h,i}$ , respectively:

$$\begin{aligned} (1 - b_i)\nabla\phi_i^{\text{lin}} + b_i\nabla\phi_{h,i} - \nabla b_i\phi_i^{\text{lin}} + \nabla b_i\phi_{h,i} \\ = \nabla\phi_i^{\text{lin}} + b_i\nabla(\phi_{h,i} - \phi_i^{\text{lin}}) + \nabla b_i(\phi_{h,i} - \phi_i^{\text{lin}}) \stackrel{\text{Cor.2.8}}{=} \nabla\phi_i^{\text{lin}} + \mathcal{O}(h), \end{aligned}$$

where in the last step we used  $b_i \in [0, 1]$  and  $|\nabla b_i| \lesssim 1$  and (2.11- $\phi_{1\text{in}|h}$ acc) from Corollary 2.8 with  $m = 0$  and  $m = 1$ , respectively. It is now of interest to compare this term with the result of taking the gradient on the other side of (5.4- $d_{h,i}$ def), denoting  $y_h := x + (d_{h,i}G_{h,i})(x)$

$$\begin{aligned} \underbrace{\nabla\phi_i^{\text{lin}}(x)}_A + \mathcal{O}(h) &= \underbrace{\nabla(\mathcal{E}_T\phi_{h,i})(y_h)}_B + \nabla d_{h,i}(x) \underbrace{(\nabla(\mathcal{E}_T\phi_{h,i})(y_h)) \cdot G_{h,i}(x)}_C \\ &\quad + \underbrace{d_{h,i}(x)(\nabla G_{h,i}(x)) \cdot \nabla(\mathcal{E}_T\phi_{h,i})(y_h)}_D \end{aligned}$$

We will first show that  $|A - B| = \mathcal{O}(h + \Delta t^{q_t+1})$ . We apply (5.5a- $\mathcal{E}_T$ acc) with  $m = 1$  from Lemma 5.2 to obtain  $\nabla(\mathcal{E}_T\phi_{h,i})(y_h) = \nabla\phi_i(y_h) + \mathcal{O}(h^{q_s} + \Delta t^{q_t+1})$ . With  $|y_h - x| \lesssim |d_{h,i}(x)||G_{h,i}(x)| \lesssim h^2 + \Delta t^{q_t+1}$ , which follows from the first estimate in (5.6b- $d_{h,i}$ bnd), (2.5- $\phi_h$ acc) and  $\|D^2\phi\|_{\infty, U} \lesssim 1$  from (2.3- $\phi$ bnd) we have

$$(B.1) \quad \nabla(\mathcal{E}_T\phi_{h,i})(y_h) = \nabla\phi_i(x) + \mathcal{O}(h) = \nabla\phi_i^{\text{lin}}(x) + \mathcal{O}(h + \Delta t^{q_t+1}) \quad \square$$

where we exploited (2.13b- $\phi^{\text{lin}}_{\text{acc}}$ ) with  $(m_s, m_t) = (1, 0)$ . Now, we achieved  $|A - B| = \mathcal{O}(h + \Delta t^{q_t+1})$ . Next, we consider  $D$ . We know already  $|d_{h,i}(x)| \lesssim h^2 + \Delta t^{q_t+1}$  and with  $(m_s, m_t) = (2, 0)$  in (2.5- $\phi_{h,\text{acc}}$ ) also  $|\nabla G_{h,i}| = |\nabla G_i| + \mathcal{O}(h^{q_s-1} + \Delta t^{q_t+1}) \lesssim 1$  and  $|\nabla(\mathcal{E}_T \phi_{h,i})(y_h)| = |\nabla \phi_i(x)| + \mathcal{O}(h) \lesssim 1$  so that  $|D| \lesssim h^2 + \Delta t^{q_t+1}$ . As a preliminary result, we can summarize  $C \nabla d_{h,i}(x) = \mathcal{O}(h + \Delta t^{q_t+1})$ .

It remains to treat  $C$ . To this end, we use the first equality of (B.1) again but additionally combine it with (5.3- $G_{h,\text{acc}}$ ) to get  $\nabla(\mathcal{E}_T \phi_{h,i})(y_h) = G_{h,i}(x) + \mathcal{O}(h + \Delta t^{q_t+1})$ . Hence, we have  $C = |G_{h,i}(x)|^2 + \mathcal{O}(h + \Delta t^{q_t+1})$ . As  $|G_{h,i}(x)|^2$  is bounded from above and below away from zero we can hence divide by  $C$  and obtain  $d_{h,i}(x) = \mathcal{O}(h + \Delta t^{q_t+1})$ .

### B.5. Proof of (6.2c- $d_{H,\text{bnd}}$ ).

*Proof.* We proceed similarly as in the proof of (3.2b- $d_{\text{bnd}}$ ) for  $m_t > 1$ . Recall the defining equation for  $d_H$  from (6.1- $d_{H,\text{def}}$ ) and defining  $\pi_H(x, t) := (x + d_H(x, t)G_H(x, t), t)$  we have

$$(6.1-d_{H,\text{def}}) \quad \mathcal{E}_T \phi_H \circ \pi_H = (1 - b)\phi^{\text{lin}} + b\phi_H = \phi^{\text{lin}} + b(\phi_H - \phi^{\text{lin}}).$$

For the time derivatives of  $b(\phi_H - \phi^{\text{lin}})$ , it holds with (2.8a- $\phi_H|_h$ ), (2.13a- $\phi^{\text{lin}}_{\text{acc}}$ ) and Assumption 2.13

$$\partial_t^{m_t} (b(\phi_H - \phi^{\text{lin}})) = \sum_{j=0}^{m_t} \binom{m_t}{j} (\partial_t^j b) (\partial_t^{m_t-j} (\phi_H - \phi^{\text{lin}})) \lesssim h^2 + \Delta t^{q_t+1-m_t}$$

With  $\partial_t^{m_t} (\mathcal{E}_T \phi_H \circ \pi_H) = \partial_t^{m_t} \phi^{\text{lin}} + \partial_t^{m_t} (b(\phi_H - \phi^{\text{lin}}))$  this implies together with another application of (2.13b- $\phi^{\text{lin}}_{\text{acc}}$ ) and (6.2a- $\mathcal{E}_T \text{acc}$ )

$$\partial_t^{m_t} (\phi \circ \pi_H - \phi) \lesssim \partial_t^{m_t} (\phi^{\text{lin}} - \phi) + h^2 + \Delta t^{q_t+1-m_t} \lesssim h^2 + \Delta t^{q_t+1-m_t}.$$

We are now in an almost identical setting as in the proof of (3.2b- $d_{\text{bnd}}$ ) for  $m_t > 1$  in Appendix A.2 before (A.7). We can proceed as in the second half of that proof with the only change that  $\pi$  is replaced by  $\pi_H$  and hence  $dG$  is replaced by  $d_H G_H$ .  $\square$

### B.6. Proof of Lemma 6.3.

*Proof.* We start with a simple splitting of the difference:

$$\begin{aligned} \|\partial_t(\Psi_H^\Gamma - \Psi^\Gamma)\|_{\infty, Q_h^\Gamma} &= \|\partial_t(d_H G_H - dG)\|_{\infty, Q_h^\Gamma} \\ &\leq \|\partial_t(d(G_H - G))\|_{\infty, Q_h^\Gamma} + \|\partial_t((d_H - d)G_H)\|_{\infty, Q_h^\Gamma} \\ &\leq \|(G_H - G)\|_{\infty, Q_h^\Gamma} \|\partial_t d\|_{\infty, Q_h^\Gamma} + \|d\|_{\infty, Q_h^\Gamma} \|\partial_t(G_H - G)\|_{\infty, Q_h^\Gamma} \\ &\quad + \|d_H - d\|_{\infty, Q_h^\Gamma} \|\partial_t G_H\|_{\infty, Q_h^\Gamma} + \|G_H\|_{\infty, Q_h^\Gamma} \|\partial_t(d_H - d)\|_{\infty, Q_h^\Gamma} = I + II + III + IV \end{aligned}$$

We treat the terms  $I$ ,  $II$ ,  $III$  and  $IV$  one after another, where sufficient estimates for the first three terms are comparably easily compiled and  $IV$  is more involved. To reduce the complexity of the proof we only treat the case where  $G_h = \nabla \phi_h$  and  $G_H = \nabla \phi_H$ , but the proof can be adapted to the case where  $G_h = P_h^\Gamma \nabla \phi_h$  and  $G_H = P_h^\Gamma \nabla \phi_H$ .

For  $I$  we obtain with (2.8b- $\phi_{H,\text{acc}}$ ) (with  $m_s = 1, m_t = 0$ ) and (3.2b- $d_{\text{bnd}}$ ) the bound  $I \lesssim (h^{q_s} + \Delta t^{q_t+1})(h^2 + \Delta t^{q_t})$  which suffices for the desired bound  $h^{q_s+1} + \Delta t^{q_t}$ . For  $II$  we use (2.8b- $\phi_{H,\text{acc}}$ ) (with  $m_t = 1, m_s = 1$ ) and (3.2a- $d_{\text{bnd}}$ ) and to get  $II \lesssim$



$(h^{q_s} + \Delta t^{q_t})(h^2 + \Delta t^{q_t+1})$ . With (2.17- $\Delta t$ bnd) this also yields a sufficient bound. For  $III$  we have  $\|\partial_t G_H\|_{\infty, Q_h^\Gamma} \leq \|\partial_t G\|_{\infty, Q_h^\Gamma} + \|\partial_t(G - G_H)\|_{\infty, Q_h^\Gamma} \lesssim 1$  with (2.8b- $\phi_H$ acc) (with  $m_t = 1$ ,  $m_s = 1$ ) and (2.3- $\phi$ bnd) and bound

$$\|d_H - d\|_{\infty, Q_h^\Gamma} \leq \|d_H - d_h\|_{\infty, Q_h^\Gamma} + \|d_h - I_{q_t}^t d\|_{\infty, Q_h^\Gamma} + \|I_{q_t}^t d - d\|_{\infty, Q_h^\Gamma} = III_a + III_b + III_c$$

where  $I_{q_t}^t d$  is the Lagrange interpolant of  $d$  at the time nodes  $t_i$ ,  $i = 0, \dots, q_t$  (note the regularity for  $d$  provided in Lemma 3.1). For  $III_a$  we have  $III_a \lesssim \Delta t^{q_t+1}$  from the previous lemma. For  $III_c$  we have  $\|I_{q_t}^t d - d\|_{\infty, Q_h^\Gamma} \lesssim \Delta t^{q_t+1} \|\partial_t^{q_t+1} d\|_{\infty, Q_h^\Gamma} \lesssim \Delta t^{q_t+1}$  with (3.2b- $d$ bnd). The expression in  $III_b$  is discrete in time and it hence suffices to bound terms on the time nodes  $i = 0, \dots, q_t$ , i.e.  $\|d_{h,i} - d_i\|_{\infty, \Omega^\Gamma}$ . Hence, with (4.5) and (5.13) we obtain the bound  $III \lesssim h^{q_s+1} + \Delta t^{q_t+1}$  which is sufficient for the desired bound. Finally, for  $IV$  we have  $\|G_H\|_{\infty, Q_h^\Gamma} \leq \|G\|_{\infty, Q_h^\Gamma} + \|G_H - G\|_{\infty, Q_h^\Gamma} \lesssim 1$  with (2.8b- $\phi_H$ acc) (with  $m_t = 0$ ,  $m_s = 1$ ) and (2.3- $\phi$ bnd).

It remains to establish a bound  $\|\partial_t(d_H - d)\|_{\infty, Q_h^\Gamma} \lesssim h^{q_s+1} + h^{q_t}$ . To this end we follow similar ideas as in the proof of (3.2b- $d$ bnd) for  $m_t = 1$ . From the definitions of  $d_H$  and  $d$  in (6.1- $d_H$ def) and (3.1- $d$ def) we have

$$\begin{aligned} \mathcal{E}_T \phi_H(x + (d_H G_H)(x, t), t) &= (1 - b(x, t)) \phi^{\text{lin}}(x, t) + b(x, t) \phi_H(x, t) \\ \phi(x + (dG)(x, t), t) &= (1 - b(x, t)) \phi^{\text{lin}}(x, t) + b(x, t) \phi(x, t) \end{aligned}$$

Subtracting both equations (and smuggling in  $\phi(x + (d_H G_H)(x, t), t)$ ) yields after dropping the arguments  $(x, t)$  for  $d_H G_H$  and  $dG$

$$\underbrace{\phi(x + d_H G_H, t) - \phi(x + dG, t)}_{=:A(x,t)} = \underbrace{(\phi - \mathcal{E}_T \phi_H)(x + d_H G_H, t)}_{=:B(x,t)} + \underbrace{b(x, t)(\phi_H - \phi)(x, t)}_{=:C(x,t)}.$$

Now deriving  $A(x, t)$  after time yields

$$\begin{aligned} \partial_t A(x, t) &= \partial_t (d_H G_H - dG) \cdot \nabla \phi(x, t) - (\partial_t \phi(x + dG, t) - \partial_t \phi(x + d_H G_H, t)) \\ &= G \cdot (\partial_t (d_H - d) G_H + \partial_t d \cdot (G_H - G)) + \partial_t (G_H - G) \cdot d + \partial_t G_H \cdot (d_H - d) - D(x, t) \\ &= \underbrace{G \cdot G_H \partial_t (d_H - d)}_{=:A_2(x,t)} + \underbrace{\partial_t d G_H \cdot (G_H - G)}_{=:A_3(x,t)} + \underbrace{\partial_t (G_H - G) \cdot d}_{=:A_3(x,t)} + \underbrace{\partial_t G_H \cdot (d_H - d)}_{=:A_4(x,t)} - D(x, t) \end{aligned}$$

which allows to isolate the desired expression  $\partial_t(d_H - d)$  and we obtain

$$|\partial_t(d_H - d)(x, t)| \leq \frac{1}{G \cdot G_H} \left( \sum_{i=2}^4 |A_i(x, t)| + |\partial_t B(x, t)| + |\partial_t C(x, t)| + |D(x, t)| \right)$$

There is  $G \cdot G_H = \|G\|^2 - G \cdot (G - G_H) \geq \|G\|(\|G\| - c(h^{q_s} + \Delta t^{q_t+1})) \gtrsim 1$  (for  $h$  and  $\Delta t$  sufficiently small) and we can hence bound the terms  $A_i$ ,  $i = 2, 3, 4$  and  $\partial_t B$ ,  $\partial_t C$  and  $D$  one after another. For  $A_2$ ,  $A_3$  and  $A_4$  we observe that the necessary bounds follow along the lines of the bound for I, II and III above.

We have that  $|\partial_t B|$  is directly in the form of the l.h.s. of (6.2a- $\mathcal{E}_T$ acc) and hence has a suitable bound. Next, we note  $|\partial_t C| \leq |\partial_t b| |\phi_H - \phi| + |b| |\partial_t(\phi_H - \phi)|$  where  $|b|, |\partial_t b| \lesssim 1$  and  $|\phi_H - \phi|, |\partial_t(\phi_H - \phi)| \lesssim h^{q_s+1} + \Delta t^{q_t}$  by (2.8b- $\phi_H$ acc). Finally, we bound  $|D|$ :

$$|D(x, t)| \lesssim \|\partial_t \nabla \phi\|_{\infty} \|\Psi_H^\Gamma - \Psi^\Gamma\|_{\infty} \lesssim \Delta t^{q_t+1} + h^{q_s+1}$$

where the last step follows from (6.4- $\Psi_H^\Gamma|_h$ ) and (5.14- $\Psi_h^\Gamma$ acc). Putting it all together yields the claim.  $\square$

### B.7. Proof of (7.12a- $\Theta_h$ acc) and (7.12b- $\Theta_h$ acc) for FE blending.

*Proof.* In the case of the FE blending, the result on  $\Omega^\Gamma$  follow directly from (5.15a- $\Theta_h^\Gamma$ acc) and (5.15b- $\Theta_h^\Gamma$ acc). It remains to show the estimates for  $\Omega_+^\Gamma \setminus \Omega^\Gamma$ . We start to tackle (7.12a- $\Theta_h$ acc), so fix  $m_t = 0, 1$  to yield with Lemma 7.2

$$\begin{aligned} \Delta t^{m_t} \|\partial_t^{m_t} (\Theta_h - \Psi)\|_{\infty, \mathcal{Q}_{h,+}^\Gamma \setminus \mathcal{Q}_h^\Gamma} &= \Delta t^{m_t} \|\mathcal{E}^{\partial\Omega^\Gamma} \partial_t^{m_t} (\Theta_h^\Gamma - \Psi^\Gamma)\|_{\infty, \mathcal{Q}_{h,+}^\Gamma \setminus \mathcal{Q}_h^\Gamma} \\ &\stackrel{(7.3a-\mathcal{E}bnd)}{\lesssim} \max_{F \in \mathcal{F}(\partial\Omega^\Gamma)} \sum_{r=0}^{q_s+1} \Delta t^{m_t} h^r \|D^r \partial_t^{m_t} (\Theta_h^\Gamma - \Psi^\Gamma)\|_{\infty, F \times I_n} \\ &\quad + \Delta t^{m_t} \|\partial_t^{m_t} (\Theta_h^\Gamma - \Psi^\Gamma)\|_{\infty, \mathcal{V}(\partial\Omega^\Gamma) \times I_n} \\ &\lesssim h^{q_s+1} + \Delta t^{q_t+1} \quad \text{by (5.15a-}\Theta_h^\Gamma\text{acc)}. \end{aligned}$$

For (7.12b- $\Theta_h$ acc) we argue similar:

$$\begin{aligned} &\|D^1 \mathcal{E}^{\partial\Omega^\Gamma} (\Theta_h^\Gamma - \Psi^\Gamma)\|_{\infty, \mathcal{Q}_{h,+}^\Gamma \setminus \mathcal{Q}_h^\Gamma} \\ &\stackrel{(7.3a-\mathcal{E}bnd)}{\lesssim} \max_{F \in \mathcal{F}(\partial\Omega^\Gamma)} \sum_{r=1}^{q_s+1} h^{r-1} \|D^r (\Theta_h^\Gamma - \Psi^\Gamma)\|_{\infty, F \times I_n} + \frac{1}{h} \|\Theta_h^\Gamma - \Psi^\Gamma\|_{\infty, \mathcal{V}(\partial\Omega^\Gamma) \times I_n} \\ &\lesssim \frac{1}{h} (h^{q_s+1} + \Delta t^{q_t+1}) \quad \text{by (5.15a-}\Theta_h^\Gamma\text{acc)}. \end{aligned}$$

With Assumption 2.12 the claim follows.  $\square$

### B.8. Proof of Lemma 8.2.

*Proof.* We start with  $\|u^e \circ \Psi^{\text{st}}\|_{H_{\square}^{0, \ell_t}(Q_{\varepsilon}^{\text{lin}})}$  and apply the setting of [11, Theorem 2.1]. In the following, we will use the notation of this paper without further explanation and refer the reader to [11] for these. We identify  $d+1$  in this text with  $d$  in [11],  $u^e \circ \Psi^{\text{st}}$  with  $h$ ,  $u^e$  with  $f$  and the components of  $\Psi^{\text{st}}$  with  $g^{(1)}, \dots, g^{(d+1)}$ . Then we investigate the constituent expressions of the norm, which are  $D^\nu(u^e \circ \Psi^{\text{st}})$  at some point  $(x, t)$  for  $\nu = (0, \dots, 0, s_t)$  with  $s_t \leq \ell_t$ . Moreover,  $n = s_t$  and we observe that all the expressions  $f_\lambda$  in [11, Theorem 2.1] are bounded by  $\|u^e\|_{H^{\ell_t}(\Psi^{\text{st}}(Q_{\varepsilon}^{\text{lin}}))}$  at  $(x, t)$ . In regards to the contribution from  $\Psi^{\text{st}}$ , we note that the indices  $\mathbf{l}_j$  must give  $\nu$  as the sum weighted with  $|\mathbf{k}_j| > 0$ . Hence,  $\mathbf{l}_j \leq \nu$ . So only bounded contributions from  $\|\Psi^{\text{st}}\|_{H_{\square}^{0, \ell_t}(Q_{\varepsilon}^{\text{lin}})}$  appear.

Next, we proceed similarly for  $\|u^e \circ \Psi^{\text{st}}\|_{H_{\square}^{\ell_s, 0}(Q_{\varepsilon}^{\text{lin}})}$ . Let  $\nu = (\nu_1, \dots, \nu_d, 0)$  be some appropriate derivation multi-index, i.e.  $n = \sum_{i=1}^d \nu_i \leq \ell_s$ . This means that again all the terms  $f_\lambda$  are bounded by  $\|u^e\|_{H^{\ell_s}(\Psi^{\text{st}}(Q_{\varepsilon}^{\text{lin}}))}$  at the point of consideration. For the derivatives of  $\Psi^{\text{st}}$ , we again note that the multi-indices  $\mathbf{l}_j$  must sum up to  $\nu$  with the according weighting and hence all these are bounded by terms from  $\|\Psi^{\text{st}}\|_{H_{\square}^{\ell_s, 0}(Q_{\varepsilon}^{\text{lin}})} \lesssim 1$ .

In relation to  $\|\partial_t(u^e \circ \Psi^{\text{st}})\|_{H_{\square}^{\ell_s, 0}(Q_{\varepsilon}^{\text{lin}})}$  we have to consider a multi-index  $\nu = (\nu_1, \dots, \nu_d, 1)$ , so that  $n = 1 + \sum_{i=1}^d \nu_i \leq \ell_s + 1$ . This causes  $\|u^e\|_{H^{\ell_s+1}(\Psi^{\text{st}}(Q_{\varepsilon}^{\text{lin}}))}$  to be an appropriate upper bound for all the  $f_\lambda$ . In relation to  $\mathbf{l}_j \leq \nu$ , all corresponding summands are contained in  $\|\Psi^{\text{st}}\|_{H_{\square}^{\ell_s, 0}(Q_{\varepsilon}^{\text{lin}})} + \|\partial_t \Psi^{\text{st}}\|_{H_{\square}^{\ell_s, 0}(Q_{\varepsilon}^{\text{lin}})}$ .

For  $\|\nabla(u^e \circ \Psi^{\text{st}})\|_{H_{\square}^{0, \ell_t}(Q_{\varepsilon}^{\text{lin}})}$ , the argument proceeds similarly with an multi-index such as  $\nu = (1, \dots, 0, \ell_t)$ ,  $n \leq \ell_t + 1$ .  $\square$

**Supplementary Material.**

$k$	$i$	FE blending		smooth blend., $w_b = 0.1$		smooth blend., $w_b = 0.2$	
		err: $L^2(T), L^2(Q_h)$		(eoc) err: $L^2(T), L^2(Q_h)$		(eoc) err: $L^2(T), L^2(Q_h)$	
1	0	$5.09 \cdot 10^{-1}$	$2.06 \cdot 10^{-1}$	$5.09 \cdot 10^{-1}$	$2.06 \cdot 10^{-1}$	$5.09 \cdot 10^{-1}$	$2.06 \cdot 10^{-1}$
1	1	$1.57 \cdot 10^{-1}$	$8.07 \cdot 10^{-2}$	(1.4) $1.57 \cdot 10^{-1}$	$8.07 \cdot 10^{-2}$	(1.4) $1.57 \cdot 10^{-1}$	$8.07 \cdot 10^{-2}$ (1.4)
2	2	$4.10 \cdot 10^{-2}$	$1.89 \cdot 10^{-2}$	(2.1) $4.10 \cdot 10^{-2}$	$1.89 \cdot 10^{-2}$	(2.1) $4.10 \cdot 10^{-2}$	$1.89 \cdot 10^{-2}$ (2.1)
3	3	$9.63 \cdot 10^{-3}$	$4.64 \cdot 10^{-3}$	(2.0) $9.63 \cdot 10^{-3}$	$4.64 \cdot 10^{-3}$	(2.0) $9.63 \cdot 10^{-3}$	$4.64 \cdot 10^{-3}$ (2.0)
4	4	$2.37 \cdot 10^{-3}$	$1.13 \cdot 10^{-3}$	(2.0) $2.37 \cdot 10^{-3}$	$1.13 \cdot 10^{-3}$	(2.0) $2.37 \cdot 10^{-3}$	$1.13 \cdot 10^{-3}$ (2.0)
5	5	$5.90 \cdot 10^{-4}$	$2.82 \cdot 10^{-4}$	(2.0) $5.90 \cdot 10^{-4}$	$2.82 \cdot 10^{-4}$	(2.0) $5.90 \cdot 10^{-4}$	$2.82 \cdot 10^{-4}$ (2.0)
6	6	$1.47 \cdot 10^{-4}$	$7.04 \cdot 10^{-5}$	(2.0) $1.47 \cdot 10^{-4}$	$7.04 \cdot 10^{-5}$	(2.0) $1.47 \cdot 10^{-4}$	$7.04 \cdot 10^{-5}$ (2.0)
3	0	$6.59 \cdot 10^{-2}$	$3.54 \cdot 10^{-2}$	$8.78 \cdot 10^{-2}$	$4.29 \cdot 10^{-2}$	$1.04 \cdot 10^{-1}$	$5.55 \cdot 10^{-2}$
1	1	$7.44 \cdot 10^{-3}$	$3.60 \cdot 10^{-3}$	(3.3) $2.06 \cdot 10^{-2}$	$8.13 \cdot 10^{-3}$	(2.4) $1.73 \cdot 10^{-2}$	$9.22 \cdot 10^{-3}$ (2.6)
2	2	$2.60 \cdot 10^{-4}$	$8.77 \cdot 10^{-5}$	(5.4) $1.46 \cdot 10^{-3}$	$9.22 \cdot 10^{-4}$	(3.1) $1.98 \cdot 10^{-3}$	$6.37 \cdot 10^{-4}$ (3.9)
3	3	$8.16 \cdot 10^{-6}$	$2.98 \cdot 10^{-6}$	(4.9) $1.54 \cdot 10^{-4}$	$4.56 \cdot 10^{-5}$	(4.3) $1.41 \cdot 10^{-5}$	$5.45 \cdot 10^{-6}$ (6.9)
4	4	$3.53 \cdot 10^{-7}$	$1.47 \cdot 10^{-7}$	(4.3) $1.40 \cdot 10^{-6}$	$5.70 \cdot 10^{-7}$	(6.3) $6.59 \cdot 10^{-7}$	$2.70 \cdot 10^{-7}$ (4.3)
5	5	$1.87 \cdot 10^{-8}$	$7.51 \cdot 10^{-9}$	(4.3) $6.93 \cdot 10^{-8}$	$2.75 \cdot 10^{-8}$	(4.4) $3.28 \cdot 10^{-8}$	$1.36 \cdot 10^{-8}$ (4.3)
5	0	$3.81 \cdot 10^{-2}$	$1.44 \cdot 10^{-2}$	$6.46 \cdot 10^{-2}$	$2.73 \cdot 10^{-2}$	$9.12 \cdot 10^{-2}$	$4.29 \cdot 10^{-2}$
1	1	$1.33 \cdot 10^{-3}$	$6.35 \cdot 10^{-4}$	(4.5) $1.49 \cdot 10^{-2}$	$6.27 \cdot 10^{-3}$	(2.1) $1.33 \cdot 10^{-2}$	$6.17 \cdot 10^{-3}$ (2.8)
2	2	$3.86 \cdot 10^{-5}$	$1.31 \cdot 10^{-5}$	(5.6) $2.19 \cdot 10^{-3}$	$8.27 \cdot 10^{-4}$	(2.9) $7.02 \cdot 10^{-4}$	$2.74 \cdot 10^{-4}$ (4.5)
3	3	$6.08 \cdot 10^{-8}$	$1.49 \cdot 10^{-8}$	(9.8) $9.66 \cdot 10^{-5}$	$2.92 \cdot 10^{-5}$	(4.8) $1.81 \cdot 10^{-6}$	$6.25 \cdot 10^{-7}$ (8.8)
4	4	$3.09 \cdot 10^{-10}$	$7.90 \cdot 10^{-11}$	(7.6) $2.20 \cdot 10^{-7}$	$8.83 \cdot 10^{-8}$	(8.4) $3.84 \cdot 10^{-8}$	$1.61 \cdot 10^{-8}$ (5.3)

TABLE 2

Numerical convergence of a stabilized  $L^2$  projection problem on an unfitted domain approximated isoparametrically, odd order  $k = 1, 3, 5$ . Observations coincide with those from the even order, cf. Table 1.

$k$	$i$	FE blending		smooth blend., $w_b = 0.1$		smooth blend., $w_b = 0.2$	
		err: $L^2(T), L^2(Q_h)$		(eoc) err: $L^2(T), L^2(Q_h)$		(eoc) err: $L^2(T), L^2(Q_h)$	
4	0	$6.09 \cdot 10^{-1}$	$3.09 \cdot 10^{-1}$	$7.36 \cdot 10^{-2}$	$3.73 \cdot 10^{-2}$	$8.69 \cdot 10^{-2}$	$5.67 \cdot 10^{-2}$
1	1	$7.00 \cdot 10^{-3}$	$2.81 \cdot 10^{-3}$	(6.8) $4.37 \cdot 10^{-2}$	$1.40 \cdot 10^{-2}$	(1.4) $2.32 \cdot 10^{-2}$	$1.36 \cdot 10^{-2}$ (2.1)
2	2	$2.16 \cdot 10^{-4}$	$8.17 \cdot 10^{-5}$	(5.1) $6.34 \cdot 10^{-3}$	$2.96 \cdot 10^{-3}$	(2.2) $2.12 \cdot 10^{-3}$	$5.47 \cdot 10^{-4}$ (4.6)
3	3	$2.16 \cdot 10^{-6}$	$6.06 \cdot 10^{-7}$	(7.1) $5.07 \cdot 10^{-4}$	$1.31 \cdot 10^{-4}$	(4.5) $9.06 \cdot 10^{-6}$	$3.94 \cdot 10^{-6}$ (7.1)
4	4	$4.29 \cdot 10^{-8}$	$1.24 \cdot 10^{-8}$	(5.6) $1.24 \cdot 10^{-6}$	$4.81 \cdot 10^{-7}$	(8.1) $3.41 \cdot 10^{-7}$	$1.48 \cdot 10^{-7}$ (4.7)
5	5	$1.29 \cdot 10^{-9}$	$3.75 \cdot 10^{-10}$	(5.1) $5.44 \cdot 10^{-8}$	$2.09 \cdot 10^{-8}$	(4.5) $1.07 \cdot 10^{-8}$	$4.77 \cdot 10^{-9}$ (5.0)

TABLE 3

Part 2 of the numerical results on interpolation (Part 1: Table 1). We specifically show the related errors for  $k = 4$  with the blending smoothness parameter chosen as  $s = 10$ . In comparison to Table 1, we observe that increasing the regularity to the value  $s = 10$  as required by our theoretical analysis is detrimental to the absolute error figures, whilst the asymptotic stays intact. We conjecture that the higher slope in e.g.  $\nabla b$  might lead to a higher constant in the error decay. We conclude that choosing parameters  $s$  lower than  $2k + 2$  in our example might be computationally advantageous.